Unraveling Chemical Compositional Changes of Biodegraded Crude Oil using Novel Chromatographic and Mass Spectrometric Techniques

By

Jeremy A. Nowak

A dissertation submitted in partial satisfaction of the

requirements for the degree of

Doctor of Philosophy

in

Chemistry

in the

Graduate Division

of the

University of California, Berkeley

Committee in charge:

Professor Allen H. Goldstein, Co-Chair
Professor Kristie Boering, Co-Chair
Professor Evan R. Williams
Professor John D. Coates

Spring 2019

Unraveling Chemical Compositional Changes of Biodegraded Crude Oil using Novel Chromatographic and Mass Spectrometric Techniques

by

Jeremy A. Nowak

Abstract

Unraveling Chemical Compositional Changes of Biodegraded Crude Oil using Novel Chromatographic and Mass Spectrometric Techniques

by

Jeremy A. Nowak

Doctor of Philosophy in Chemistry

University of California, Berkeley

Professor Allen H. Goldstein, Co-Chair
Professor Kristie Boering, Co-Chair

Crude oil is an immensely complex mixture that contains thousands of distinct elemental compositions with hydrogen, carbon, oxygen, nitrogen, and sulfur atoms. The chemical fingerprint of a crude oil varies depending on its origin and degree of weathering, a phenomenon which includes biodegradation. This dissertation focuses on chemical composition of crude oil and its biodegradation with an emphasis on biosouring, an enzymatic process in which Sulfate Reducing microbial Communities (SRCs) reduce sulfate, thiosulfate, and elemental sulfur to sulfide. Biosouring in crude oil reservoirs results in hydrogen sulfide production, precipitation of metal sulfide complexes, increased industrial costs of petroleum production, and exposure issues for personnel. Potential treatment strategies for biosouring include the injection of nitrate or perchlorate anions into crude oil reservoirs. The objectives of this dissertation include development of new analytical techniques and their application to characterize the chemical composition of crude oil, and how it changes during biosouring and treatments, including substrate consumption and product formation.

Chapter 1 introduces the motivations for the research and analytical methods applied, including single and multi-dimensional gas chromatography with vacuum ultraviolet ionization and time-of-flight mass spectrometry (GC-VUV-TOF and GCxGC-VUV-TOF), gas chromatography combined with variable ionization time-of-flight-mass spectrometry (GC-Select-eV-TOF-MS), and Fourier transform ion cyclotron resonance mass spectrometry (FT-ICR MS) combined with electrospray ionization. Chapter 1 then describes the experiments done examining biotransformations under different reducing environments and with different crude oils.

The ability to structurally characterize and isomerically quantify crude oil hydrocarbons relevant to refined fuels such as motor oil, diesel, and gasoline represents an extreme challenge for chromatographic and mass spectrometric techniques. In Chapter 2, GC×GC-VUV-TOF is applied using a tunable vacuum ultraviolet soft photoionization source, the Chemical Dynamics Beamline 9.0.2 of the Advanced Light Source at the Lawrence Berkeley National Laboratory, to directly characterize and isomerically sum the contributions of aromatic and aliphatic species to hydrocarbon classes of four crude oils. When the VUV beam is tuned to 10.5 ± 0.2 eV, both aromatic and aliphatic crude oil hydrocarbons are ionized to reveal the complete chemical abundance of C_9–C_{30} hydrocarbons. When the VUV beam is tuned to 9.0 ± 0.2 eV only aromatic hydrocarbons are ionized, allowing separation of the aliphatic and aromatic fractions of the crude

oil hydrocarbon chemical classes in an efficient manner while maintaining isomeric quantification. This technique provides an effective tool to determine the isomerically summed aromatic and aliphatic hydrocarbon compositions of crude oil, providing information that goes beyond typical GC×GC separations of the most dominant hydrocarbon isomers.

A comprehensive analysis of changes in crude oil chemical composition during biosouring and experimental treatments is presented in Chapter 3. Analyses using GC-VUV-TOF and FT-ICR MS combined with electrospray ionization were applied in this chapter to identify hydrocarbon degradation patterns and product formations in crude oil samples from biosoured, nitrate-treated, and perchlorate-treated bioreactor column experiments. Crude oil hydrocarbons were selectively transformed based on molecular weight and compound class in the biosouring control environment. Both the nitrate and the perchlorate treatments significantly reduced sulfide production; however, the nitrate treatment enhanced crude oil biotransformation, while the perchlorate treatment inhibited crude oil biotransformation. Nitrogen- and oxygen-containing biodegradation products, particularly with chemical formulas consistent with monocarboxylic and dicarboxylic acids containing 10−60 carbon atoms, were observed in the oil samples from both the souring control and the nitrate-treated columns but were not observed in the oil samples from the perchlorate-treated column. These results demonstrate that hydrocarbon degradation and product formation of crude oil can span hydrocarbon isomers and molecular weights up to C_{60} and double-bond equivalent classes ranging from straight-chain alkanes to polycyclic aromatic hydrocarbons. These results also strongly suggest that perchlorate injections may provide a preferred strategy to treat biosouring through inhibition of biotransformation.

Microbial catabolism is a natural biological process that can sour crude oil reservoirs, transform spilled oil, and is an engineering tool in hydrocarbon pollution remediation strategies. In Chapter 4, differences in hydrocarbon structure (such as degree of branching or position of alkyl substituents) are examined to determine how they affect relative catabolic degradation of alkanes, monocycloalkanes, and monoaromatic hydrocarbons in order to determine which compounds are altered most by these processes and which are recalcitrant. GC-Select-eV-TOF-MS at 14 eV was used to characterize catabolic patterns of hydrocarbon isomers in crude oil from four different oil fields exposed to a single complex microbial community. Changes in alkanes, monocycloalkanes, and monoaromatic hydrocarbons are comprehensively characterized to identify differences in biodegradation as a function of degree of branching and alkyl position. Hydrocarbon isomers with terminal alkyl branches were more prone to biodegradation than those with methyl groups further from the terminal position. Compounds with alkyl branches adjacent to each other experience less biodegradation than isomers with nonadjacent methyl groups. These patterns were consistent regardless of hydrocarbon structural class or oil composition, implying that isomeric structure, including the shape of the carbon chain and the alkyl position, dictates patterns of catabolism of hydrocarbons of a particular molecular class. The patterns identified in this chapter demonstrate that microbial metabolism leaves a distinct signature from other transformation processes occurring in spilled oil, such as atmospheric oxidation or evaporation, allowing the effects of biodegradation to be distinguished from those of other processes acting upon weathered oil.

A summary of research implications and ideas for further research directions, including incorporation of isotope labeled tracers to track a compound's specific biodegradation pathway and characterization of volatile organic compounds (VOCs) from biodegrading microbial communities, are provided in Chapter 5.

Table of Contents

Acknowledgments

I would like to first acknowledge my advisor, Allen Goldstein. His ability to multitask teaching, organize vastly different projects across the scientific spectrum, and provide the mentorship and kindness that is vital for graduate students has inspired me throughout my graduate career. I would not be where I am today without him and for that, I thank you very much. I would also like to thank the other professors at UC-Berkeley who provided much needed intellectual discussion and advice on experimental techniques throughout my research, chiefly Professors John Coates and Evan Williams. Thank you to the other scientists and staff in both the Goldstein group, the Wilson group, and the MagLab who guided me throughout those long beamtime and magnet time hours: Kevin Wilson, Bruce Rude, Robin Weber, Greg Drozd, Huan Chen, and Amy McKenna. I also want to thank my beamtime buddy, Michael Jacobs, who drove me home from the ALS at 4 AM and kept me awake with the help of snacks, baseball, and lots of soda.

My mom and dad, Barbara and Michael Nowak, have gone above and beyond parental duties during my PhD. From calls home at 3 AM complaining that nothing was working, to stress talks regarding paper writing or quals, to just needing to vent about grad school, my parents have always picked up the phone and listened to my musings and/or rants. I love both of you very much.

I would not have been able to complete my PhD without the support of the amazing chemistry graduate community at UC-Berkeley and my friends back in Boston. Eric Liu, thanks for listening to my stories of research, dating, and Bay area shenanigans. Whenever I've wanted to travel or drag you somewhere, you always say yes. Grad school wouldn't have been as successful if not for your encouragement and ability to keep me grounded.

Andreana Rosnik has been my housemate, best friend, confidant, and moral compass for the past five years. It seems like yesterday we moved into Ashby. These five years have flown by in some parts, dragged in others, and have made for some fantastic stories. Thanks for always offering emotional and intellectual support at a moment's notice. You are one of the best people I know.

I cannot imagine life after graduate school where I don't share an office with Ellyn Gray. We've watched hundreds of hours of baseball and football together (go Sox, Dodgers, and Pats!) and I know I would not have made it through my PhD without your constant cheerleading and emotional support on research and life. Thanks for being an amazing person Ellyn and I already miss seeing you every day.

And for everybody who has been a part of parties, movie nights, or barbecues at Ashby, thank you for being a part of my graduate school story and making it an amazing ride.

Chapter 1:

Introduction

1.1 Motivation of Work

One of the major analytical challenges in chromatographic and mass spectrometric techniques is the characterization of the chemical components of crude oil. Crude oil is an immensely complex organic mixture that can contain thousands of different molecules with different elemental compositions.[1,2] While the mixture can consist of organic compounds containing nitrogen, oxygen, or sulfur heteroatoms, over 90% of a crude oil's chemical composition is dominated by pure hydrocarbons.[3] Further complicating comprehensive crude oil characterization is how the chemical signature of an oil varies depending on geographic origin or degree of environmental weathering.[4,5] Crude oil from the Gulf of Mexico has a different chemical signature than crude oil from Scandinavia. Oil that appears as a surface slick after a spill will have a different chemical signature from oil obtained directly from a wellhead due to both weathering and the dissolution of water-soluble components. Previous work has extensively studied the effects of dissolution, photolysis, and evaporation on the chemical composition of crude oils from different reservoirs.[6-8]

This dissertation explores the effects of biotransformation on crude oil hydrocarbons in the context of the industrial process of biological souring, hereafter referred to as biosouring. Souring in general refers to the reduction of sulfate (SO_4^{2-}), thiosulfate ($S_2O_3^{2-}$), or elemental sulfur to sulfide (S^{2-}).[9] Non-biogenic souring occurs due to the thermal degradation of sulfur-containing hydrocarbons or thermochemical sulfate reduction. Biosouring occurs via the enzymatic reduction of sulfate to sulfide to form hydrogen sulfide (H_2S) by Sulfate Reducing microbial Communities (SRCs), such as Deltaproteobacteria and Firmicutes, found in the crude oil reservoir or seawater.[10] While biosouring can occur during primary oil recovery procedures, where only natural subterranean pressure is used to extract oil from a reservoir,[11] it most often is observed during secondary recovery techniques.

Secondary recovery of crude oil from an offshore reservoir is an enhanced oil recovery process which involves the injection of pressurized seawater into the reservoir's wellhead in order to displace oil toward a production well.[12] The oil-water mixture is collected in the production well and sent to an oil-water separator, where the oil is extracted for further refinement. The recovered water, now called produced water, is supplemented with additional seawater and re-injected into the reservoir to continue the secondary recovery process. This industrial process increases the crude oil production lifetime of the offshore reservoir compared to that of a reservoir solely relying on natural subterranean pressure for oil recovery. The seawater used in this secondary recovery technique lowers the temperature of the oil reservoir in the area near the injection well. This decrease in temperature creates an optimal environment for the growth of mesophilic microorganisms, such as SRCs.[13] The seawater typically contains 25-30 mM sulfate anions, which provide an abundant electron acceptor for SRC activity and sulfate reduction.[14] The metabolic reduction of sulfate by SRCs increases the sulfide concentrations in the produced water and crude oil.

When the biosoured crude oil and produced water contain high concentrations of sulfide, metal sulfide complexes precipitate and corrode oil reservoir infrastructure, including oil-water

separation units, production wells, and pipelines used to transport oil.[15] These precipitated complexes often lead to facility failures with large associated costs. In addition to the infrastructure costs, H_2S is a toxic gas that leads to poor air quality and human health concerns for personnel working in and around a crude oil reservoir.[16] These regulatory concerns are of extreme relevance to the crude oil industry with respect to worker safety issues and reservoir operating licenses.

The crude oil industry employs a variety of different strategies for controlling biosouring in a reservoir, including both physical and chemical treatments. Sulfide scavengers, including amines or sodium hydroxide, can be incorporated to reduce sulfide concentrations. New reservoir infrastructure can be constructed to capture H_2S gas.[9] One of the most popular traditional biosouring chemical treatments is the incorporation of biocides. Biocides can be injected into oil-separators and production wells in order to reduce the relative abundance of SRCs and remove microbiological deposits from pipelines.[17] These chemical treatments, including glutaraldehyde, formaldehyde, and benzalkonium chloride, are expensive because they typically require continuous injection into the reservoir to be effective.[18] Furthermore, the effectiveness of biocide treatments is maximized near the injection port in the reservoir matrix and decreases with distance from the port.[19] It is therefore extremely difficult to predict the efficacy of these treatment strategies in the mitigation of biosouring.

The most established current approach for biosouring control is the injection of nitrate (NO_3^-) anions into a crude oil reservoir. These anions act as alternate preferential electron acceptors for microbial communities in place of sulfate. The metabolic pathways of nitrate-reducing bacteria (NRB) are thermodynamically favorable when compared to the pathways of analogous sulfate reduction.[20-21] While nitrate injections have been tested in both laboratory and field studies,[20-22] the overall effectiveness is poorly understood. As the concentration of nitrate depletes near the injection well of the reservoir, sulfate reduction may still be active deeper in the oil field.[23] Nitrite, a metabolic intermediate of nitrate reduction, can be toxic to SRCs but is also chemically and biologically labile and has a reduced half-life in a reservoir matrix.[24] These limitations require large nitrate injection concentrations to prevent depletion and to maximize nitrite production. This requirement may not be economically or logistically feasible in a large crude oil reservoir.

Perchlorate injections have been reported as an effective solution to biosouring.[25] Like nitrate reduction, perchlorate reduction is thermodynamically favorable relative to sulfate reduction. Previous studies have demonstrated that perchlorate is specifically inhibitory to sulfate reduction and that dissimilatory perchlorate-reducing bacteria (DPRB) can outcompete SRCs. DPRBs also directly oxidize sulfide to sulfur as a metabolic end product.[26-28]

The importance of microbial biotransformation of crude oil hydrocarbons has been increasingly realized in the context of industrial petroleum production,[29] environmental oil spills,[30] and enhanced oil recovery from subsurface oil reservoirs.[31] Evidence of hydrocarbon biotransformation has previously been observed in metabolite profiling of subsurface oil reservoirs,[31] incubation studies of crude oil with known microbial inocula,[32] and gasoline amended aquifers.[33] Crude oil biodegradation studies typically select lower molecular weight compounds to serve as biotransformation markers, such as $C_4 - C_{10}$ straight-chain alkanes and monoaromatic hydrocarbons, rather than tracking complete suites of hydrocarbon isomers of varying chemical sizes or compound classes.[29, 31-33]

In the specific industrial process of biosouring, little is known as to the extent of biotransformation of labile crude oil hydrocarbons, including substrate consumption and biological product formation, in a sulfate-reducing biosouring environment, a nitrate-reducing

biosouring treatment environment, or a perchlorate-reducing biosouring treatment environment. The objective of this dissertation is to employ novel chromatographic and mass spectrometric analytical techniques to comprehensively characterize changes in a crude oil's chemical composition in each of these three environments and to identify how biotransformation patterns change as a function of hydrocarbon isomeric structure.

1.2 Novel Ionization Sources and Ultrahigh Resolution Mass Spectrometry

Gas chromatographic (GC) techniques are traditionally used in crude oil and fuel analyses to characterize and quantify organic compounds ranging in carbon number (N_C) from C_9-C_{30} with double equivalent chemical class (N_{DBE}) of 0-10,[34] where N_{DBE} for a hydrocarbon is defined as

$$N_{DBE}(C_xH_y)=X - Y/2 + 1 \quad (1)$$

This technique is especially useful for the characterization of refined fuels obtained from crude oil, including gasoline, diesel, and motor oil.[35,36] GC typically couples a volatility separation of the hydrocarbons with a flame ionization detector (FID) or electron ionization mass spectrometer (EI MS). Due to a crude oil's chemical complexity, much of the organic mass co-elutes as an unresolved complex mixture (UCM)[37] in the resulting chromatogram, which complicates mass spectra interpretation and compound identification. EI, a hard ionization technique (~70 eV) achieved by generating electrons from a heated filament in a vacuum chamber, imparts a large excess of energy to organic molecules, resulting in fragmentation that complicates compound identification on a molecular level.[36,37] Two-dimensional gas chromatography with electron ionization mass spectrometry (GC×GC-EI-MS) enhances compound separation and peak capacity by over 10-fold compared to GC-MS.[38-40] The addition of a second polar column in GC×GC-EI-MS allows aromatic compounds of the same volatility as aliphatic compounds to separate in the second dimension of the chromatogram, facilitating the acquisition of cleaner mass spectra and more easily quantifiable peak areas. However, even the most advanced GC×GC separation has its limitations in the characterization of oils and fuels. Aliphatic hydrocarbons are not well-retained on the polar column and contribute to UCM in crude oil even when using GCxGC-EI-MS. It is also difficult to resolve the exponential increase in hydrocarbon constitutional isomers as molecular weight increases,[41] even with high resolution GC×GC-EI-MS, and often only the most concentrated species are quantifiable. It can therefore be challenging to use either GC-EI-MS or GC×GC-EI-MS to achieve a comprehensive quantitative summary of hydrocarbon distributions that considers the contribution of structural isomers based on volatility, polarity, chemical structure, and aromaticity.

Further complicating both GC and GC×GC separation is the fact that at $N_{DBE} \geq 4$, both pure aromatic, pure aliphatic, and heavily alkylated aromatic hydrocarbons are present with the same chemical formulas in crude oil and fuels. It becomes increasingly difficult to separate and quantify how much material is aliphatic versus aromatic as N_C and N_{DBE} increase due to the aforementioned exponential increase in isomers and the similar polarities of heavier aliphatic compounds and heavily alkylated aromatic compounds.

Chapter 2 of this dissertation details the incorporation of GC×GC coupled with tunable synchrotron vacuum ultraviolet photoionization and time-of-flight mass spectrometry (GC×GC-VUV-TOF). The VUV beam at the Advanced Light Source at the Lawrence Berkeley National Laboratory (ALS-LBNL) provides a soft ionization source (8–30 eV) with high photon flux to

reduce hydrocarbon fragmentation and enhance the signal of the molecular ion compared to that of EI. This tunable technique allows complete classes of GC-amendable crude oil hydrocarbons to be integrated, summed, and characterized based on molecular weight, N_C, degree of branching, N_{DBE}, and aromaticity. Four crude oils from different origins (the North Sea, Texas, Azerbaijan, and the Gulf of Mexico) are used to demonstrate the ability of this technique to characterize each oil's distinct chemical composition.

Limitations of the GC-VUV-TOF technique include the fact that it can only characterize organic compounds up to the molecular volatility limit of the GC columns (~320°C) and that polar compounds containing multiple oxygen or nitrogen atoms may not elute through the GC columns.[42] Furthermore, it is challenging to separate and characterize compounds of similar volatilities with similar molecular weights using this technique because the resolution of the TOF instrument is approximately 4000. In order to overcome these chromatographic and mass spectrometric limitations, this work incorporates ultrahigh resolution Fourier transform ion cyclotron resonance mass spectrometry (FT-ICR MS) combined with atmospheric pressure ionization, specifically electrospray ionization (ESI), to selectively characterize polar crude oil components, such as those containing nitrogen or oxygen heteroatoms, without boiling point limitations. This technique routinely achieves resolving power sufficient to separate compounds that differ in mass by less than the mass of an electron in a single mass spectrum ($m/\Delta m_{50\%} \approx$ 1,000,000, in which $\Delta m_{50\%}$ is the mass spectral peak width at half maximum peak height at m/z=500).[43-45] While FT-ICR MS cannot resolve structural isomers or characterize hydrocarbons based on the degree of aromaticity like the GC-VUV-TOF technique can, it can resolve compounds in crude oil up to C_{80} with a N_{DBE} of 30, thereby dramatically expanding the analytical window of resolvable compounds in a biotransformed oil. Further details regarding FT-ICR MS are given in Chapter 3.

In order to overcome the limited access for beamtime to use the GC-VUV-TOF technique at the Advanced Light Source, crude oils were also analyzed via gas chromatography with variable electron ionization time-of-flight mass spectrometry (GC-Select-eV-TOF-MS), which became available in the laboratory during the course of this PhD. This new technique uses the combination of chromatographic resolution and soft electron ionization at 14 eV to minimize hydrocarbon fragmentation to characterize the crude oil's composition in the same manner as the GC-VUV-TOF technique. The ion source of this instrument can be tuned between 10 and 70 eV. It also possesses a tandem ionization capability, where two mass spectra can be obtained simultaneously at two distinct ionization energies. The GC-Select-eV-TOF-MS technique was applied for all the analyses presented in Chapter 4.

1.3 Bioreactor Column Experiments

Chapter 3 details bioreactor column experiments used to study crude oil biotransformations related to biosouring. The experimental setup was designed by Pravin Shrestha, Yi Liu, and Dana Loutey in Professor John Coates's research group. Custom designed glass columns were packed with a slurry of sand and crude oil from a North Sea reservoir. The column conditions, including temperature, flow rate, and geochemistry, were designed to mimic the conditions of the actual reservoir. H_2S was measured as a proxy for SRC activity to determine the extent of biosouring in duplicate columns. Once the columns had significantly soured, pulsed doses of nitrate or perchlorate began in separate duplicate columns. One column was left untreated to maintain the biosouring environment as a control column. Column liquid containing crude oil was periodically

extracted over a 70 day period and analyzed via the aforementioned analytical techniques in order to identify changes, derived from biosouring, in the crude oil's chemical composition. Total microbial community analysis and 16S rRNA genetic sequencing was used to link changes in the crude oil's chemical composition to shifts in the overall microbial community structure of the inocula in the columns.

1.4 Microcosm Bottle Experiments

In order to expand on the experimental results from the bioreactor column studies detailed in Chapter 3, Chapter 4 of this dissertation specifically focuses on biotransformation patterns of lower molecular weight hydrocarbons from different crude oils. The experimental setup was designed by Pravin Shrestha, Yi Liu, and Anchal Mehra in Professor John Coates's research group. Oils from four different crude oil fields, studied in extensive analytical detail in Chapter 2, were combined with autoclaved seawater from the San Francisco Bay in separate anaerobic microcosm bottles. They were inoculated with the same complex strain of sulfate-reducing microbial enrichments obtained from the bioreactor column study. A microbiologically active environment was established for 20 weeks in order to further understand how hydrocarbon structure affects biodegradation.

1.5 References

(1) Marshall, A. G.; Rodgers, R. P. Petroleomics: the next grand challenge for chemical analysis. *Acc. Chem. Res*, **2004**, *37*, (1), 53–59.

(2) Marshall, A. G.; Rodgers, R. P. Petroleomics: chemistry of the underworld. *Proc. Natl. Acad. Sci.* **2008**, *105*, (47), 18090-18095.

(3) Colati, K. A. P.; Dalmaschio, G. P.; de Castro, E. V. R.; Gomes, A. O.; Vaz, B. G.; Romão, W. Monitoring the liquid/liquid extraction of naphthenic acids in brazilian crude oil using electrospray ionization FT-ICR mass spectrometry (ESI FT-ICR MS). *Fuel*. **2013**, *108*, 647-655.

(4) Chen, H.; Hou, A.; Corilo, Y. E.; Lin, Q.; Lu, J.; Mendelssohn, I. A.; Zhang, R.; Rodgers, R.P.; McKenna, A.M. 4 years after the Deepwater Horizon Spill: Molecular transformation of Macondo well oil in Louisiana salt marsh sediments revealed by FT-ICR mass spectrometry. *Environ. Sci. Tech.* **2016**, *50*, (17), 9061-9069.

(5) Ruddy, B. M.; Huettel, M.; Kostka, J. E.; Lobodin, V. V.; Bythell, B. J.; McKenna, A. M.; Aeppli, C.; Reddy, C. M.; Nelson, R. K.; Marshall, A. G.; Rodgers, R. P. Targeted petroleomics: analytical investigation of Macondo well oil oxidation products from Pensacola Beach. *Energy Fuels*. **2014**, *28*, (6), 4043-4050.

(6) Drozd, G. T.; Worton, D. R.; Aeppli, C.; Reddy, C. M.; Zhang, H.; Variano, E.; Goldstein, A. G. Modeling comprehensive chemical composition of weathered oil following a marine spill to predict ozone and potential secondary aerosol formation and constraint transport pathways. *J. Geophys. Res. Oceans.* **2015**, *120*, (11), 7300-7315.

(7) Worton, D.; Zhang, H.; Isaacman, G.; Chan, A.; Wilson, K.; Goldstein, A. Comprehensive Chemical Characterization of Hydrocarbons in NIST Standard Reference Material 2779 Gulf of Mexico Crude Oil. *Environ. Sci. Tech.* **2015**, *49*, (22), 13130-13138.

(8) Wang, Z.; Fingas, M. Differentiation of the source of spilled oil and monitoring of the oil weathering process using gas chromatography-mass spectrometry. *Journal of Chromatography A*. **1995**, 712 (2), 321− 343.

(9) Gieg, L. M.; Jack, T. R.; Foght, J. M. Biological souring and mitigation in oil reservoirs. *Applied Microbiology and Biotechnology*. **2011**, *92* (2), 263-282.

(10) Liamleam, W.; Annachhatre, A. P. Electron donors for biological sulfate reduction. *Biotechnology Advances.* **2007**, *25*, (5), 452-463.

(11) Agrawal, A.; Vanbroekhoven, K.; Lal, B. Diversity of culturable sulfidogenic bacteria in two oil-water separation tanks in the north-eastern oil fields of India. *Anaerobe.* **2010**, *16*, (1), 12-18.

(12) Youssef, N.; Elshahed, M. S.; McInerney, M. J. Microbial processes in oil fields: culprits, problems, and opportunities. *Advances in Applied Microbiology*. **2009**, *66*, 141-251.

(13) Greene, E. A.; Hubert, C.; Nemati, M.; Jenneman, G. E.; Voordouw, G. Nitrite reductase activity of sulphate-reducing bacteria prevents their inhibition by nitrate-reducing, sulphide-oxidizing bacteria. *Environmental microbiology*. **2003**, *5* (7), 607-617.

(14) Tang, K.; Baskaran, V.; Nemati, M. Bacteria of the sulphur cycle: An overview of microbiology, biokinetics and their role in petroleum and mining industries. *Biochemical Engineering Journal*. **2009**, *44*, 73-94.

(15) Williamson, N. Chapter 18: Health and safety issues from the production of hydrogen sulphide. *Applied Microbiology and Molecular Biology of Oilfield Systems*. **2008**, *13*, 151-157.

(16) Hubbard, C. G.; Cheng, Y.; Engelbrektson, A.; Druhan, J. L.; Li, L.; Ajo-Franklin, J. B.; Coates, J. D.; Conrad, M.E. Isotopic insights into microbial sulfur cycling in oil reservoirs. *Frontiers in Microbiology.* **2014**. *5*, 1-12.

(17) Smart, J. S.; Smith, G, L.; Pigging and chemical treatment for oil and gas pipelines. *Corrosion Prevention and Control***. 1992**, *31* (1), 47-50.

(18) Videla, H. A.; Herrera, L. K. Microbiologically infused corrosion: looking to the future. *International Microbiology*. **2005**, *8*, (3), 169-180.

(19) Lavania, M.; Sarma, P. M.; Mandal, A. K.; Cheema, S.; Lal, B. Efficacy of natural biocide on control of microbial induced corrosion in oil pipelines mediated by *Desulfovibrio vulgaris* and *Desulfovibrio gigas*. *Journal of Environmental Sciences*. **2011**, *23*, (8), 1394-1402.

(20) Voordouw, G.; Grigoryan, A.A.; Lambo, A.; Lin, S.P.; Park, H.S.; Jack, T.R.; Coombe, D.; Clay, B.; Zhang, F.; Ertmoed, R.; Miner, K.; Arensdorf, J.J. Sulfide remediation by pulsed injection of nitrate into a low temperature Canadian heavy oil reservoir. *Environmental Science & Technology*. **2009**, *43* (24), 9512-9518.

(21) Callbeck, C.M.; Agrawal, A.; Voordouw, G. Acetate production from oil under sulfate-reducing conditions in bioreactors injected with sulfate and nitrate. *Appl Environ Microbiol*. **2013**, *79* (16), 5059-5068.

(22) Grigoryan, A.A.; Cornish, S.L.; Buziak, B.; Lin, S.; Cavallaro, A.; Arensdorf, J.J.; Voordouw, G. Competitive oxidation of volatile fatty acids by sulfate- and nitrate-reducing bacteria from an oil field in Argentina. *Appl. Environ. Microbiol.* **2008**, *74* (14), 4324-4335.

(23) Callbeck, C.; Dong, X.; Chatterjee, I.; Agrawal, A.; Caffrey, S.; Sensen, C. Microbial community succession in a bioreactor modeling a souring low-temperature oil reservoir subjected to nitrate injection. *Appl. Microbiol. Biotechnol*. **2001**, *91* (3), 799–810.

(24) Hubert, C.; Nemati, M.; Jenneman, G.; Voordouw, G. Containment of biogenic sulfide production in continuous up-flow packed-bed bioreactors with nitrate or nitrite. *Biotech. Prog.* **2003**, *19* (2), 338-345.

(25) Engelbrektson, A.; Hubbard, C. G.; Tom, L. M.; Boussina, A.; Jin, Y. T.; Wong, H.; Piceno, Y. M.; Carlson H. K.; Conrad, M. E.; Anderson, G.; Coates, J. D. Inhibition of microbial sulfate reduction in a flow-through column system by (per)chlorarte treatment. *Frontiers in Microbiology*. **2014**, *5*, 1-11.

(26) Baeuerle, P. A.; Huttner, W. B. Chlorate—a potent inhibitor of protein sulfation in intact cells. *Biochem. Biophys. Res. Commun*. **1986**, *141* (2), 870–877.

(27) Coates, J. D.; Achenbach, L. Microbial perchlorate reduction: rocket-fueled metabolism. A. *Nat. Rev. Microbiol*. **2004**, *2* (7), 569–580.

(28) Gregoire, P.; Engelbrektson, A.; Hubbard, C. G.; Metlagel, Z.; Csencsits. R.; Auer, M. Control of sulfideogenesis through bio-oxidation of H_2S coupled to (per)chlorate reduction. *Environ. Microbiol*. **2014**, *6* (16), 558-564.

(29) Gieg, L. M.; Davidova, I. A.; Duncan, K. E.; Suflita, J. M. Methanogenesis, sulfate reduction and crude oil biodegradation in hot Alaskan oilfields. *Environmental Microbiology*. **2010**, *12* (11), 3074-3086.

(30) Drozd, G. T.; Worton, D. R.; Aeppli, C.; Reddy, C. M.; Zhang, H.; Variano, E.; Goldstein, A. G. Modeling comprehensive chemical composition of weathered oil following a marine spill to predict ozone and potential secondary aerosol formation and constraint transport pathways. *J. Geophys. Res. Oceans.* **2015**, *120*, (11), 7300-7315.

(31) Aitken, C. M.; Jones, D. M.; Larter, S. R. Anaerobic hydrocarbon biodegradation in deep subsurface oil reservoirs. *Nature*. **2004**, *431* (7006), 291-294.

(32) Townsend, G. T.; Prince, R. C.; Suflita, J. M. Anaerobic oxidation of crude oil hydrocarbons by the resident microorganisms of a contaminated anoxic aquifer. *Environ. Sci. Technol*. **2003**, *37* (22), 5213–5218.

(33) Townsend, G. T.; Prince, R. C.; Suflita, J. M. Anaerobic biodegradation of alicyclic constituents of gasoline and natural gas condensate by bacteria from an anoxic aquifer. *FEMS Microbiology Ecology*. **2004**, *49* (1), 129–135.

(34) McLafferty, F. W.; Turecek, F., *Interpretation of Mass Spectra, 4th ed.* University Science Books: Mill Valley, CA, 1993.

(35) Fingas, M. *Handbook of Oil Spill Science and Technology*. **2015**.

(36) Reddy, C. M.; Quinn, J. G. GC-MS analysis of total petroleum hydrocarbons and polycyclic aromatic hydrocarbons in seawater samples after the north cape oil spill. *Marine Pollution Bulletin*. **1999**, *38*, 126-135.

(37) White, H. K.; Xu, L.; Hartmann, P.; Quinn, J. G.; Reddy, C. M. Unresolved complex mixture (UCM) in coastal environments is derived from fossil sources. *Environ. Sci. Technol*. **2013**, *47*, 726-731.

(38) Liu, Z. Y.; Phillips, J. B. Comprehensive 2-dimensional gas chromatography using an on column thermal modulator interface. *Journal of Chromatographic Science*, **1991**, 29, (6), 227-231.

(39) Nelson, R. K.; Kile, B. S.; Plata, D. L.; Sylva, S. P.; Xu, L.; Reddy, C. M.; Gaines, R. B.; Frysinger, G. S.; Reichenbach, S. E. Tracking the weathering of an oil spill with comprehensive two-dimensional gas chromatography. *Environmental Forensics*. **2006**, *7*, (1), 33-44.

(40) Gros, J.; Reddy, C. M.; Aeppli, C.; Nelson, R. K., Carmichael, C. A.; Arey, J. S. Resolving biodegradation patterns of persistent saturated hydrocarbons in weathered oil samples from the Deepwater Horizon disaster. *Environ. Sci. Tech.* **2014**, *48*, (3), 1628-1637.

(41) Goldstein, A. H.; Galbally, I. E. Known and unexplored organic constituents in the earth's atmosphere. *Environ. Sci. Technol*. **2007**, 41, (5), 1514−1521.

(42) Isaacman, G.; Wilson, K.; Chan, A.; Worton, D.; Kimmel, J.; Nah, T.; Hohaus, T.; Gonin, M.; Kroll, J. H.; Worsnop, D. R.; Goldstein, A. H. Improved resolution of hydrocarbon structures and constitutional isomers in complex mixtures using gas chromatography-vacuum ultraviolet-mass spectrometry. *Anal. Chem*. **2012**, *84* (5), 2335−2342.

(43) Marshall, A. G.; Hendrickson, C. L.; Jackson, G. S. Fourier transform ion cyclotron resonance mass spectrometry: a primer. *Mass Spectrom. Rev.* **1998**, *17* (1), 1-35.

(44) McKenna, A. M.; Williams, J. T.; Putman, J. C.; Aeppli, C. Reddy, C. M.; Valentine, D. L.; Lemkau, K. L.; Kellermann, M. Y.; Savory, J. J.; Kaiser, N. K.; Marhsall, A. G.; Rodgers, R. P. Unprecedented ultrahigh resolution FT-ICR mass spectrometry and parts-per-billion mass accuracy enable direct characterization of nickel and vanadyl porphyrins in petroleum from natural seeps. *Energy Fuels*. **2014**, *28* (4), 2454-2464.

(45) Kaiser, N.; Savory, J.; McKenna, A.; Quinn, J.; Hendrickson, C. L. Electrically compensated fourier transform ion cyclotron resonance cell for complex mixture mass analysis. *Anal. Chem*. **2011**, *83* (17), 6907−6910.

Chapter 2

Quantification of isomerically summed hydrocarbon contributions to crude oil by carbon number, double bond equivalent, and aromaticity using gas chromatography with tunable vacuum ultraviolet ionization

This chapter is adapted from:

Jeremy A. Nowak, Robert J. Weber, Allen H. Goldstein
"Quantification of isomerically summed hydrocarbon contributions to crude oil by carbon number, double bond equivalent, and aromaticity using gas chromatography with tunable vacuum ultraviolet ionization"
The Analyst, **2018**, 143, 1396-1405

2.1 Abstract

The ability to structurally characterize and isomerically quantify crude oil hydrocarbons relevant to refined fuels such as motor oil, diesel, and gasoline represents an extreme challenge for chromatographic and mass spectrometric techniques. This chapter incorporates two-dimensional gas chromatography coupled to a tunable vacuum ultraviolet soft photoionization source, the Chemical Dynamics Beamline 9.0.2 of the Advanced Light Source at the Lawrence Berkeley National Laboratory, with a time-of-flight mass spectrometer (GCxGC-VUV-TOF) to directly characterize and isomerically sum the contributions of aromatic and aliphatic species to hydrocarbon classes of four crude oils. When the VUV beam is tuned to 10.5 ± 0.2 eV, both aromatic and aliphatic crude oil hydrocarbons are ionized to reveal the complete chemical abundance of C_9-C_{30} hydrocarbons. When the VUV beam is tuned to 9.0 ± 0.2 eV only aromatic hydrocarbons are ionized, allowing separation of the aliphatic and aromatic fractions of the crude oil hydrocarbon chemical classes in an efficient manner while maintaining isomeric quantification. This technique provides an effective tool to determine the isomerically summed aromatic and aliphatic hydrocarbon compositions of crude oil, providing information that goes beyond typical GC x GC separations of the most dominant hydrocarbon isomers.

2.2 Introduction

Crude oil is a complex mixture containing tens of thousands of distinct organic species,[1,2] dominated primarily by hydrocarbons (~90%).[3] The composition of a crude oil varies depending on its origin and degree of weathering,[4,5] as hydrocarbons become photooxidized, biodegraded, or subjected to abiotic environmental processes. While the range of crude oil hydrocarbons has been observed up to C_{80} with a double bond equivalent (N_{DBE})[6] chemical class up to 30,[2] refined fuels such as diesel, gasoline, and motor oil mostly consist of hydrocarbons below C_{30} in a N_{DBE} range of 0-10.[7-9] Hydrocarbons in these refined fuels increase in aromatic and aliphatic compound complexity as the carbon number (N_C) and the potential number of isomers of the compound both increase, particularly as $N_C \geq 9$. This dissertation chapter focuses on the characterization of those

C_9-C_{30} hydrocarbons of crude oils pertaining to the aforementioned refined fuels that are amendable to separation in the GC system.

There have been many chromatographic and mass spectrometric advancements to characterize both crude oils and their fuel derivatives as a function of hydrocarbon content. Liquid chromatographic (LC) separations distinguish resins, aromatic compounds, saturated compounds, and acidic compounds in crude oil,[10,11] but are insufficient for separating compounds of increased alkylation in a higher boiling range. LC also does not isomerically quantify compounds of a specific N_C[9,10] and the analysis processes are often time-consuming and prone to sample loss.

Ultrahigh resolution Fourier transform ion cyclotron mass spectrometry (FT-ICR MS) allows the identification of unique elemental compositions in crude oil between C_{10}-C_{80} and N_{DBE}=0-30.[1,2,4,5] FT-ICR MS analysis of crude oil is typically performed using electrospray ionization (ESI), which targets polar compounds,[5,12] or atmospheric pressure photoionization (APPI), which targets nonpolar compounds and sulfur containing species.[13] While these soft ionization methods retain molecular ions necessary for molecular formula identification, they have difficulty ionizing pure hydrocarbons without significant ion suppression or reduced ionization efficiency. Even when pure hydrocarbons are ionized in FT-ICR MS,[12] this technique is unable to offer structural characterizations of hydrocarbons or differentiate hydrocarbon isomers in a single N_{DBE} chemical class at a particular N_C. Attempts at combining ion mobility/mass spectrometry (IM/MS) with FT-ICR MS have provided limited isomeric separation of predominantly heteroatom containing crude oil components rather than separation of pure hydrocarbons.[14,15] Furthermore, FT-ICR MS relies on characterizing molecular formulas in terms of relative abundances in a mass spectrum rather than quantifying them based on mass fractions of a particular N_C or N_{DBE}.[1,2,4,5]

Gas chromatographic (GC) techniques are traditionally used in gasoline, diesel, and motor oil analyses when there is no necessity to characterize compounds up to C_{80} and N_{DBE}=30, as these heavier non-GC amendable species are rarely found in the aforementioned fuels.[7-9] Traditional GC techniques are often limited to amendable hydrocarbons up to C_{30}, due to the temperature limitations of columns and transfer lines (~320^{o}C). GC typically couples a volatility separation of the hydrocarbons with a flame ionization detector (FID) or electron ionization mass spectrometer (EI MS).[16,17] Due to the crude oil's or fuel's chemical complexity, much of the organic mass co-elutes as an unresolved complex mixture (UCM) in the resulting chromatogram,[18] which complicates mass spectra interpretation and compound identification. EI, a hard ionization technique (~70 eV), imparts a large excess of energy to organic molecules, resulting in fragmentation that complicates compound identification on a molecular level.[16-18] GC has been combined with FT-ICR MS,[19] but EI fragmented compounds >155 amu, making molecular identification of heavier compounds difficult. GC has also been previously combined with atmospheric pressure chemical ionization (APCI) and FT-ICR MS,[20] but the results illustrated limited isomeric separation of hydrocarbons with the same elemental composition and retention time as well as limited characterization of structural contributions to a particular N_{DBE} class of one N_C.

Two-dimensional gas chromatography with electron ionization mass spectrometry (GCxGC-EI-MS) enhances compound separation and peak capacity by over 10-fold compared to GC-MS.[21-23] The addition of a second polar column in GCxGC-EI-MS allows aromatic compounds of the same volatility as aliphatic compounds to separate in the second dimension of the chromatogram, facilitating the acquisition of cleaner mass spectra and more easily quantifiable peak areas. However, even the most advanced GCxGC separation has its limitations in the

characterization of oils and fuels. As the number of carbon atoms in molecules increases, the number of possible hydrocarbon constitutional isomers becomes exponentially larger (>10^3 isomers of alkanes with N_C=15 and >10^5 isomers of alkanes with N_C=20),[24] making it difficult to resolve these individual species even with high resolution GCxGC-EI-MS. While cycloalkanes and alkylbenzenes are more easily identifiable in the second dimension of a GCxGC chromatogram than they are in a chromatogram using traditional GC-MS with EI, only the most concentrated species are quantifiable and it remains difficult to quantify the total range of isomers of a hydrocarbon class. It can therefore be challenging to use GCxGC-EI-MS to achieve a comprehensive quantitative summary of hydrocarbon distributions that takes into account the contribution of structural isomers based on volatility, polarity, and chemical structure.

Further complicating advanced GCxGC separation is the fact that at $N_{DBE} \geq 4$, both pure aromatic, pure aliphatic, and heavily alkylated aromatic hydrocarbons are present with the same chemical formulas in crude oil and fuels. It becomes increasingly difficult to separate and quantify how much material is aliphatic versus aromatic as N_C and N_{DBE} increase due to the aforementioned exponential increase in isomers and the similar polarities of heavier aliphatic compounds and heavily alkylated aromatic compounds.[25]

In order to quantify both the isomeric hydrocarbon content and the aromatic distributions of crude oil hydrocarbons relevant to refined fuels, this chapter incorporates GCxGC coupled with tunable synchrotron vacuum ultraviolet photoionization and time-of-flight mass spectrometry (GCxGC-VUV-TOF).[25,26] The VUV beam at the Advanced Light Source at the Lawrence Berkeley National Laboratory provides a soft ionization source (8-30 eV, less than the 70 eV ionization energy of typical "hard" electron ionization) with high photon flux (~10^{16} photons/s)[25] to reduce hydrocarbon fragmentation and enhance the signal of the molecular ion compared to that of EI. This technique allows complete classes of GC-amendable hydrocarbons to be integrated, summed, and characterized based on molecular weight, N_C, degree of branching, and N_{DBE},[25,26] which is represented for only hydrocarbons in this chapter by

$$N_{DBE}(C_xH_y)=X-Y/2+1 \quad (1)$$

Unlike other soft photoionization methods combined with GC that rely on a rare gas excimer lamp to ionize petroleum alkanes at only one ionization energy,[27,28,] the VUV beam can be tuned to different photoionization energies. While previous studies have also incorporated tunable synchrotron VUV photoionization mass spectrometry to analyze heavy oils and aromatic crude oil hydrocarbons,[29-31] those investigations did not combine chromatographic resolution with soft ionization to isomerically sum both aliphatic and aromatic hydrocarbon fractions of those C_9-C_{30} compounds relevant to fuels. This investigation combines GCxGC-MS with tunable synchrotron VUV photoionization energies to determine the N_C dependent and isomerically summed aromatic and aliphatic fractions, as a function of mass loading, of GC-amendable hydrocarbons of four crude oils from different locations. VUV radiation at 10.5 eV was chosen as the ionization energy to ionize all aliphatic and aromatic hydrocarbons, thereby simultaneously maximizing the signal from the molecular ion needed for quantification and minimizing signal interferents from fragment ions. Ionization energies greater than 10.5 eV result in greater compound fragmentation and reduced molecular ion signal, making it more difficult to accurately and isomerically sum both the aromatic and aliphatic hydrocarbon fractions. VUV radiation at 9.0 eV ionizes aromatic species without significantly ionizing aliphatic hydrocarbons,[32] which allows the molecular ion signal of aromatic hydrocarbons to be maximized while minimizing both fragmentation of aromatic hydrocarbons and interfering ions from aliphatic compounds. Aromatic fractions, representing those compounds that contain at least one aromatic functional group, of

isomerically summed hydrocarbon molecular formulas can then be determined based on the response ratios of hydrocarbon signals obtained at 9.0 eV versus 10.5 eV ionization energy ($R_{9.0/10.5}$). This tunable soft ionization method allows immediate quantification, isomeric summarization, and aromatic characterization of those crude oil hydrocarbons relevant to refined fuels. The ability to efficiently quantify and distinguish isomerically summed aliphatic from aromatic fractions of one hydrocarbon mass and N_{DBE} is useful to characterize crude oil hydrocarbons for environmental modeling, fingerprinting of the hydrocarbon component of fuels for industrial applications, examining environmental weathering pathways, and understanding the impacts of oil spills in the environment.[34]

2.3 Experimental Section

2.3.1 Oil Samples

Crude oil samples were obtained from four sources: the North Sea, the Gulf of Mexico, Texas, and Azerbaijan. The oils were dissolved in chloroform (HPLC grade, Sigma-Aldrich, St. Louis, MO, USA) prior to analysis. Densities were determined by weighing a known volume of the original crude oil (Mettler AB104 analytical balance, Toledo, Columbus, OH, USA). API gravities (in degrees) of the oils were calculated using the equation below, where SG is the specific gravity of crude oil:

$$\text{API Gravity} = 141.5/\text{SG} - 131.5 \quad (2)$$

2.3.2 GCxGC-VUV-TOF

Oil dissolved in chloroform was directly injected, without prior fractionation or chromatographic separation, via a septumless head into a liquid nitrogen cooled inlet (-40°C) with a fused silica liner (CIS4, Gerstel Inc, Linthicum, MD, USA). The sample was transferred to the gas chromatograph (GC, Agilent 7890, Santa Clara, CA, USA) by heating the liner to 320°C at 10°C/s. Analytes were separated based on volatility using a nonpolar column (60 m x 0.25 mm x 0.25 um Rxi-5Sil-MS; Restek, Bellefonte, PA, USA) followed by polarity using a medium-polarity second dimension column (1 m x 0.25 mm x 0.25 um Rtx-200MS; Restek, Bellefonte, PA, USA), with a helium gas flow rate of 2 mL/min. A dual-stage thermal modulator (Zoex, Houston, TX, USA) consisting of a guard column (1 m x 0.25 mm Rxi; Restek, Bellefonte, PA, USA) cryogenically focused the first column effluent and rapidly heated the analyte every 2.4 s via a 400 ms hot jet pulse into the second column. The GC program began at 40°C, ramped at 3.5°C/minute to 320°C, and was held isothermal for a final 10 minutes. These temperatures provide an upper limit of amendable hydrocarbons of C_{30}. The second column was placed in a secondary oven maintained 15°C above the main oven temperature. This system created an orthogonal separation of the analyte based on volatility in the 1st-dimension and polarity in the 2nd-dimension.

The analyte from the second column was transferred from the GC to a 170°C ion source via a 270°C transfer line. These temperatures reduce the thermal energy imparted to the hydrocarbons and subsequently reduce compound fragmentation.[25,26] Analytes were ionized with 10.5 ± 0.2 eV or 9.0 ± 0.2 eV VUV photoionization with a photon flux of ~10^{16} photons/s and detected using a time-of-flight mass spectrometer (TOF, Tofwerk, Thun, Switzerland) with $m/\Delta m_{50\%} \approx 4000$. The VUV beam was from the Chemical Dynamics Beamline 9.0.2 of the Advanced Light Source at the Lawrence Berkeley National Laboratory. Mass spectra were

collected at 100 Hz and data processing was performed using custom code written in Igor 6.3.7 (Wavemetrics).[26] To correct for thermal transfer efficiency of high- and low-volatility analytes through the GC column, a series of perdeuterated alkanes (Sigma-Aldrich, St. Louis, MO, USA) from C_{10}-C_{30} were used as an internal standard in 10.5 eV analyses to establish a relationship between transfer efficiency and retention time. Perdeuterated polycyclic aromatic hydrocarbons (PAHs) (Sigma-Aldrich, St. Louis, MO, USA) were used to correct for thermal transfer efficiency in the 9.0 eV analyses (when alkane ionization is negligible).

2.3.3 Data Visualization for Isomeric Summarization

Supplemental Figure 2.1a illustrates a chromatogram of molecular ion mass versus first dimension retention time of the Gulf of Mexico oil obtained using GCxGC-VUV-TOF at 10.5 eV ionization energy. In this figure the second-dimension separation is not visible. Increasing molecular mass is observed as the GC retention time increases, as is to be expected with heavier compounds of decreasing volatility. Supplemental Figure 2.1b illustrates the mass spectrum as a function of chromatographic retention time for the isomers of hydrocarbons with 20 carbon atoms in the Gulf of Mexico oil, showing their classification by mass and N_{DBE} under 10.5 eV VUV ionization. N_{DBE}=0 represents alkanes and N_{DBE}=6 represents a mixture of hexacycloalkanes and aromatic species. PAHs of $N_{DBE} \geq 7$ were also observed, but are not shown in Supplemental Figure 2.1b for simplicity. The volatility separation based on retention time successfully distinguishes aliphatic compounds and PAHs of equal molecular mass. Additionally, hydrocarbon volatility of N_{DBE}=0 compounds increases with branching of the straight-chain alkane, therefore branched isomers elute earlier in the chromatogram than the straight-chain hydrocarbon.[7] The enhancement of the molecular ion under VUV ionization, combined with chromatographic separation by volatility, distinguishes the branched isomers from the straight-chain alkane of the same N_C. Supplemental Figure 2.1c demonstrates this concept by showing the single ion chromatogram (SIC) of pentadecane (m/Q=212, $C_{15}H_{32}$) of the Gulf of Mexico oil, where the straight-chain alkane and its branched isomers are clearly distinguished.

In addition to retaining molecular ions necessary for hydrocarbon classification and quantification, Supplemental Figure 2.2 illustrates the advantages of GCxGC-VUV-TOF over traditional GCxGC-EI-MS. Supplemental Figures 2.2a and 2.2b illustrate the complete GCxGC-EI-TOF chromatogram at 70 eV ionization energy and the complete GCxGC-VUV-TOF chromatogram at 10.5 eV ionization energy, respectively, of mass versus first dimension retention time of the Gulf of Mexico oil. While the isomers of heavier molecular weight and lower volatility compounds are observable and quantifiable at 10.5 eV, they are not quantifiable at 70 eV. Fragmentation of hydrocarbon isomers is also increased in the chromatogram at 70 eV, as illustrated by the increase in signal between m/Q=100-200. Supplemental Figure 2.2c further illustrates the advantages of GCxGC-VUV-TOF over traditional GCxGC-EI-MS by depicting m/Q=326 ($C_{24}H_{38}$ N_{DBE}=6) hydrocarbon isomers using the two techniques. In the GCxGC-EI-MS total ion chromatogram in Supplemental Figure 2.2c, only a few most concentrated isomers are identifiable as individual peaks corresponding to peaks in the single ion GCxGC-VUV-MS chromatogram of m/Q=326. Most of the signal for $C_{24}H_{38}$ is from the extremely large number of unresolved isomers eluting between 55 and 70 minutes, which are not separable using GCxGC-EI-MS. It is extremely difficult to separate or resolve the numerous isomers present at much lower concentrations (>10^5 isomers could be present with N_C=20).[24] It is difficult, time consuming, and perhaps impossible to isomerically separate and quantify all of these hydrocarbons, especially as

N_C further increases, to achieve complete chemical characterization of a compound class. GCxGC-VUV-TOF represents these $C_{24}H_{38}$ compounds in Supplemental Figure 2.2c as a single chromatographic trace using the molecular ion. By integrating across the trace and summing the signal of the complete range of isomers of a particular hydrocarbon molecular ion, we achieve the ability to quantify the complete mass of these isomers. This methodology extends across all GC-amendable molecular weights and compound classes, allowing to isomerically sum compounds more easily and to a greater analytical extent than even in the most advanced GCxGC-EI-MS separation.

2.3.4 Differences in chromatograms at 9.0 eV and 10.5 eV

All aliphatic and aromatic compounds are ionized using GCxGC-VUV-TOF with 10.5 eV VUV energy to reveal the chemical composition of crude oil hydrocarbons from C_9-C_{30} with N_{DBE}=0-10. Under 9.0 eV ionization energy, only the aromatic species are ionized. Figure 2.1 shows the mass spectrum as a function of chromatographic retention time for the isomers of hydrocarbons with 20 carbons atoms (C_{20}) in the Gulf of Mexico oil, showing their classification by mass and N_{DBE} under 10.5 and 9.0 eV VUV ionization (2.1a and 2.1b, respectively). All N_{DBE}=0-10 hydrocarbons are ionized in the 10.5 eV chromatogram, while only N_{DBE}=4-6 aromatic compounds and PAHs (N_{DBE}=7-10, not shown here for simplicity) are ionized in the 9.0 eV chromatogram. There is some detection of aliphatic compounds at 9.0 eV, but the ionization efficiency is <5% of that at 10.5 eV and is therefore considered negligible in these analyses. Supplemental Figure 2.3 shows two-dimensional chromatograms of a known standard hydrocarbon mixture to further illustrate the use of tunable VUV ionization to selectively ionize hydrocarbons depending on molecular structure.

2.3.5 Calculating N_C-Dependent Aromatic Fractions of N_{DBE} Classes

In this dissertation, aromatic fraction is defined as the fraction of isomers of a hydrocarbon molecular formula, based on N_C and N_{DBE}, that contain an aromatic functional group. An aromatic fraction of 1 represents isomerically summed species that contain no aliphatic character, such as methyl naphthalenes or anthracene. We assumed that compounds of N_{DBE}=4 with fewer than 14 carbon atoms are entirely aromatic (aromatic fraction=1). As the aromatic fraction decreases from 1, aliphatic contributions to an isomerically summed compound increase in the form of alkyl side chains or pure cycloalkanes. Isomers of a hydrocarbon molecular formula with an aromatic fraction <1 therefore can consist of pure aromatic compounds, aliphatic compounds, mixtures of compounds containing fused aromatic and cyclic rings, etc. An aromatic fraction of 0 represents an isomerically summed molecular formula that contains no aromaticity, and therefore consists entirely of alkanes, including branched alkanes and cycloalkanes.

The response ratio of hydrocarbon signals obtained by integrating across a molecular formula at 9.0 eV versus 10.5 eV ionization energy ($R_{9.0/10.5}$) is indicative of the aromatic fraction in a specific N_{DBE} as a function of N_C. It should be noted that $R_{9.0/10.5} \neq 1$ even if all isomers of a molecular formula are completely aromatic. For instance, $C_{10}H_{14}$ represents isomers of alkylated benzenes with ten carbon atoms. While a combination of double bonded cyclic compounds could theoretically possess a chemical formula of $C_{10}H_{14}$, the likelihood of finding such compounds in crude oils or refined fuels is low, as they do not generally contain alkenes.[7,35] $R_{9.0/10.5}$ of these $C_{10}H_{14}$ alkylated benzenes is still less than 1 due to the decreased photoionization efficiencies of

aromatic hydrocarbons at 9.0 versus 10.5 eV ionization energies.[33] As the length of the alkyl side chain group in heavier N_{DBE}=4-6 compounds increases, there is an increasing trend in ionization energy that leads to a lower response at 9.0 eV and thus a lower $R_{9.0/10.5}$.[32,33] Therefore, there is a N_C dependence in $R_{9.0/10.5}$ for alkylated aromatic compounds.

To calibrate for $R_{9.0/10.5}$ of the hydrocarbons as a function of N_C and N_{DBE} in the oils, authentic standards (Sigma-Aldrich, St. Louis, MO, USA), including alkanes, branched alkanes, cycloalkanes, alkylbenzenes, hopanes, steranes, PAHs, and alkylated PAHs were analyzed at 9.0 eV and 10.5 eV. The ratio of these hydrocarbon signals is referred to as $R_{standard}$. Figure 2.2 shows $R_{9.0/10.5}$ for a standard mixture of hydrocarbons consisting of the aforementioned species. Compounds with $N_{DBE} < 4$ in this standard mixture are not aromatic and have a $R_{9.0/10.5} < 0.05$, corroborating the fact that the photoionization probability of aliphatic compounds is extremely low at 9.0 eV. $R_{9.0/10.5}$ for alkylbenzenes decreases with increasing N_C and becomes indistinguishable from $R_{9.0/10.5}$ for tetracyclic steranes above C_{25}. PAHs have a $R_{9.0/10.5}$ of 0.45-0.50 independent of molecular weight. To estimate the response ratios between 9.0 eV and 10.5 eV energies for purely aliphatic components of N_{DBE}=4, 5, and 6 ($R_{aliphatic}$), the trend in response ratios observed in the N_{DBE}=0, 1, 2, and 3 classes, which cannot include aromatic rings, is extrapolated. Using the N_C dependent values for the aromatic and aliphatic hydrocarbon signal responses, the aromatic fraction of an isomerically summed molecular formula is calculated as

$$\text{Aromatic Fraction}=[R_{9.0/10.5}-R_{aliphatic}]/(R_{standard}) \quad (3)$$

When N_C in an isomerically summed N_{DBE}=4 molecular formula exceeds 25, the aromatic hydrocarbon isomers have a similar $R_{9.0/10.5}$ to that of tetracyclic steranes and therefore the aromatic fraction cannot be discerned by this method.

2.4 Results and Discussion

2.4.1 Crude Oil Chemical Composition

The calculated densities and API gravities of the four crude oils are given in Table 2.1. Based on the API gravities, the Azerbaijan and Texas oils are classified as light and the Gulf of Mexico and North Sea oils are medium-heavy. All four oils were initially analyzed using GCxGC-VUV-TOF with 10.5 eV photoionization energy. Figure 2.3 illustrates the distribution of each oil's GC-amendable isomerically summed hydrocarbon mass fractions (measured in milligram per kilogram injected oil) as a function of both N_C and N_{DBE}. ~60-65% of the measured mass fractions of the hydrocarbons in the Texas and Azerbaijan oils are between the C_9-C_{19} hydrocarbons. The mass fraction distributions of the hydrocarbons in the North Sea and Gulf of Mexico oils are similar, with ~50% of the mass fractions split between C_9-C_{19} and C_{20}-C_{30} species. The Texas and Azerbaijan oils contain ~70% of the total measured hydrocarbon mass fraction within completely aliphatic compound classes, N_{DBE}=0-3. Only ~60% of the total measured hydrocarbon mass fractions of the North Sea and Gulf of Mexico oils belongs to N_{DBE}=0-3.

GCxGC-VUV-TOF at 10.5 eV ionization energy also provides separation of crude oil alkanes based on their degree of branching. Alkanes can be classified by retention time based on the degree of branching B_X, where x represents the number of alkyl branches from methyl (B1) to hexamethyl (B6). For simplicity, each branch is assumed to represent a methyl group, rather than ethyl, propyl, etc. Supplemental Figure 2.4 illustrates the isomerically summed mass fractions of

the branched alkanes in each of the oils as a function of N_C and degree of branching (B1-B6). B1 branched alkanes dominate the branched alkanes in the Texas oil. The branched signatures of both the Gulf of Mexico and North Sea oils exhibit similar mass distributions, corroborating the similarities in the hydrocarbon compositions of these two oils seen in Figure 2.1. The Azerbaijan oil has a similar branched alkane distribution to that of the North Sea and Gulf of Mexico oils, but the Azerbaijan oil contains substantially higher mass fractions of B4-B6 branched alkanes between C_{19}-C_{30}.

2.4.2 Response Ratios at 9.0 eV and 10.5 eV Ionization Energies

Supplemental Figures 2.5, 2.6, and 2.7 display overlayed SICs with arbitrary units of intensity at 9.0 eV and 10.5 eV ionization energies for $C_{18}H_{30}$ (N_{DBE}=4), $C_{20}H_{32}$ (N_{DBE}=5), and $C_{20}H_{30}$ (N_{DBE}=6), respectively, for all four oils. The signal peaks that are present in the 10.5 eV SICs, but not in the 9.0 eV SICs, represent aliphatic isomers that are not ionized at 9.0 eV. $R_{9.0/10.5}$ of the integrated signal of the summed isomers of N_{DBE}=4, 5, and 6 hydrocarbons was calculated for each oil and plotted as a function of N_C in Supplemental Figure 2.8. $R_{9.0/10.5}$ decreases with increasing molecular weight independent of an oil's source, indicating that aliphatic contributions in the form of alkyl groups, cyclic rings, etc. to these isomerically summed compound classes increase with N_C.

As previously discussed and illustrated, traditional GCxGC-EI-MS separates aliphatic and aromatic compounds based on both volatility and polarity, but the exponential increase in the number of constitutional isomers as N_C increases makes quantification of the whole chemical class by N_C and N_{DBE} challenging and time-consuming. Only concentrated compounds are identifiable and quantifiable in GCxGC space as N_C increases, therefore it becomes increasingly difficult to isomerically sum and distinguish aliphatic compounds from aromatic compounds as molecular weight increases. In order to test this structural separation method based on ionization energies, Table 2.2 displays the ratio of aromatic components to the total aromatic plus aliphatic components of nine isomerically summed hydrocarbon molecular formulas in the North Sea oil, spanning a range of molecular weights. This ratio was calculated using the second-dimension separation of GCxGC-EI-MS and tunable GCxGC-VUV-TOF. As N_C grows from N_C=16 to N_C=24 in N_{DBE}=4, 5, and 6, it becomes difficult to separate and quantify isomers of a given hydrocarbon. The calculated ratios using the GCxGC-EI-MS separation differ from those calculated using tunable GCxGC-VUV-TOF by ~35-65% as N_C increases. This comparison of experimental techniques illustrates the increased fraction of isomers which are not measured using GCxGC-EI-MS as the oil's chemical complexity increases. The mass closure afforded by summing the isomers of hydrocarbons of higher molecular weights, as well as the structural separations afforded by the tunable ionization energies, present tunable GCxGC-VUV-TOF as an analytical tool that can efficiently and quantitatively characterize sums of hydrocarbon isomers found in crude oil to a greater extent than GCxGC-EI-MS separation can alone.

2.4.3 N_{DBE}=7-10 Response Ratios

At 10.5 eV, the SICs of molecular weights pertaining to N_{DBE}=8 hydrocarbons contain fragments of larger aliphatic hydrocarbons, making it difficult to discern the total pure N_{DBE}=8 hydrocarbon content in the GCxGC-VUV-TOF chromatogram. Supplemental Figure 2.9 illustrates this concept using the SIC of m/Q=196 ($C_{15}H_{16}$ N_{DBE}=8) at 10.5 eV. Portions of the

chromatographic trace align with retention times of heavier straight-chain and branched alkanes. The $C_{15}H_{16}$ molecular mass also corresponds with fragment ions from alkanes such as $C_{17}H_{36}$ and $C_{20}H_{42}$, following the loss of hydrogens and alkyl groups. Therefore at 10.5 eV, the chromatographic trace of $C_{15}H_{16}$ includes signal from $C_{15}H_{16}$ isomers and aliphatic fragments of higher molecular weight species. At 9.0 eV, these aliphatic compounds are not ionized and the interference from fragment ions is negligible. While the 9.0 eV data can detect the total aromatic contribution to a N_{DBE}=8 molecular formula, an aromatic fraction of this isomerically summed molecular formula cannot be calculated due to the interfering fragment ions in the 10.5 eV signal.

Figure 2.4b further illustrates this concept by overlaying the Gulf of Mexico oil's $C_{15}H_{16}$ (N_{DBE}=8) SICs (with arbitrary units of intensity) at both 10.5 eV and 9.0 eV ionization energies. Branched aliphatic hydrocarbons fragment more than straight-chain aliphatic compounds, thus the larger fragments in the 10.5 eV trace in Figure 2.4b correspond to fragments of branched compounds of a higher molecular weight whose retention times overlap with those of the lower molecular weight $C_{15}H_{16}$ isomers. At 9.0 eV, the aliphatic compounds are not ionized and the N_{DBE}=8 SIC consists purely of aromatic hydrocarbons with no observable interferences from fragmentation. This observation was consistent in all molecular formulas pertaining to N_{DBE}=8 hydrocarbons in all four oils.

Figures 2.4a, 2.4c, and 2.4d display the overlapping 9.0 eV and 10.5 eV SICs (with arbitrary units of intensity) for $C_{15}H_{18}$ (N_{DBE}=7), $C_{15}H_{14}$ (N_{DBE}=9), and $C_{15}H_{12}$ (N_{DBE}=10) of the Gulf of Mexico oil. Unlike in the SIC of $C_{15}H_{16}$ at 10.5 eV, there were no observable interferences from fragmentation of heavier aliphatic compounds in these PAH SICs at 10.5 eV and $R_{9.0/10.5}$ values could be estimated. This observation was consistent in all molecular formulas pertaining to N_{DBE}=7, 9, and 10 compounds in all four oils. Supplementary Figure 2.10 shows $R_{9.0/10.5}$ of the integrated signal of the summed isomers of N_{DBE}=7, 9, and 10 compounds for all four oils as a function of N_C. All of the oils have a $R_{9.0/10.5}$ of ~0.4-0.6 in the aforementioned compound classes independent of N_C. There is no decrease in $R_{9.0/10.5}$ as was observed in the N_{DBE}=4, 5, and 6 $R_{9.0/10.5}$, implying that N_{DBE}=7, 9, and 10 hydrocarbons in these oils consist of pure PAHs with minimal aliphatic isomers.

2.4.4 Aromatic Fraction Calculations

The measured $R_{9.0/10.5}$ of N_{DBE}=4, 5, and 6 hydrocarbons, along with $R_{aliphatic}$ and $R_{standard}$, is used to calculate the N_C-dependent isomerically summed aromatic fraction of each N_{DBE} in each oil using Equation 3.

Figures 2.5a-2.5c present the isomerically summed aromatic fractions of N_{DBE}=4, 5, and 6 hydrocarbons of each oil as a function of N_C. The Gulf of Mexico oil contains the largest fraction of isomerically summed aromatic hydrocarbons of the four oils used across all N_C in N_{DBE}=4-6. This oil contains ~1.5-2.0 times higher fractions of isomerically summed aromatic material across the N_{DBE}=4, 5, and 6 compound classes when compared to those of the other three oils. The Azerbaijan oil has the lowest isomerically summed aromatic fraction in the N_{DBE}=4 class, while the Texas oil has a ~1.5-2.0 times higher isomerically summed aromatic fraction than that of the North Sea oil in the C_{15}-C_{25} range of N_{DBE}=4. The North Sea, Texas, and Azerbaijan oils all possess similar isomerically summed aromatic fractions at N_{DBE}=5 across all N_C. At N_{DBE}=6, the isomerically summed aromatic fraction from C_{15}-C_{25} in the North Sea oil is ~1.3-1.6 times that of the Texas and Azerbaijan oils, revealing that the North Sea oil is structurally similar to the Gulf of

Mexico oil in the N_{DBE}=6 class and consists of more aromatic material than the Texas and Azerbaijan oils in the N_{DBE}=6 class.

This chapter shows that as molecular weight increases in N_{DBE}=4-6 classes, the fraction of isomers of a hydrocarbon molecular formula that are purely aromatic decreases. This pattern implies that hydrocarbon structures consisting of benzenes or alkylated benzenes decrease in concentration as N_C grows across N_{DBE}=4-6, and structures consisting of fused cyclic rings increase in concentration in the same scenario. It can therefore be concluded from this chapter that in N_{DBE}=4-6, isomerically summed heavier hydrocarbons are more likely to consist of fused cyclic rings and cycloalkanes than pure alkylated benzenes or a combination of aromatic functional groups and cyclic rings. Therefore, aliphatic contributions to the N_{DBE}=4-6 compound classes in all of these oils become more prevalent as molecular weight increases across one isomerically summed compound class.

2.5 Conclusions

Tunable soft VUV photoionization coupled to GCxGC-MS offers a fast, efficient, and unique analytical technique to further characterize and quantify the chemical complexity of crude oil hydrocarbons in the molecular range relevant to refined fuels such as gasoline, diesel, and motor oil beyond that of traditional GCxGC-EI-MS separation. Soft ionization at 10.5 eV allows the full range of isomeric hydrocarbons to be summed as a function of N_C, N_{DBE} chemical class, and the degree of branching. By altering the energy of the VUV beam between 10.5 eV and 9.0 eV, hydrocarbon isomers with $N_{DBE} \geq 4$ are successfully ionized into aliphatic and aromatic fractions as a function of N_C while maintaining the ability to isomerically sum mass fractions. This chapter provides a novel chromatographic and mass spectrometric tool to constrain and strengthen existing models of crude oil hydrocarbon characterization with applications to oil spills, microbial transformations, and environmental impacts. Tunable soft ionization is a powerful analytical tool which can be applied to isomerically sum and further characterize crude oil hydrocarbons beyond that of traditional compound class and carbon number labels.

2.6 Acknowledgments

The authors acknowledge the Energy Biosciences Institute (EBI) for funding this work under project 86217. The authors also acknowledge Kevin Wilson and Bruce Rude for their assistance at the Chemical Dynamics Beamline 9.0.2 at the Advanced Light Source, Coty Jen for GCxGC-VUV-TOF instrumental setup and transport, and Professor John Coates for access to the oils and advice.

2.7 References

(1) Marshall, A. G.; Rodgers, R. P. Petroleomics: the next grand challenge for chemical analysis. *Acc. Chem. Res*, **2004**, *37*, (1), 53–59.

(2) Marshall, A. G.; Rodgers, R. P. Petroleomics: chemistry of the underworld. *Proc. Natl. Acad. Sci.* **2008**, *105*, (47), 18090-18095.

(3) Colati, K. A. P.; Dalmaschio, G. P.; de Castro, E. V. R.; Gomes, A. O.; Vaz, B. G.; Romão, W. Monitoring the liquid/liquid extraction of naphthenic acids in brazilian crude oil using electrospray ionization FT-ICR mass spectrometry (ESI FT-ICR MS). *Fuel*. **2013**, *108*, 647-655.

(4) Chen, H.; Hou, A.; Corilo, Y. E.; Lin, Q.; Lu, J.; Mendelssohn, I. A.; Zhang, R.; Rodgers, R.P.; McKenna, A.M. 4 years after the Deepwater Horizon Spill: Molecular transformation of Macondo well oil in Louisiana salt marsh sediments revealed by FT-ICR mass spectrometry. *Environ. Sci. Tech.* **2016**, *50*, (17), 9061-9069.

(5) Ruddy, B. M.; Huettel, M.; Kostka, J. E.; Lobodin, V. V.; Bythell, B. J.; McKenna, A. M.; Aeppli, C.; Reddy, C. M.; Nelson, R. K.; Marshall, A. G.; Rodgers, R. P. Targeted petroleomics: analytical investigation of Macondo well oil oxidation products from Pensacola Beach. *Energy Fuels*. **2014**, *28*, (6), 4043-4050.

(6) McLafferty, F. W.; Turecek, F., *Interpretation of Mass Spectra, 4th ed.* University Science Books: Mill Valley, CA, 1993.

(7) Worton, D. R.; Isaacman, G.; Gentner, D. R.; Dallmann, T. R.; Chan, A. W. H.; Ruehl, C.; Kirchstetter, T. W.; Wilson, K. R.; Harley, R. A.; Goldstein, A. H. Lubricating oil dominates primary organic aerosol emissions from motor vehicles. *Environ. Sci. Tech.* **2014**, *48*, (7), 3698-3706.

(8) Prince, R. C.; Parkerton, R. P.; Lee, C. The primary aerobic biodegradation of gasoline hydrocarbons. *Environ. Sci. Tech.* **2007**, *41*, 3316-3321.

(9) Adam, F.; Bertoncini, F.; Thiébaut, D.; Esnault, S.; Espinat, D.; Hennion, M. C. Towards comprehensive hydrocarbons analysis of middle distillates by LC-GCxGC. *Journal of Chromatographic Science*. **2007**, *45*, 643-649.

(10) Demirbas, A.; Taylan, O. Removing of resins from crude oils. *Petrol. Sci. Tech.* **2016**, *34*, 771-777.

(11) Islas-Flores, C. A.; Buenrostro-Gonzalez, E.; Lira-Galeana, C. Fractionation of Petroleum Resins by Normal and Reverse Phase Liquid Chromatography. *Fuel*. **2006**, *85*, (12), 1842-1850.

(12) Lobodin, V. V.; Juyal, P.; McKenna, A. M.; Rodgers, R. P.; Marshall, A. G. Tetramethylammonium hydroxide as a reagent for complex mixture analysis by negative ion electrospray ionization mass spectrometry. *Anal. Chem.* **2013,** *85* (16), 7803-7808.

(13) McKenna, A. M.; Williams, J. T.; Putman, J. C.; Aeppli, C. Reddy, C. M.; Valentine, D. L.; Lemkau, K. L.; Kellermann, M. Y.; Savory, J. J.; Kaiser, N. K.; Marhsall, A. G.; Rodgers, R. P. Unprecedented ultrahigh resolution FT-ICR mass spectrometry and parts-per-billion mass accuracy enable direct characterization of nickel and vanadyl porphyrins in petroleum from natural seeps. *Energy & Fuels*. **2014**, *28* (4), 2454-2464.

(14) Fernandez-Lima, F. A.; Becker, C.; McKenna, A. M.; Rodgers, R. P.; Marshall, A. G.; Russell, D. H. Petroleum crude oil characterization by IMS-MS and FTICR MS. *Anal. Chem*. **2009,** *81*, 9441-9947.

(15) Farenc, M.; Corilo, Y. E.; Lalli, P. M.; Riches, E.; Rodgers, R. P.; Afonso, C.; Giusti, P. Comparison of atmospheric pressure ionization for the analysis of heavy petroleum fractions with ion mobility-mass spectrometry. *Energy & Fuels*. **2016**, *30*, 8896-8903.

(16) Wang, Z.; Fingas, M. Differentiation of the source of spilled oil and monitoring of the oil weathering process using gas chromatography-mass spectrometry. *Journal of Chromatography A*. **1995**, 712 (2), 321− 343.

(17) Reddy, C. M.; Quinn, J. G. GC-MS analysis of total petroleum hydrocarbons and polycyclic aromatic hydrocarbons in seawater samples after the *North Cape* oil spill. *Marine Pollution Bulletin*. **1999**, *38*, (2), 126-135.

(18) White, H. K.; Xu, L.; Hartmann, P.; Quinn, J. G.; Reddy, C. M. Unresolved complex mixture (UCM) in coastal environments is derived from fossil sources. *Environ. Sci. Technol*. **2013**, *47*, 726-731.

(19) Szulejko, J. E.; Solouki, T. Potential Analytical Applications of Interfacing a GC to an FT-ICR MS: Fingerprinting complex sample matrixes. *Anal. Chem*. **2002,** *74*, 3434-3442.

(20) Barrow, M. P.; Peru, K. M.; Headley, J. V. An added dimension: GC atmospheric chemical ionization FTICR MS and the Athabasca oil sands. *Anal. Chem*. **2014,** *86*, 8281-8288.

(21) Liu, Z. Y.; Phillips, J. B. Comprehensive 2-dimensional gas chromatography using an on column thermal modulator interface. *Journal of Chromatographic Science*, **1991**, 29, (6), 227-231.

(22) Nelson, R. K.; Kile, B. S.; Plata, D. L.; Sylva, S. P.; Xu, L.; Reddy, C. M.; Gaines, R. B.; Frysinger, G. S.; Reichenbach, S. E. Tracking the weathering of an oil spill with comprehensive two-dimensional gas chromatography. *Environmental Forensics*. **2006**, *7*, (1), 33-44.

(23) Gros, J.; Reddy, C. M.; Aeppli, C.; Nelson, R. K., Carmichael, C. A.; Arey, J. S. Resolving biodegradation patterns of persistent saturated hydrocarbons in weathered oil samples from the Deepwater Horizon disaster. *Environ. Sci. Tech.* **2014**, *48*, (3), 1628-1637.

(24) Goldstein, A. H.; Galbally, I. E. Known and unexplored organic constituents in the earth's atmosphere. *Environ. Sci. Technol*. **2007**, 41, (5), 1514−1521.

(25) Isaacman, G.; Wilson, K.; Chan, A.; Worton, D.; Kimmel, J.; Nah, T.; Hohaus, T.; Gonin, M.; Kroll, J. H.; Worsnop, D. R.; Goldstein, A. H. Improved Resolution of Hydrocarbon Structures and Constitutional Isomers in Complex Mixtures Using Gas Chromatography-Vacuum Ultraviolet-Mass Spectrometry. *Anal. Chem*. **2012**, *84*, (5), 2335− 2342.

(26) Worton, D.; Zhang, H.; Isaacman, G.; Chan, A.; Wilson, K.; Goldstein, A. Comprehensive Chemical Characterization of Hydrocarbons in NIST Standard Reference Material 2779 Gulf of Mexico Crude Oil. *Environ. Sci. Tech.* **2015**, *49*, (22), 13130-13138.

(27) Geibler, R.; Saraji-Bozorgzad, M.; Streibel, T.; Kaisersberger, E.; Denner, T.; Zimmermann, R. Investigation of different crude oils applying thermal analysis/mass spectrometry with soft photoionization. *J. Therm. Anal. Calorim.* **2009**, *96*, 813-820.

(28) Wohlfahrt, S.; Fischer, M.; Saraji-Bozorgzad, M.; Matuschek, G.; Streibel, T.; Post, E.; Denner, T.; Zimmermann, R. Rapid comprehensive characterization of crude oils by thermogravimetry coupled to fast modulated gas chromatography-single photon ionization time-of-flight mass spectrometry. *Anal. Bioanal. Chem.* **2013**, *405*, 7107-7116.

(29) Chen, J.; Jia, L.; Zhao, L.; Lu, X.; Guo, W.; Weng, J.; Qi, F. Analysis of Petroleum Aromatics by Laser-Induced Acoustic Desorption/Tunable Synchrotron Vacuum Ultraviolet Photoionization Mass Spectrometry. *Energy & Fuels*. **2013**, *27*, 2010-2017.

(30) Guo, W.; Bi, Y.; Guo, H.; Pan, Y.; Qi, F.; Deng, W.; Shan, H. Infrared laser desorption /vacuum ultraviolet photoionization mass spectrometry of petroleum saturates: a new experimental approach for the analysis of heavy oils. *Rapid Commun. Mass Spectrom.* **2008**, *22*, 4025–4028.

(31) Jia, L.; Weng, J.; Zhou, Z.; Qi, F.; Guo, W.; Zhao, L.; Chen, J. Note: Laser-induced acoustic desorption/synchrotron vacuum ultraviolet photoionization mass spectrometry for analysis of fragile compounds and heavy oils. *Rev. Sci. Instrum.* **2012**, *83*, 026105.

(32) Adam, T.; Zimmermann, R. Determination of single photon ionization cross sections for quantitative analysis of complex organic mixtures. *Anal. Bioanal. Chem.* **2007**, *389*, (6), 1941-1951.

(33) NIST Chemistry WebBook, NIST Standard Reference Database Number 69 (http://webbook.nist.gov/).

(34) Drozd, G. T.; Worton, D. R.; Aeppli, C.; Reddy, C. M.; Zhang, H.; Variano, E.; Goldstein, A. G. Modeling comprehensive chemical composition of weathered oil following a marine spill to predict ozone and potential secondary aerosol formation and constraint transport pathways. *J. Geophys. Res. Oceans.* **2015**, *120*, (11), 7300-7315.

(35) Mao, D.; Van De Weghe, H.; Lookman, R.; Vanermen, G.; De Brucker, N.; Diels, L. Resolving the unresolved complex mixture in motor oils using high-performance liquid chromatography followed by comprehensive two-dimensional gas chromatography. *Fuel*. **2009**, *88*, (2), 312−318.

2.8 Tables and Figures

Table 2.1. Densities and API gravities of the Gulf of Mexico, North Sea, Azerbaijan, and Texas oils.

	Density (g cm^{-3})	API Gravity (degrees)
Gulf of Mexico Oil	~0.92	~22.0
North Sea Oil	~0.91	~22.5
Azerbaijan Oil	~0.85	~35.0
Texas Oil	~0.83	~40.0

Table 2.2. Ratio of aromatic components to total aromatic plus aliphatic components (± standard deviations) of isomerically summed hydrocarbon molecular formulas in the North Sea oil measured by traditional GCxGC-EI-MS versus by tunable GCxGC-VUV-TOF. Hydrocarbons containing 16, 20, or 24 carbon atoms and double bond equivalents of 4, 5, and 6, which could contain either 1 or 0 aromatic rings, are included to illustrate the increased fraction of isomers which are not measured using EI-MS as the chemical complexity increases.

	Ratio Aromatic: Total EI-MS	Ratio Aromatic: Total Tunable VUV
$C_{16}H_{26}$ (N_{DBE}=4)	0.29 ± 0.04	0.27 ± 0.06
$C_{16}H_{24}$ (N_{DBE}=5)	0.48 ± 0.07	0.46 ± 0.05
$C_{16}H_{22}$ (N_{DBE}=6)	0.50 ± 0.03	0.48 ± 0.02
$C_{20}H_{34}$ (N_{DBE}=4)	0.11 ± 0.08	0.16 ± 0.04
$C_{20}H_{32}$ (N_{DBE}=5)	0.21 ± 0.04	0.31 ± 0.08
$C_{20}H_{30}$ (N_{DBE}=6)	0.23 ± 0.06	0.39 ± 0.03
$C_{24}H_{42}$ (N_{DBE}=4)	0.08 ± 0.02	0.13 ± 0.01
$C_{24}H_{40}$ (N_{DBE}=5)	0.17 ± 0.08	0.25 ± 0.02
$C_{24}H_{38}$ (N_{DBE}=6)	0.11 ± 0.05	0.31 ± 0.02

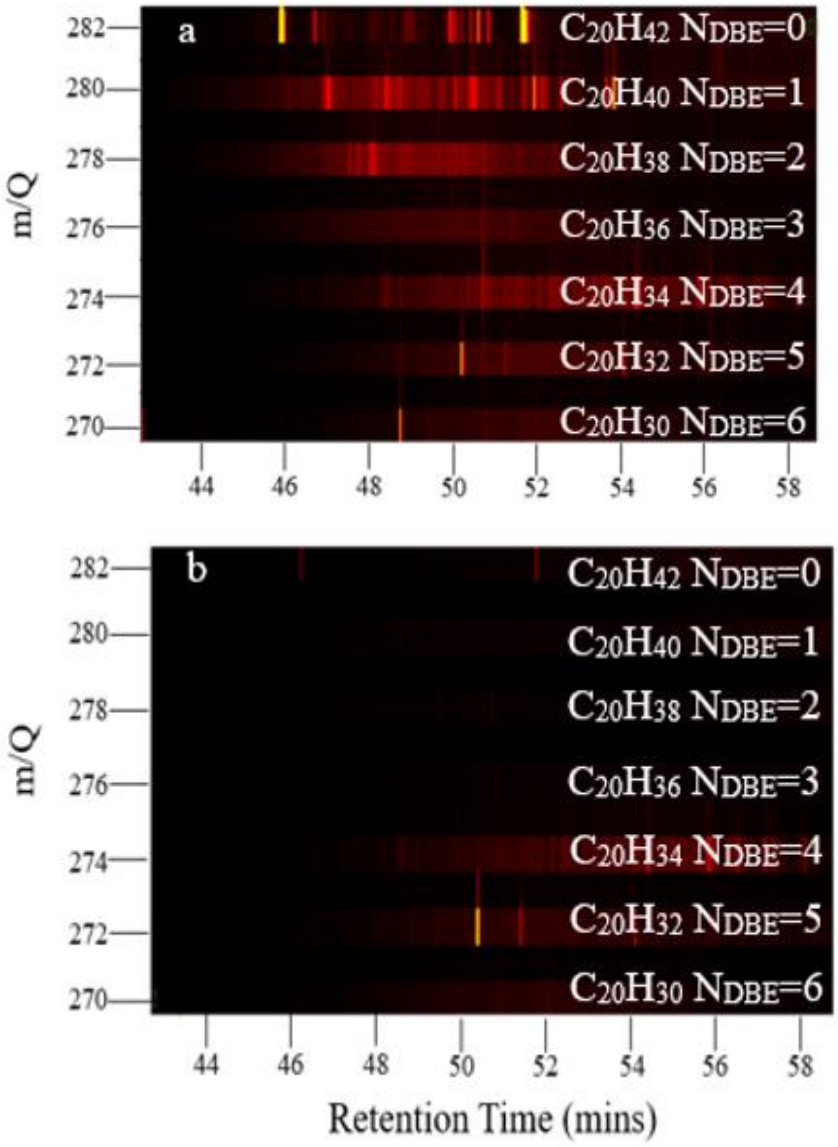

Figure 2.1. Mass spectrum as a function of chromatographic retention time for the isomers of hydrocarbons with 20 carbon atoms (C_{20}) in the Gulf of Mexico Oil, showing their classification by mass and corresponding double bond equivalents (N_{DBE}) under (a) 10.5 and (b) 9.0 eV VUV ionization.

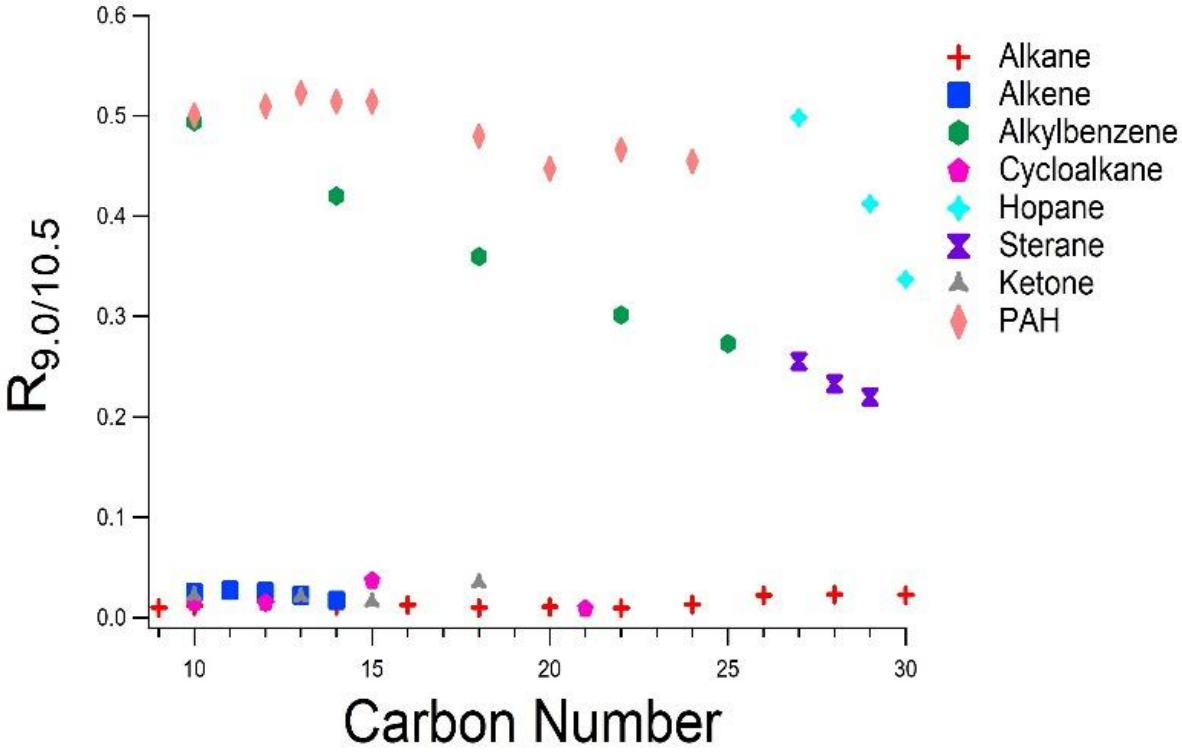

Figure 2.2. Ratio of hydrocarbon signal responses at 9.0 and 10.5 eV ionization energies ($R_{9.0/10.5}$) for a standard mixture of hydrocarbons, including alkanes, alkenes, cycloalkanes, ketones, hopanes, steranes, alkylbenzenes, and polycyclic aromatic hydrocarbons (PAHs).

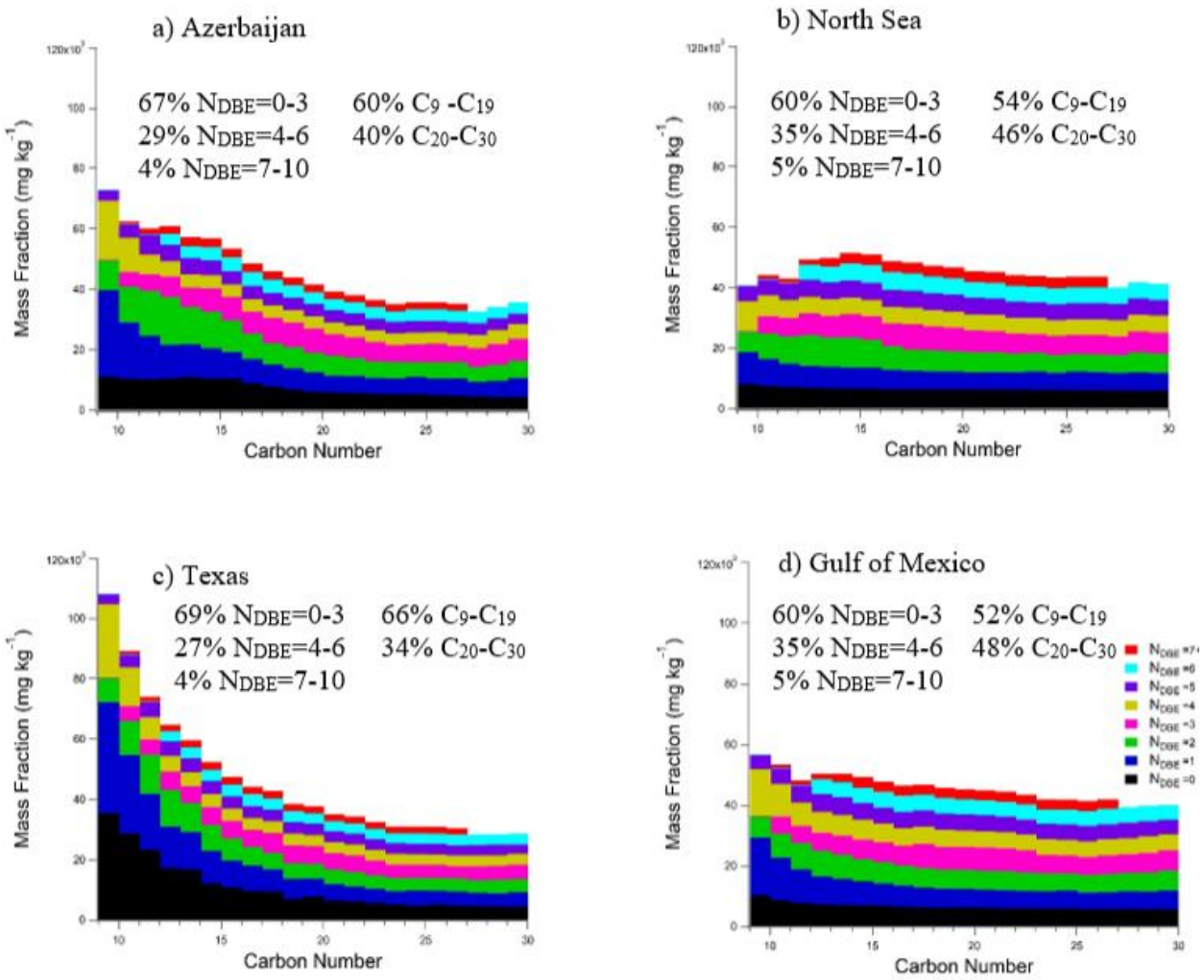

Figure 2.3. Distribution of GC-amendable isomerically summed hydrocarbon mass fractions as a function of both the number of carbon atoms and double bond equivalents (N_{DBE}) for oils from a) Azerbaijan, b) North Sea, c) Texas, and d) Gulf of Mexico.

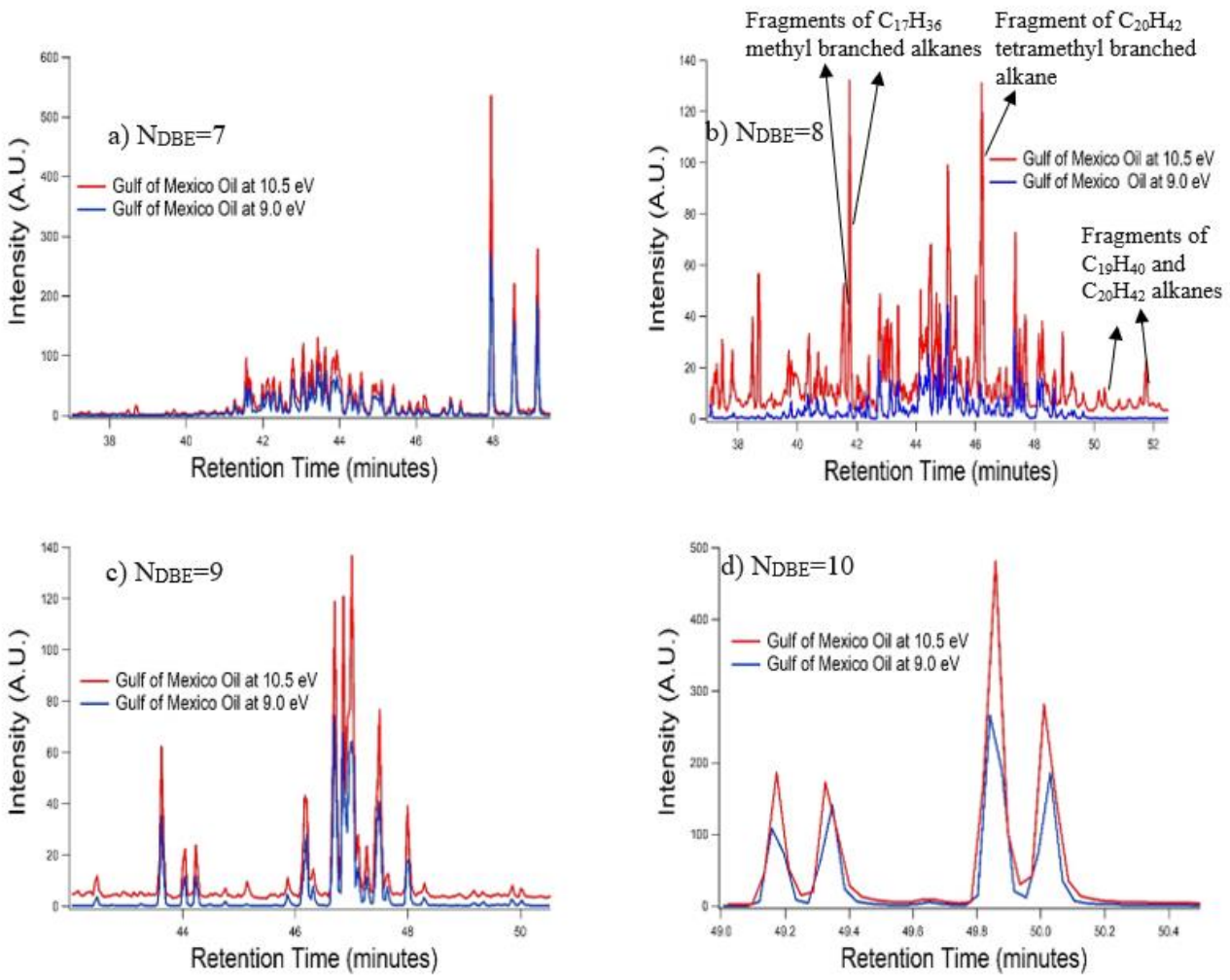

Figure 2.4. Single ion chromatograms (SICs) with arbitrary units of intensity (A.U.) of Gulf of Mexico oil for a) $C_{15}H_{18}$ (N_{DBE}=7), b) $C_{15}H_{16}$ (N_{DBE}=8), c) $C_{15}H_{14}$ (N_{DBE}=9), and d) $C_{15}H_{12}$ (N_{DBE}=10) at both 10.5 and 9.0 eV ionization energies. The $C_{15}H_{16}$ N_{DBE}=8 SIC at 10.5 eV includes signal from $C_{15}H_{16}$ isomers and aliphatic fragments of higher molecular weight species (e.g. $C_{17}H_{36}$, $C_{19}H_{40}$, $C_{20}H_{42}$) with overlapping retention times. The N_{DBE}=7, 9, and 10 SICs at 10.5 eV contain no observable interferences from fragmentation.

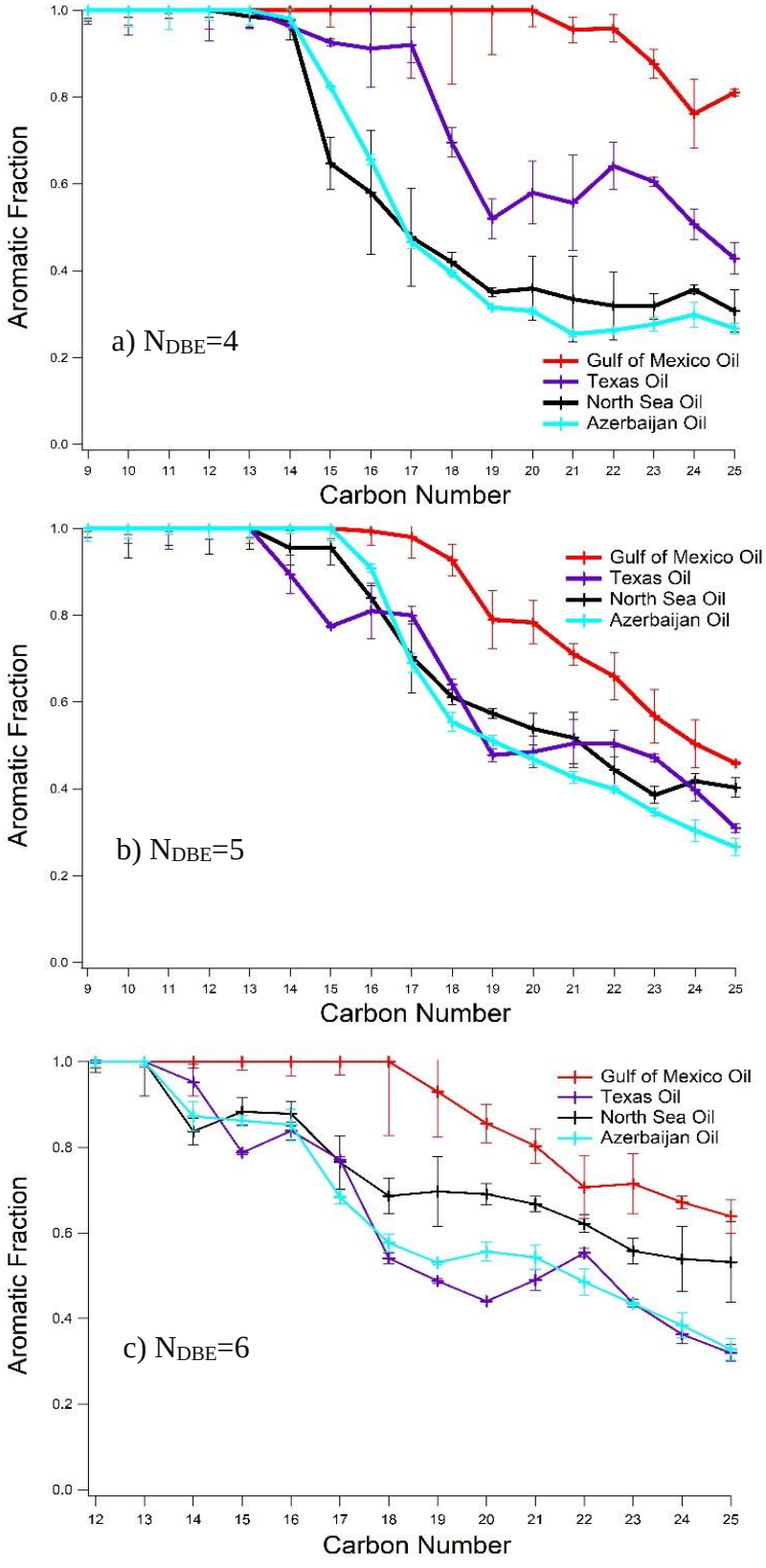

Figure 2.5. Aromatic mass fractions as a function of carbon number for the four oils, indicated by color, in three classes of double bond equivalents: N_{DBE}=4, 5, and 6 (a, b, and c, respectively).

2.9 Supplemental Information

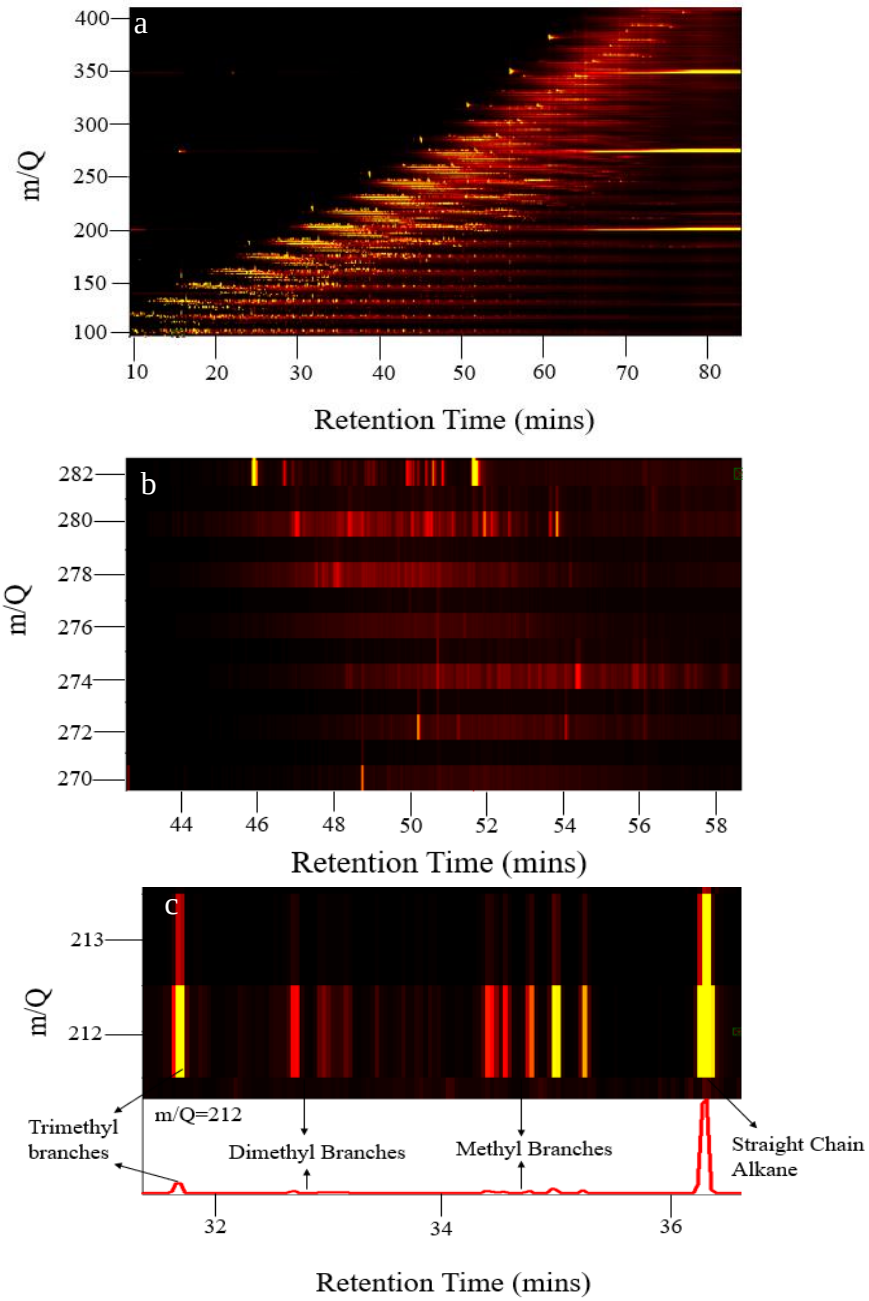

Supplemental Figure 2.1. (a) Complete GCxGC-VUV-TOF chromatogram at 10.5 eV ionization energy of molecular ion mass versus first dimension retention time of the Gulf of Mexico oil. (b) Mass spectrum as a function of chromatographic retention time for the isomers of hydrocarbons with 20 carbon atoms in the Gulf of Mexico oil, showing their classification by mass and N_{DBE} under 10.5 eV VUV ionization. N_{DBE}=0 represents alkanes and N_{DBE}=6 represents a mixture of hexacycloalkanes and aromatic species. (c) Single ion chromatogram (SIC) of pentadecane (m/Q=212, $C_{15}H_{32}$) of the Gulf of Mexico oil, where the straight-chain alkane and its branched isomers are clearly distinguished.

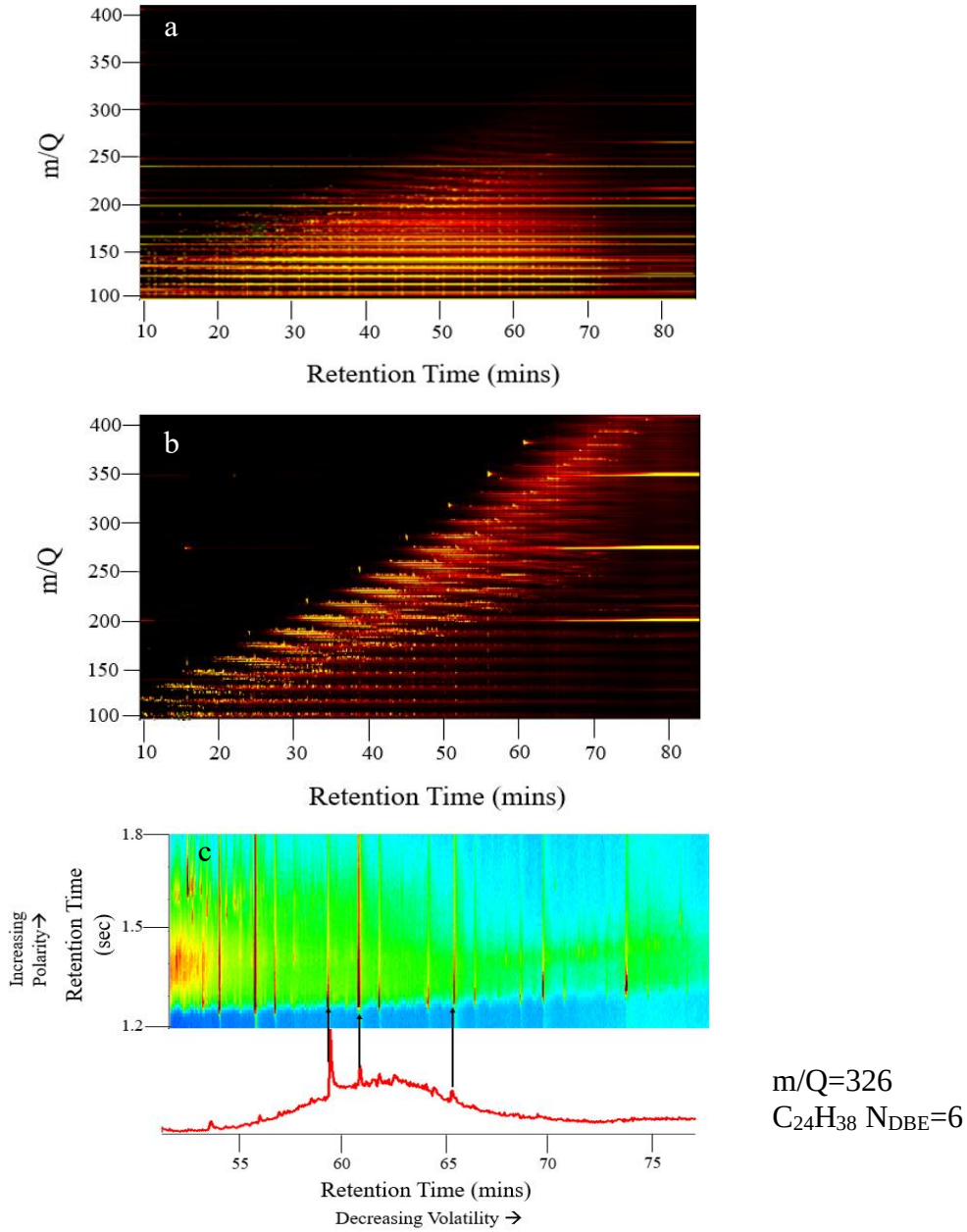

Supplemental Figure 2.2. (a) Complete GCxGC-EI-TOF chromatogram at 70 eV ionization energy of mass versus first dimension retention time of the Gulf of Mexico oil. (b) Complete GCxGC-VUV-TOF chromatogram at 10.5 eV ionization energy of molecular ion mass versus first dimension retention time of the Gulf of Mexico oil. (c) In the GCxGC-EI-MS total ion chromatogram (top), only a few most concentrated isomers are identifiable as individual peaks corresponding to peaks in the single ion GC-VUV-MS chromatogram of m/Q=326 ($C_{24}H_{38}$ N_{DBE}=6) (bottom). Most of the signal for $C_{24}H_{38}$ is from the extremely large number of unresolved isomers eluting between 55 and 70 minutes, which are not separable using GCxGC-EI-MS. GC-VUV-TOF represents these compounds as a single chromatographic trace using the molecular ion, allowing quantification of the sum of all isomers for this carbon number and double bond equivalent by integrating across the signal.

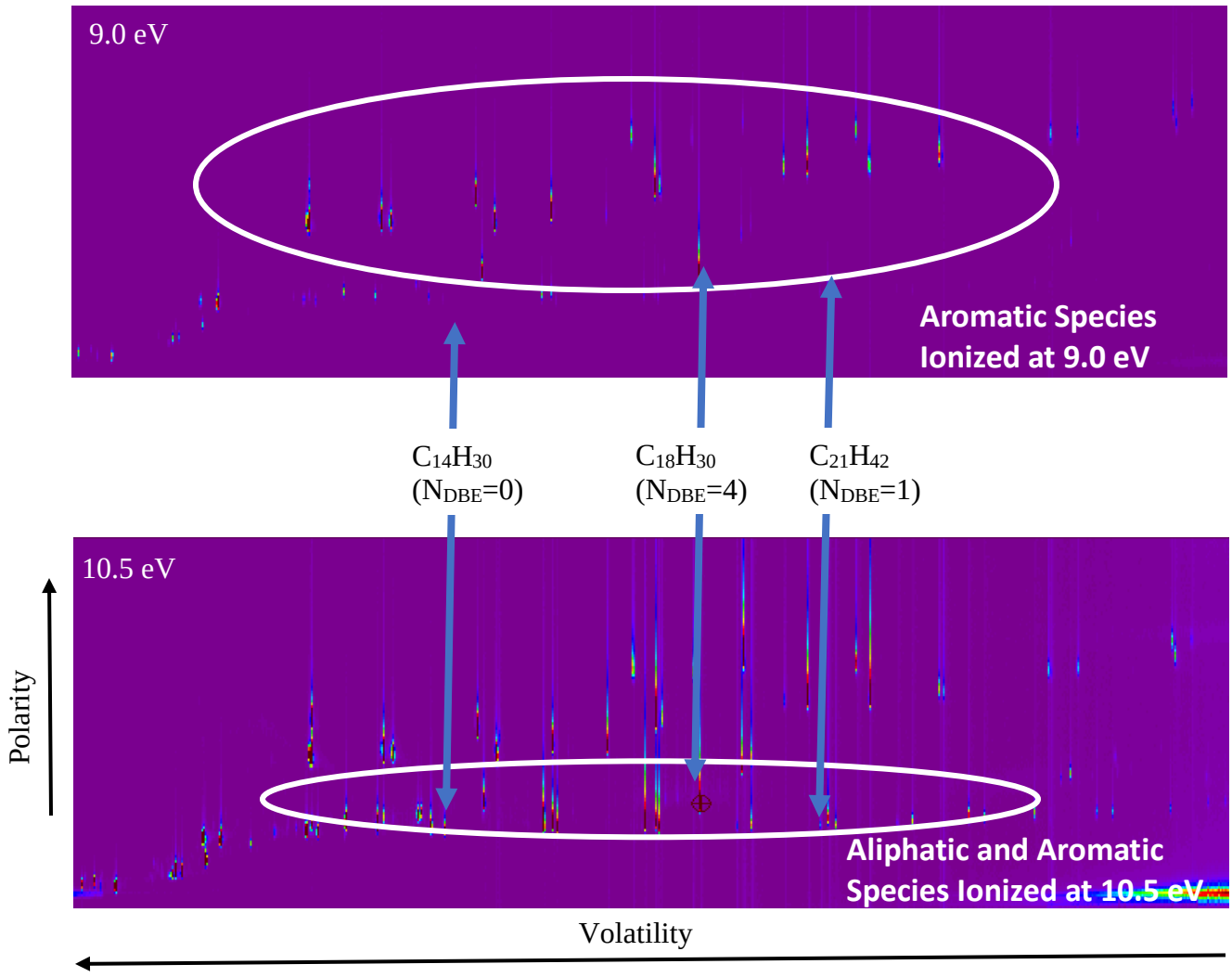

Supplemental Figure 2.3. Two-dimensional chromatograms of a known standard hydrocarbon mixture consisting of both aliphatic (labeled N_{DBE}=0 or 1) and aromatic species (labeled N_{DBE}=4), analyzed at 9.0 eV and 10.5 eV ionization energies. Tunable VUV ionizes hydrocarbons depending on molecular structure, with the aromatic species selectively ionized at 9.0 eV.

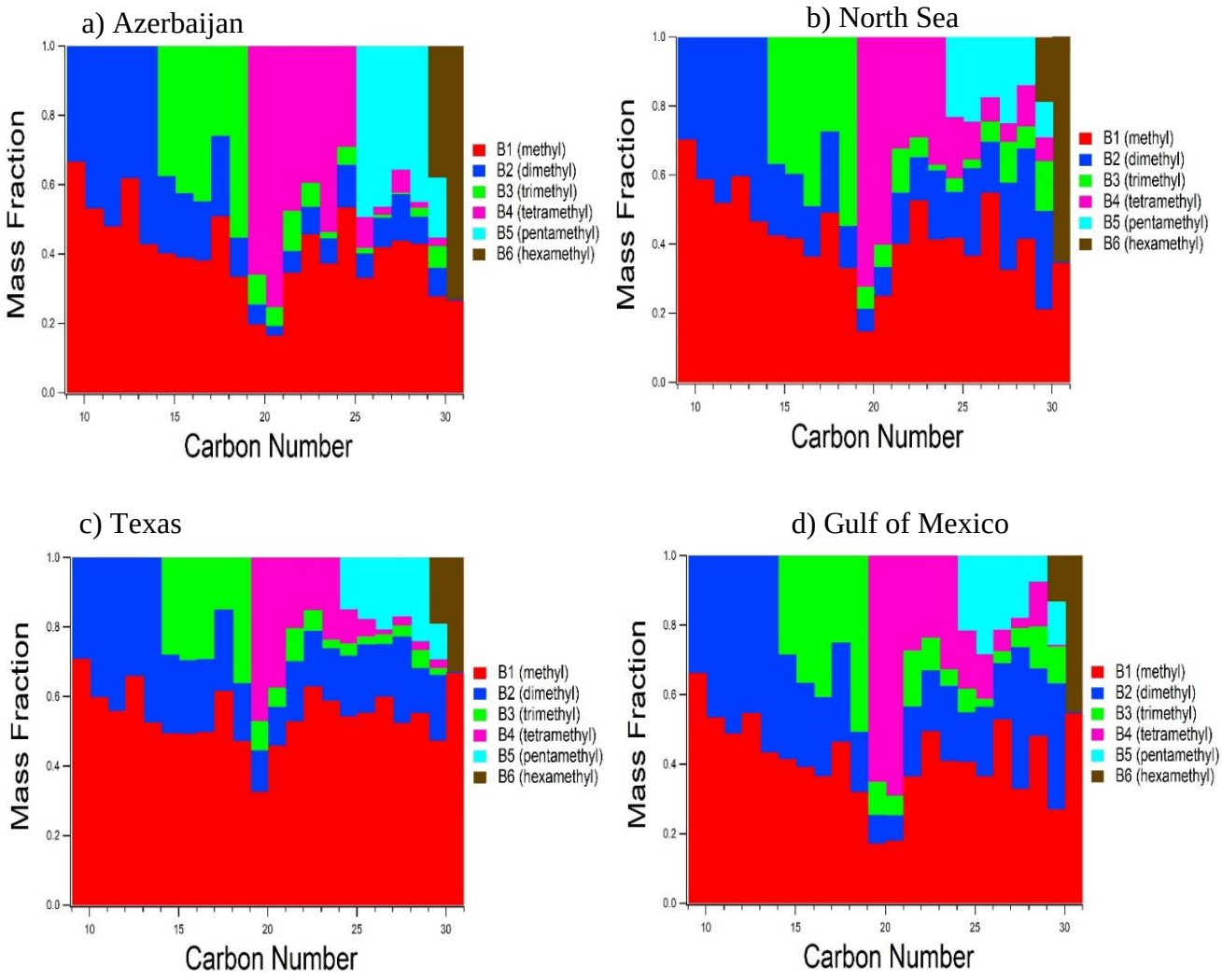

Supplemental Figure 2.4. Isomerically summed mass fractions of the branched alkanes as a function of carbon number and degree of branching for oils from a) Azerbaijan, b) North Sea, c) Texas, and d) Gulf of Mexico.

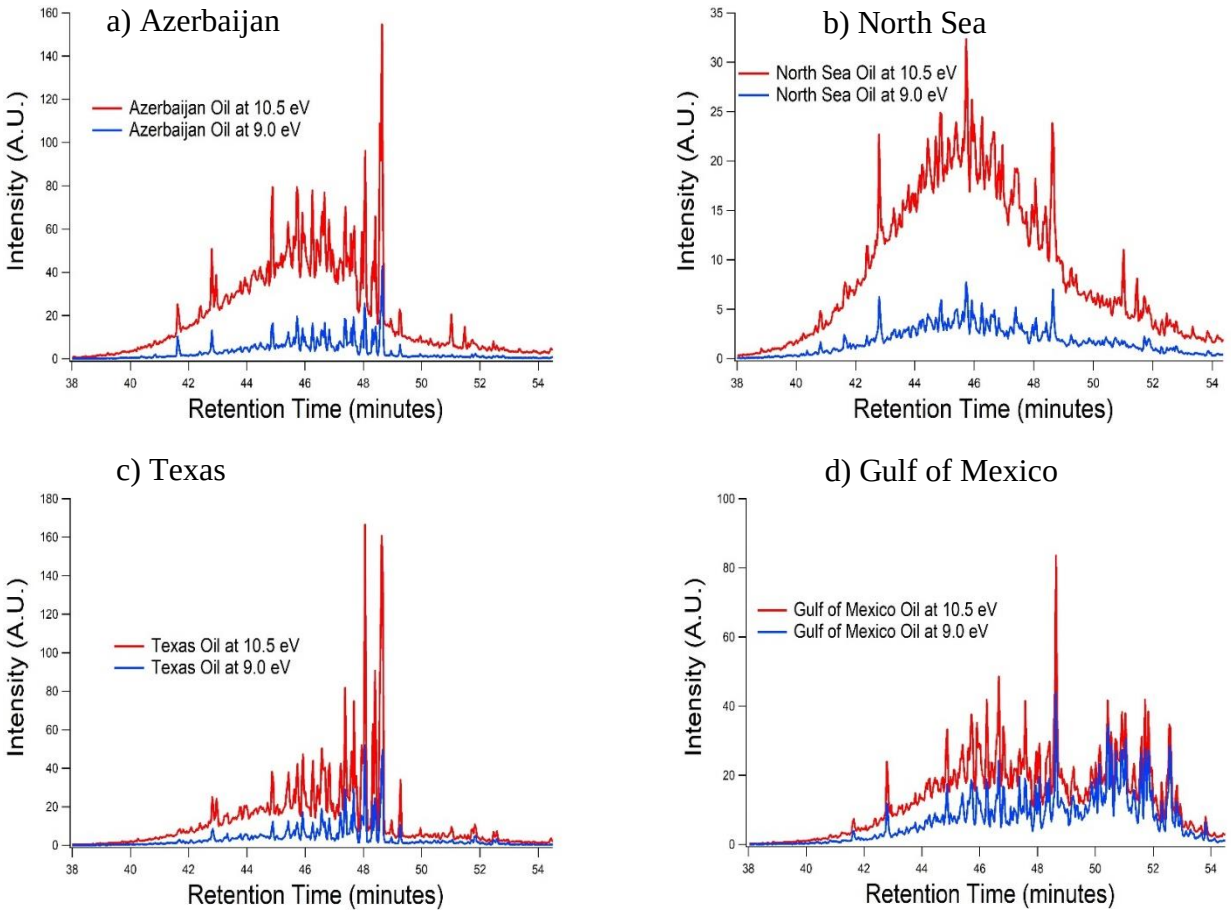

Supplemental Figure 2.5. Overlayed single ion chromatograms with arbitrary units of intensity (A.U.) at 9.0 eV and 10.5 eV ionization energies for $C_{18}H_{30}$ (N_{DBE}=4, m/Q=246) for oils from a) Azerbaijan, b) North Sea, c) Texas, and d) Gulf of Mexico.

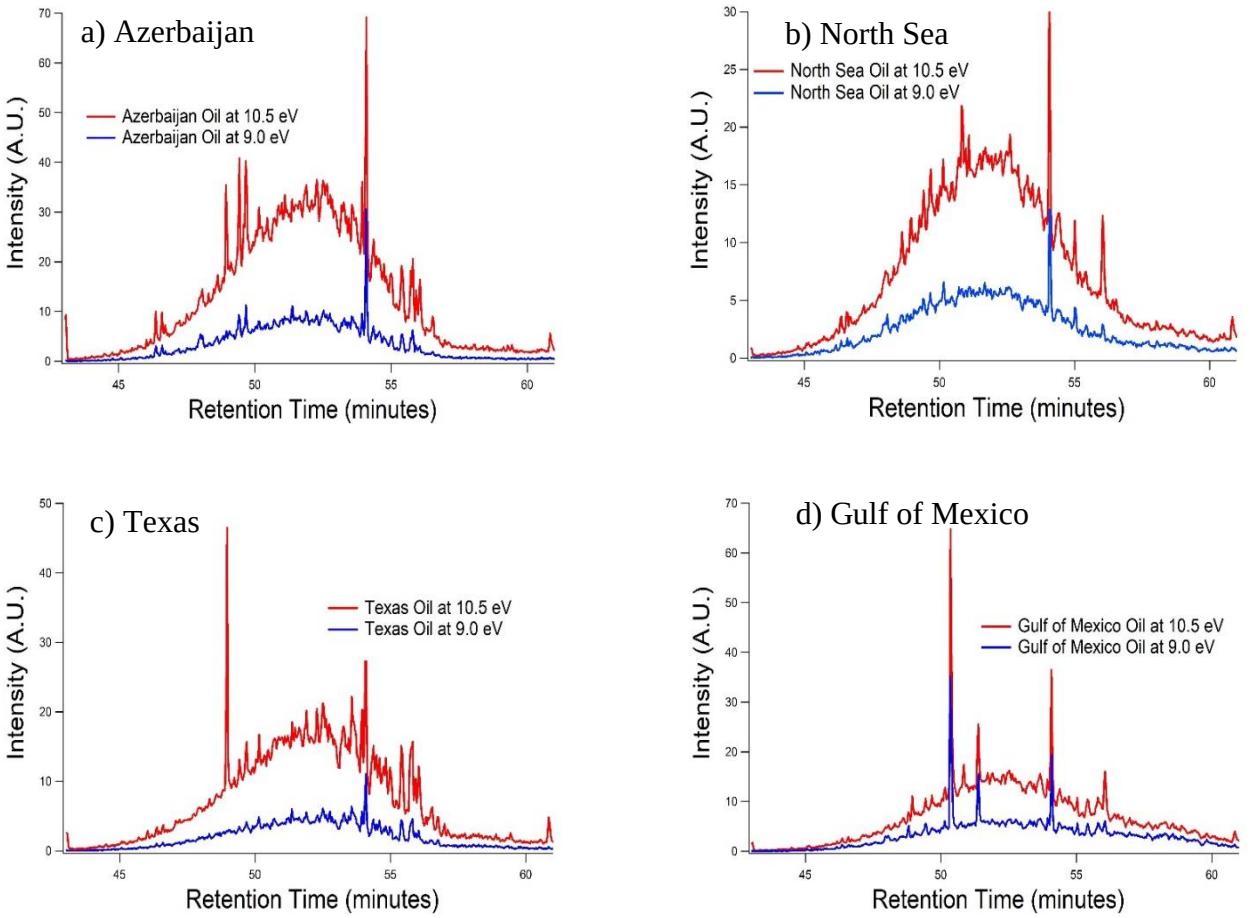

Supplemental Figure 2.6. Overlayed single ion chromatograms with arbitrary units of intensity (A.U.) at 9.0 and 10.5 eV ionization energies for $C_{20}H_{32}$ (N_{DBE}=5, m/Q=272) for oils from a) Azerbaijan, b) North Sea, c) Texas, and d) Gulf of Mexico.

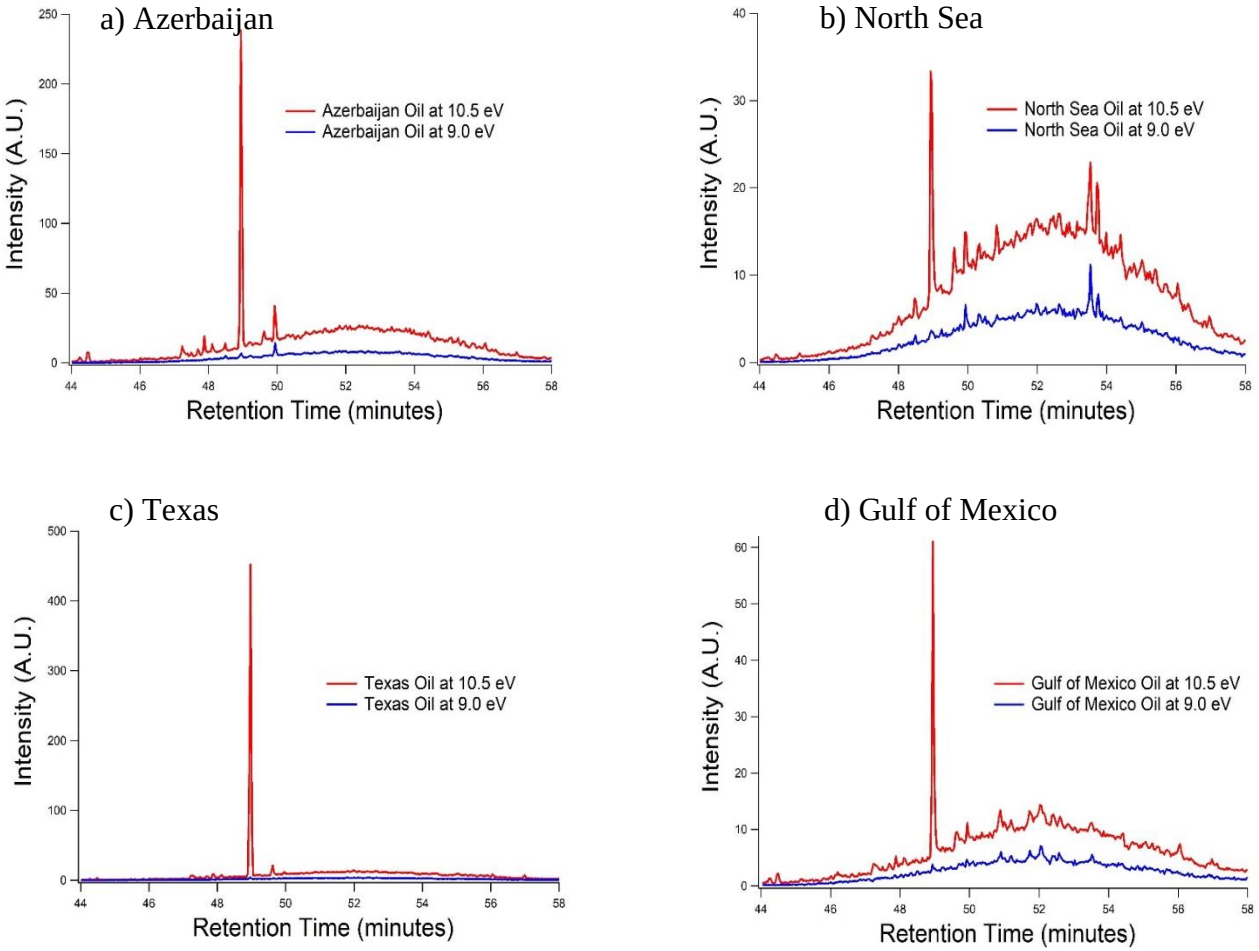

Supplemental Figure 2.7. Overlayed single ion chromatograms with arbitrary units of intensity (A.U.) at 9.0 and 10.5 eV ionization energies for $C_{20}H_{30}$ (N_{DBE}=6, m/Q=270) for oils from a) Azerbaijan, b) North Sea, c) Texas, and d) Gulf of Mexico. The signal present at ~49 minutes in all four oils is that of the ^{13}C isotope of the C_{19} alkane, which is ionized in the 10.5 eV runs, but not in the 9.0 eV runs.

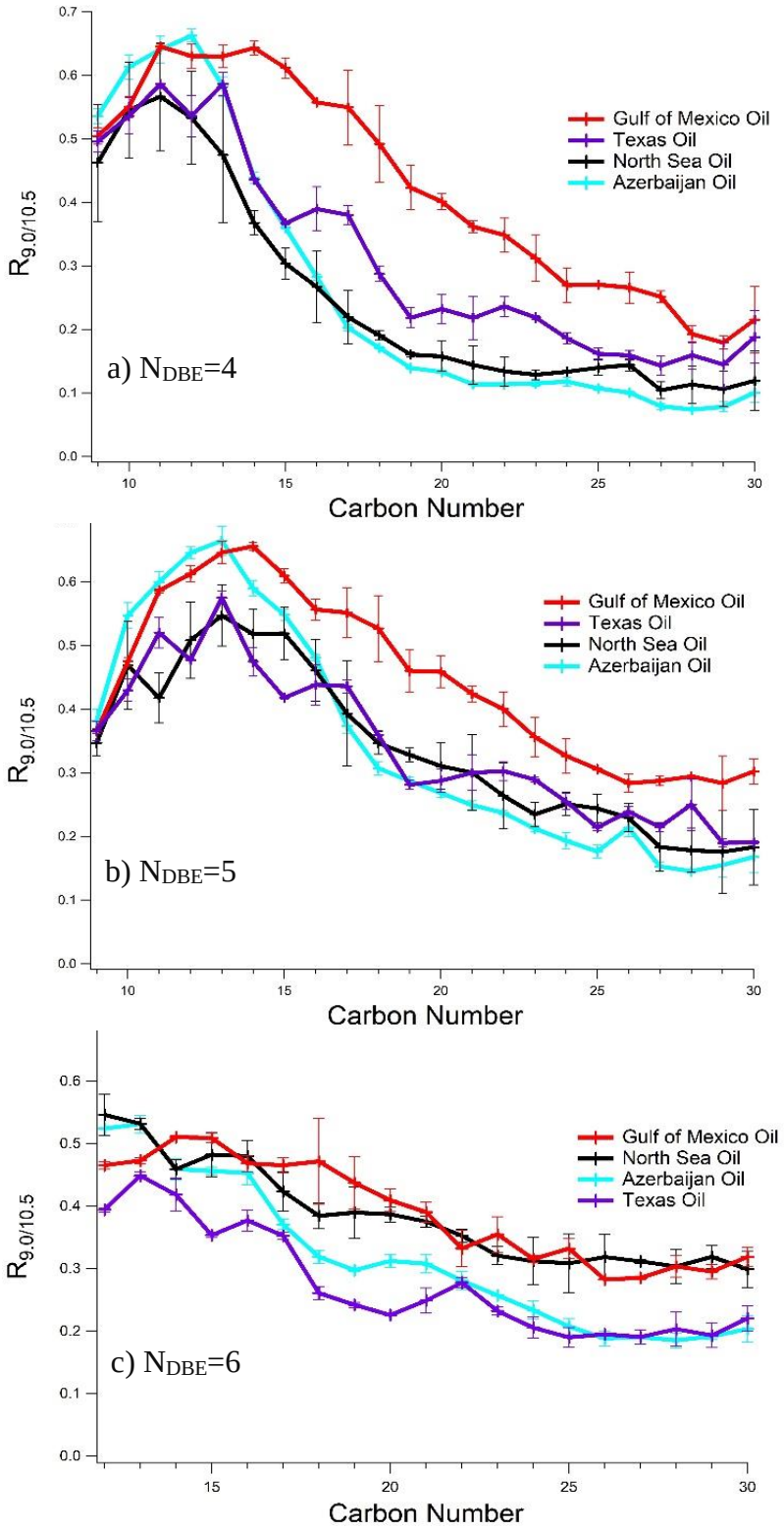

Supplemental Figure 2.8. Ratio of signal responses at 9.0 and 10.5 eV ionization energies ($R_{9.0/10.5}$) as a function of carbon number for oils from Azerbaijan, North Sea, Texas, and Gulf of Mexico, indicated by color, in three classes of double bond equivalents: N_{DBE}=4, 5, and 6 (a, b, and c, respectively).

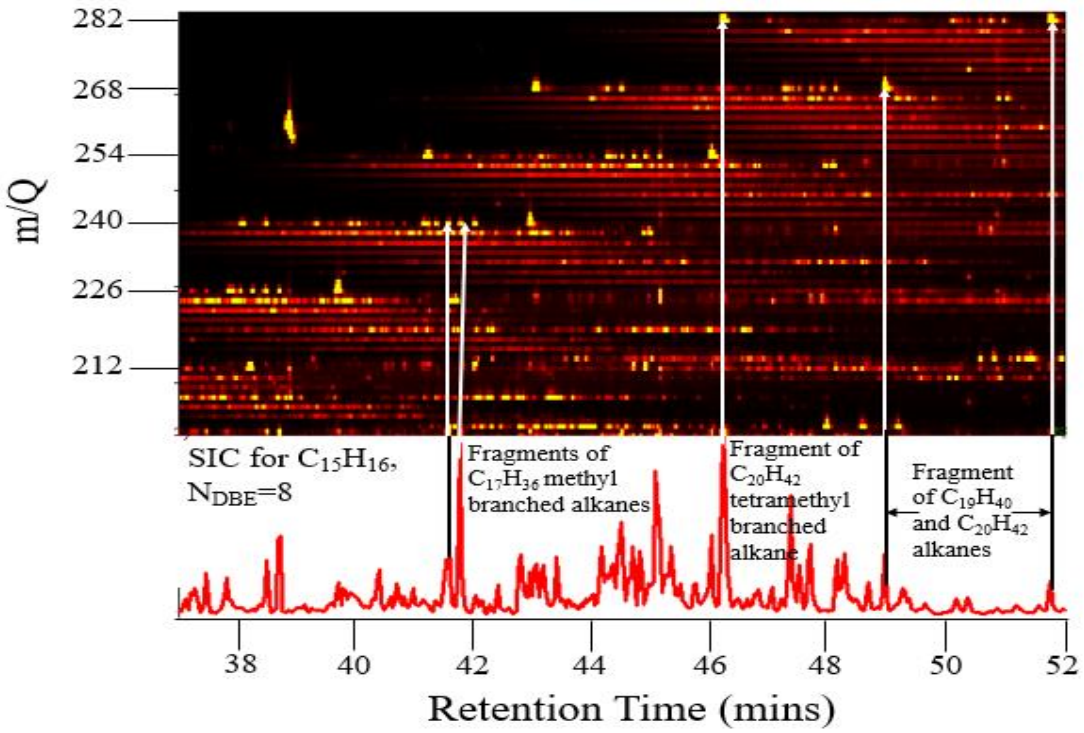

Supplemental Figure 2.9. Single ion chromatogram (SIC) of m/Q=196 (equivalent to $C_{15}H_{16}$, N_{DBE}=8) and mass spectrum versus retention time chromatogram at 10.5 eV. The SIC includes signal from $C_{15}H_{16}$ isomers and aliphatic fragments of higher molecular weight species (e.g. $C_{17}H_{36}$, $C_{19}H_{40}$, $C_{20}H_{42}$).

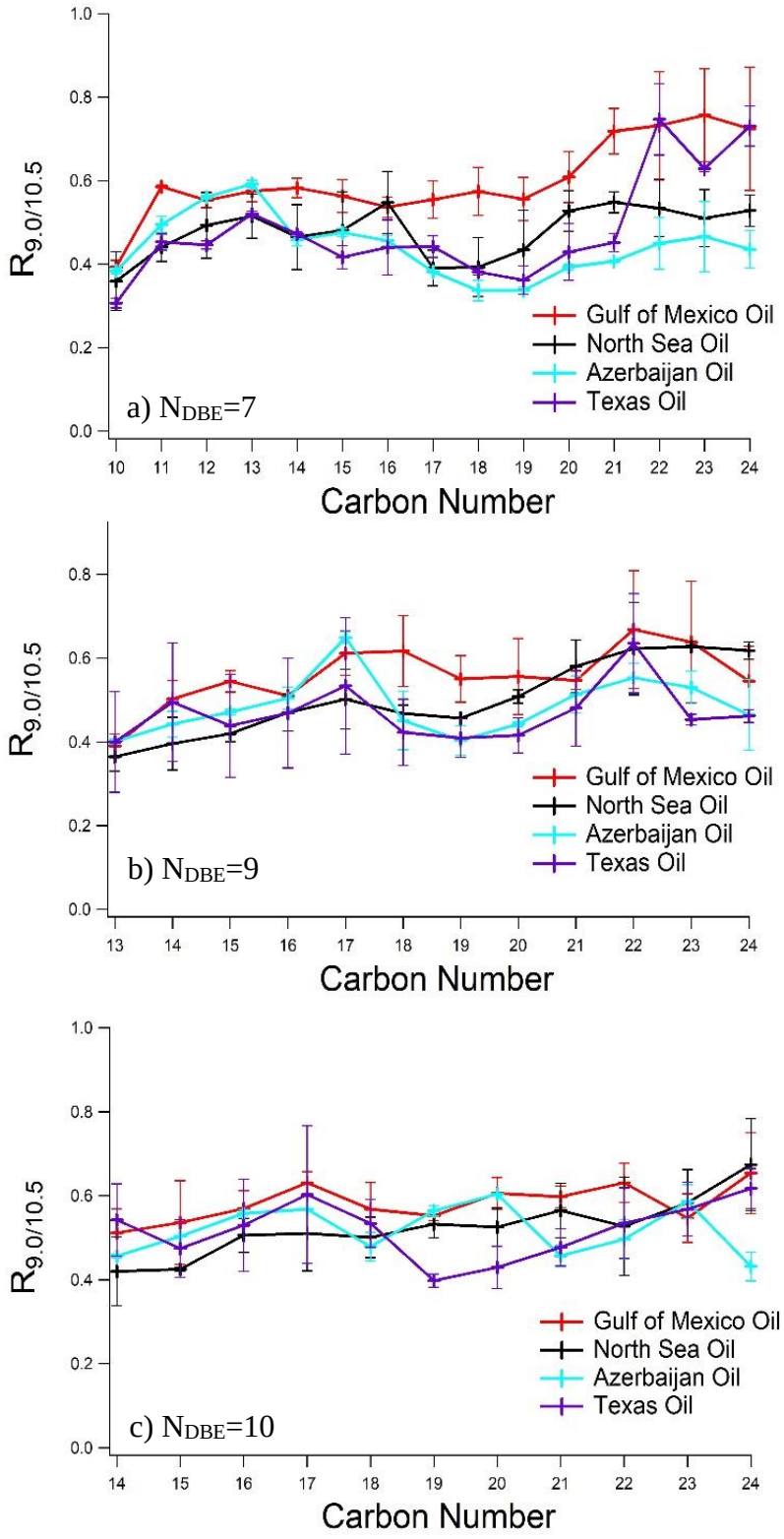

Supplemental Figure 2.10. Ratio of signal responses at 9.0 and 10.5 eV ionization energies ($R_{9.0/10.5}$) as a function of carbon number for oils from Azerbaijan, North Sea, Texas, and Gulf of Mexico, indicated by color, in three classes of double bond equivalents: N_{DBE}=7, 9, and 10 (a, b, and c, respectively).

Chapter 3

Comprehensive Analysis of Changes in Crude Oil Chemical Composition during Biosouring and Treatments

This chapter is adapted from:

Jeremy A. Nowak, Pravin M. Shrestha, Robert J. Weber, Amy M. McKenna, Huan Chen, John D. Coates, Allen H. Goldstein
"Comprehensive Analysis of Changes in Crude Oil Chemical Composition during Biosouring and Treatments"
Environmental Science & Technology, **2018**, *52*(3): 1290–1300

3.1 Abstract

Biosouring in crude oil reservoirs by sulfate-reducing microbial communities (SRCs) results in hydrogen sulfide production, precipitation of metal sulfide complexes, increased industrial costs of petroleum production, and exposure issues for personnel. Potential treatment strategies include nitrate or perchlorate injections into reservoirs. Gas chromatography with vacuum ultraviolet ionization and high-resolution time-of-flight mass spectrometry (GC-VUV-TOF) and Fourier transform ion cyclotron resonance mass spectrometry (FT-ICR MS) combined with electrospray ionization were applied in this chapter to identify hydrocarbon degradation patterns and product formations in crude oil samples from biosoured, nitrate-treated, and perchlorate-treated bioreactor column experiments. Crude oil hydrocarbons were selectively transformed based on molecular weight and compound class in the biosouring control environment. Both the nitrate and the perchlorate treatments significantly reduced sulfide production; however, the nitrate treatment enhanced crude oil biotransformation, while the perchlorate treatment inhibited crude oil biotransformation. Nitrogen- and oxygen-containing biodegradation products, particularly with chemical formulas consistent with monocarboxylic and dicarboxylic acids containing 10−60 carbon atoms, were observed in the oil samples from both the souring control and the nitrate-treated columns, but were not observed in the oil samples from the perchlorate-treated column. These results demonstrate that hydrocarbon degradation and product formation of crude oil can span hydrocarbon isomers and molecular weights up to C_{60} and double-bond equivalent classes ranging from straight-chain alkanes to polycyclic aromatic hydrocarbons. These results also strongly suggest that perchlorate injections provide a preferred strategy to treat biosouring through inhibition of biotransformation.

3.2 Introduction

Secondary recovery of crude oil from an offshore reservoir is an enhanced oil recovery process which involves the injection of pressurized seawater and produced water into the reservoir's wellhead in order to displace oil towards a production well.[1] This industrial process increases the crude oil production lifetime of the offshore reservoir compared to that of a reservoir solely relying on natural subterranean pressure for oil recovery.[2,3] The seawater lowers the temperature of the oil reservoir in the area near the injection well. This decrease in temperature

creates an optimal environment for the growth of mesophilic microbes such as Sulfate Reducing microbial Communities (SRCs).[4,5] These microbial communities in the injected seawater initiate biosouring, a metabolic process which reduces sulfate (SO_4^{2-}) to sulfide (S^{2-}) to form hydrogen sulfide (H_2S).[5] This compound is explosive, flammable, toxic, and potentially hazardous to personnel working near the reservoir.[6,7] Elevated sulfide concentrations initiated by sulfidogenesis lead to the precipitation of metal sulfide complexes that corrode pipelines and oil-water separators.[6,7] These precipitated complexes can lead to facility failure with large associated costs.[7]

Strategies for controlling biosouring have included the applications of sulfate analogs and biocides.[8,9] These treatments have seen limited success due to their costs and restricted efficiencies, as they only inhibit specific strains of SRCs.[2,8,9] The most established current approach for souring control is the injection of nitrate (NO_3^-) anions into a crude oil reservoir. These anions act as alternate electron acceptors for microbial communities in place of sulfate.[1,10] The metabolic pathways of nitrate-reducing bacteria (NRB) are thermodynamically favorable when compared to the pathways of analogous sulfate reduction.[11] While nitrate injections have been tested in both laboratory[11,12] and field studies,[10] the overall effectiveness is poorly understood. As the concentration of nitrate depletes near the injection well of the reservoir, sulfate reduction may still be active deeper in the oil field.[10,13] Nitrite, a metabolic intermediate of nitrate reduction, can be toxic to SRCs, but is also chemically and biologically labile and has a reduced half-life in a reservoir matrix.[13,14] These limitations require large nitrate injection concentrations to prevent depletion and to maximize nitrite production. This requirement may not be economically or logistically feasible in a crude oil reservoir.

Perchlorate injections have recently been reported as an effective solution for souring control.[10,15] Like nitrate reduction, perchlorate reduction is thermodynamically favorable relative to sulfate reduction (E^o= +797 mV for ClO_4^-/Cl^- and E^o= -217 mV for SO_4^{2-}/S^{2-}). Previous studies have demonstrated that perchlorate is specifically inhibitory to sulfate reduction[16] and that dissimilatory perchlorate-reducing bacteria (DPRB) can outcompete SRCs. Furthermore, DPRB also directly oxidize sulfide to sulfur as a metabolic end product, removing it from the produced fluids.[17,18]

The importance of microbial biotransformation of crude oil hydrocarbons has been increasingly realized in the context of industrial petroleum production,[19] environmental oil spills,[20] and enhanced oil recovery from subsurface oil reservoirs.[21] Evidence of hydrocarbon biodegradation has previously been observed in metabolite profiling of subsurface oil reservoirs,[21] incubation studies of crude oil with known microbial inocula,[22] and gasoline amended aquifers.[23] Previous studies have investigated thermochemical sulfate reduction coupled to transformation of Gulf coast oils.[24] Microbiological sulfate, nitrate, and perchlorate reduction in conjunction with crude oil biotransformation remain poorly understood. Furthermore, biodegradation studies typically incorporate select compounds to serve as biotransformation markers, such as C_4-C_{10} straight-chain alkanes and monoaromatic compounds,[21-23] rather than tracking complete suites of hydrocarbon isomers of varying chemical sizes or compound classes. In this chapter, comprehensive chemical analyses provide insight into crude oil biotransformation, including hydrocarbon degradation and product formation, to understand the impacts of biosouring and its potential treatments on crude oil's chemical composition.

Traditional gas chromatographic (GC) techniques used in crude oil analysis typically couple a volatility separation of the oil's components with a flame ionization detector (FID) or electronic ionization mass spectrometer (EI MS).[25,26] Due to crude oil's chemical complexity, much of the organic mass co-elutes as an unresolved complex mixture (UCM),[27] a phenomenon

which complicates mass spectra interpretation and compound identification. This chapter incorporates two complementary techniques to resolve UCM and understand biotransformation of soured, nitrate treated, and perchlorate treated crude oil from a 70 day experimental representative of the *in situ* crude oil reservoir. Gas chromatography combined with vacuum ultraviolet ionization and time-of-flight mass spectrometry (GC-VUV-TOF) can comprehensively summarize the chemical composition of hydrocarbon isomers of complex organic mixtures, such as crude oil, up to the molecular volatility limit of the GC columns (~320ºC).[28] Ultrahigh resolution Fourier transform ion cyclotron resonance mass spectrometry (FT-ICR MS) combined with atmospheric pressure ionization, such as electrospray ionization, can selectively characterize polar and nonpolar crude oil components without boiling point limitations.[29-31] This technique routinely achieves resolving power sufficient to separate compounds that differ in mass by less than the mass of an electron in a single mass spectrum ($m/\Delta m_{50\%} \approx 1{,}000{,}000$, in which $\Delta m_{50\%}$ is the mass spectral peak width at half-maximum peak height at m/z 500).[32-34] Ultrahigh resolution FT-ICR MS can identify compositional changes to biotransformed crude oil through comparison of molecular differences in oil samples from different stages of souring or treatment. Details of the GC-VUV-TOF and FT-ICR MS techniques are described in the Supplemental Information section (Section 3.8) of this chapter.

3.3 Materials and Methods

3.3.1 Experimental Protocol

Bioreactor columns were established as described in detail in Shrestha et al.[35] Briefly, custom designed 1 m x 10 cm glass columns were packed with a slurry of ~6 kg of pure sand (Iota Quartz, New Canaan, CT, USA) and 4.5 liters of North Sea crude oil. The columns were maintained at 40°C, mimicking the average temperature of an offshore oil reservoir. Seawater and produced water, obtained directly from a North Sea oil field in a 60:40 ratio, were injected through the columns at 189 µl/min to establish a 2-week residence time, mimicking the residence time of the seawater injected into an offshore oil reservoir. A mixture of volatile fatty acids, based on the empirically determined content of the North Sea oil reservoir's produced waters (acetate 565 µM; butyrate 19 µM; propionate 23 µM; formate 74 µM), was continuously added to all of the columns. As the experiment progressed, >70% of the initial oil in all of the columns was washed out by the bioreactor flow system. The observed transformations reported in this chapter represent those of the residual oil rather than the initial bulk oil.

Hydrogen sulfide was measured as a proxy for SRC activity. When the columns were soured and the sulfide concentrations were stable (>0.68 mM), pulsed doses of nitrate (weekly doses of ~17.5 mM) and perchlorate (weekly doses of ~17 mM) began in separate duplicate columns. One additional column was left untreated, to maintain the biosouring environment as a control column. Column liquid containing crude oil was extracted from a sampling port on each column using a 1 mL glass syringe (Hamilton, Reno, NV, USA). The liquid was then placed into a vial containing 1 mL of chloroform (HPLC grade, Si gma-Aldrich, St. Louis, MO, USA). Oil samples from the nitrate and perchlorate treated columns were extracted at days 0, 21, 42, and 70 of treatment. Control oil samples from the biosouring column were extracted at the corresponding days 0, 28, 43, and 70. Water samples were continuously extracted from the columns for sulfide analysis. The Cline assay was used to determine sulfide concentrations in these water samples.[36]

3.3.2 Chromatographic Technique

Oil samples were analyzed via GC-VUV-TOF (Supplemental Figure 3.1), which extends the analytical capabilities of GC-MS and two-dimensional gas chromatography-mass spectrometry (GCxGC-MS) to allow a complete characterization of C_9-C_{30} crude oil hydrocarbon isomers as a function of both carbon number and structural class. Oil was directly injected via a septumless head into a liquid nitrogen cooled inlet (-40ºC) on a fused silica liner (CIS4, Gerstel Inc, Linthicum, MD, USA). The sample was transferred to the gas chromatograph (GC, Agilent 7890, Santa Clara, CA, USA) by heating the liner to 320ºC at 10ºC/s. The chemical components of the oil (hereafter referred to as "analyte") were separated based on volatility using a nonpolar column (60 m x 0.25 mm x 0.25 um Rxi-5Sil-MS; Restek, Bellefonte, PA, USA), with a helium gas flow rate of 2 mL/min. The GC program began at 40ºC and the ramp rate was 3.5ºC/minute. The program ended at a maximum temperature of 320ºC with a 10-minute final hold time. The analyte was transferred from the GC to a 170ºC ion source via a 270ºC transfer line and ionized with 10.5 ± 0.2 eV VUV photoionization. The ions were detected using a high-resolution ($m/\Delta m_{50\%} \approx 4000$) time-of-flight mass spectrometer (TOF, Tofwerk, Thun, Switzerland). The VUV beam was from the Chemical Dynamics Beamline 9.0.2 of the Advanced Light Source at the Lawrence Berkeley National Laboratory. An ionization energy of 10.5 eV was chosen to detect all parent ions and to minimize contributions from fragment ions that could create UCM. Mass spectra were collected at 100 Hz, then averaged to 0.5 Hz to deconvolute mass spectral peaks in high-resolution post processing peak fitting. High-mass-resolution data processing was done using custom code written in Igor 6.3.7 (Wavemetrics).[37] Measurement calibrations followed previously established methods described in Chan et al[38] and Worton et al.[37] These methods are described in detail in the Supplemental Information section (Section 3.8) of this chapter.

3.3.3 FT-ICR MS Technique

Ultrahigh resolution FT-ICR MS analysis was done at the National High Magnetic Field Laboratory at Florida State University to expand the analytical window beyond those hydrocarbons measurable using GC-VUV-TOF in order to observe compounds $>C_{30}$ and to identify heteroatom containing chemical formulas.[39] All solvents used in this chapter were HPLC grade (Sigma-Aldrich, St Louis, MO, USA). During sample preparation, 1 gram of oil was diluted with 1 mL of toluene that was further diluted with equal parts methanol spiked with either 0.25% by volume tetramethylammonium hydroxide (TMAH) for negative electrospray ionization (-ESI) FT-ICR MS[40] or 8% by volume formic acid for positive electrospray ionization (+ESI) FT-ICR MS analysis.[41]

Positive ion electrospray ionization selectively ionizes basic compounds through protonation via formic acid to form quasimolecular ions $[M+H]^+$.[41] Negative ion electrospray ionization selectively ionizes acidic species through deprotonation via TMAH to form quasimolecular ions $[M-H]^-$.[40] When combined with ultrahigh resolution FT-ICR MS and Kendrick mass sorting,[31,33] these ionization techniques provide sub-ppm mass accuracy necessary for elemental composition assignments to polar compounds in transformed crude oil.[42] Molecular formulas are grouped by heteroatom class (species with the same $C_cH_hN_nO_oS_s$ elemental composition differing only by the degree of alkylation) based on relative abundance in the mass spectrum to identify products in biotransformed crude oil when compared to the parent crude oil. Details regarding the ionization sources, FT-ICR MS instrumentation, broadband phase correction,

and frequency-to-mass conversion are provided in the Supplemental Information section (Section 3.8) of this chapter.

3.4 Results and Discussion

3.4.1 Crude Oil Chemical Composition and Sulfide Production

The distribution of the parent crude oil's GC-amendable measured hydrocarbon mass fraction (milligrams per kilogram injected oil) as a function of both carbon number and double bond equivalent (N_{DBE})[43] is shown in Figure 3.1a. N_{DBE} for a pure hydrocarbon is determined by Equation 1:

$$N_{DBE}(C_xH_y)=X-Y/2+1 \quad (1)$$

When using N_{DBE} to classify crude oil hydrocarbons, N_{DBE}=0 represents normal and branched alkanes, N_{DBE}=1 represents monocycloalkanes, N_{DBE}=4 represents monoaromatic compounds and four alkyl ringed steranes, and N_{DBE}=7 represents polycyclic aromatic hydrocarbons (PAHs). Crude oil contains little to no olefinic compounds due to the compounds' instability and reactivity.[44,45] Crude oil N_{DBE} hydrocarbon classes can therefore be assumed to represent the number of cyclic rings and aromaticity rather than the number of non-aromatic double bonds.

A ~50% split of the mass fractions in the parent crude oil between GC-amendable C_9-C_{19} and C_{20}-C_{30} species is illustrated in Figure 3.1a. Approximately 60% of the total measured hydrocarbon mass fraction represents purely aliphatic compound classes (N_{DBE}=0-3) and 40% represents classes with a $N_{DBE} \geq 4$ that can contain aromatic rings.

The differences in sulfide production among the untreated souring control column, the nitrate treated column, and the perchlorate treated column are illustrated in Figure 3.1b. Sulfide concentrations in the biosouring control column fluctuated between 0.3-1.4 mM over the 70 day experiment. These levels were indicative of sulfate reduction by SRCs throughout the experimental timeline. After 18 days of nitrate treatment and 40 days of perchlorate treatment in the respective treated columns, sulfide concentrations dropped to 0 mM, indicating effective biosouring control. The decrease in sulfide concentrations correlated with an increase in sulfate concentrations in the treated columns.

Oil samples were analyzed by GC-VUV-TOF to document the transformation of crude oil hydrocarbons in all three columns as a function of time. All hydrocarbon concentrations reported were normalized to a $C_{30}H_{52}$ hopane recalcitrant biomarker.[46] The normalized concentration of each compound in the biodegraded oil, based on carbon number and N_{DBE}, was compared to its original concentration in the parent crude oil to determine the percent of the compound remaining in the transformed crude oil. Day zero in all timelines represents the timepoint when the biosouring treatments began in the soured columns.

3.4.2 Straight-Chain Alkane Transformations

The patterns of straight-chain alkane (N_{DBE}=0) biotransformations are different among oil samples from the biosouring control, nitrate treated, and perchlorate treated columns, implying that biotransformation patterns of the crude oil's chemical composition change if the microbial environment is sulfate-reducing, nitrate-reducing, or perchlorate-reducing. Figure 3.2a depicts

how straight-chain alkanes, ranging in size from C_{10}-C_{14}, in all oil samples from the three columns were degraded to ~60-80% of the initial parent oil concentrations prior to the beginning of treatment at day 0. In the oil samples from the biosouring control column, the C_{10}-C_{14} straight-chain alkanes were transformed to ~25-70% of the parent oil concentrations in the first 43 days of the experiment, but remained recalcitrant for the final 27 days (Figure 3.2a). This incomplete transformation of straight-chain alkanes in a sulfate-reducing environment has previously been observed in long-term microbial incubation studies with crude oil.[47] Straight-chain alkanes ranging from C_{15}-C_{18} in the oil from the souring control column were reduced to ~85-90% of the original concentrations after 70 days, and C_{19}-C_{29} straight-chain alkanes underwent minimal (less than 5%) transformation during souring. Previous studies have similarly shown crude oil degrading microbial communities transforming straight-chain C_4-C_{15} alkanes before degrading larger C_{16}-C_{30} alkanes under sulfate-reducing conditions, in agreement with these findings.[47,48]

The introduction of nitrate and perchlorate anions into the soured column led to large changes in crude oil biotransformations when compared to the transformations of the hydrocarbons in the souring control oil. Nitrate introduction led to a rapid increase in C_{12}-C_{29} straight-chain alkane transformations in the oil, without dependence on molecular weight. After 21 days, these compounds were depleted to ~40-60% of the original parent oil concentrations (Figure 3.2b). At the end of the 70 day experiment, all straight-chain alkanes in the oil samples from the nitrate treated column were transformed to ~30-40% of the original concentrations in the parent crude oil. Introduction of perchlorate into the soured column rapidly inhibited the transformation of straight-chain alkanes in the oil (Figure 3.2c). Over the complete 70 day perchlorate treatment, straight-chain alkanes in the oil were transformed <10% when compared to the concentrations in the parent crude oil. The lack of straight-chain alkane transformations in the presence of perchlorate suggests that DPRB were unable to utilize crude oil as an electron donor or carbon source to drive metabolism.

Metabolic intermediates such as nitrite were detected in the treatment environments, providing evidence that the anaerobic processes of nitrate and perchlorate reduction by microbial communities occurred. Total microbial community analysis revealed an increase in the relative abundances of functional NRB and DPRB communities in the respective columns upon introduction of nitrate or perchlorate as the electron acceptor. This microbiological evidence corroborates the biological origin of the crude oil hydrocarbon transformations observed in this chapter, implying that these differences in hydrocarbon transformation patterns stem from differences in the relative abundances of microbial communities, their activities, and the availability of a dominant terminal electron acceptor.

3.4.3 Biotransformations of Monocycloalkanes

Transformations of isomerically summed monocycloalkanes in oil samples from the untreated biosouring control, nitrate treated, and perchlorate treated columns are shown in Supplemental Figure 3.2. The C_{10}-C_{12} monocycloalkane concentrations in oil samples from all three columns were reduced to ~45-75% of the initial concentrations in the parent crude oil at day 0, before biosouring treatment began. This depletion is similar to the depletions in the straight-chain alkanes observed during the same time period. After 43 days of souring, the C_{10}-C_{19} crude oil monocycloalkanes in the control column were transformed to ~25-85% of the original parent oil concentrations. These same compounds were only transformed an additional ~1-10% between 43 and 70 days. In contrast, the C_{20}-C_{29} monocycloalkanes in oil samples from the biosouring

control column underwent little to no change in concentration throughout the timeline. This observed hydrocarbon transformation pattern agrees with earlier studies suggesting that microbial communities transform C_{10}-C_{15} aliphatic compounds (including straight-chain alkanes and monocycloalkanes) before transforming C_{20}-C_{30} aliphatic compounds.[22,47]

Transformations of isomerically summed monocycloalkanes in oil samples from the nitrate and perchlorate treated columns exhibited similar patterns to those of the straight-chain alkane transformations in each respective treatment. There was a ~40-60% reduction in the concentration of monocycloalkanes, independent of molecular weight, in oil samples from the nitrate treated column when compared to the monocycloalkane concentrations in the parent crude oil. The C_{10}-C_{29} monocycloalkanes in oil samples from the perchlorate treated column underwent a <10% change in concentration throughout the experiment. The similarities between the biotransformation patterns of both monocycloalkanes and straight-chain alkanes in oil samples from the nitrate and perchlorate treated columns support the conclusion that nitrate enhances crude oil hydrocarbon biotransformation while perchlorate inhibits biotransformation. Microbial community analysis illustrates the abundances of NRB and DPRB in the respective treatments, confirming the biological differences in environments with a different dominant electron acceptor. The microbiological results from 16S rRNA sequencing suggest that the DPRB found in the columns are not hydrocarbon degraders, therefore their presence and activity do not result in crude oil biotransformations.[35] As these microbial communities are not known to degrade crude oil hydrocarbons in order to drive their metabolic processes, it is unlikely that the DPRB communities adapted to transform these classes of hydrocarbons. This microbial community analysis was done outside of the scope of this dissertation in a collaboration with Professor John Coates's research group.

3.4.4 Biotransformations of Monoaromatic Compounds

The N_{DBE}=4 compound class consists of monoaromatic species and steranes with four aliphatic rings. Transformation of toluene and ethylbenzene by different pure culture isolates of sulfate-reducing microorganisms has been well documented.[49,50] This chapter utilizes GC-VUV-TOF data to quantify how the isomeric sum of all C_{10}-C_{29} monoaromatic compounds and steranes is transformed as a function of time, going beyond previous studies which focused on transformations of a limited number of aromatic species.[49,50] Transformations of monoaromatic species in oil samples from the biosouring control, nitrate treated, and perchlorate treated columns are illustrated in Figure 3.3. In all oil samples from the three columns, there was a ~20-40% reduction in concentration of the C_{10}-C_{11} monoaromatic species when compared to the parent oil concentrations at day 0, similar to the depletions observed in the N_{DBE}=0 and N_{DBE}=1 compound classes prior to treatment. In oil samples from the biosouring control column, C_{24}-C_{26} monoaromatic species were reduced to ~70-75% of the original parent oil concentrations after 28 days (Figure 3.3a), while the concentrations of C_{10}-C_{23} monoaromatic compounds underwent minimal (<10%) change compared to the parent crude oil concentrations during the same time span. Between 28 and 43 days of souring, C_{10}-C_{23} monoaromatic species in oil samples from the control column were depleted to ~60-85% of the initial parent oil concentrations at a transformation rate ~10-fold faster than that of the same compounds between 0 and 28 days. Larger C_{24}-C_{26} monoaromatic species continued to be transformed to ~50-60% of the parent crude oil concentrations after 43 days of souring at a rate ~1.5-fold faster than that of the same compounds between 0 and 28 days. The C_{10}-C_{23} monoaromatic species were depleted an additional ~10%

when compared to the first 43 days during the final 27 days of souring, but the C_{24}-C_{26} monoaromatic species were only depleted an additional ~5% when compared to the first 43 days during the same time span. The C_{27}-C_{29} steranes in oil samples from the control column underwent minimal transformation throughout the entirety of the biosouring experiment and are considered to be recalcitrant markers.[46]

The transformation patterns of monoaromatic compounds in oil samples from the biosouring control column differed from those patterns observed in the N_{DBE}=0 and N_{DBE}=1 compound classes. As the amount of available aliphatic hydrocarbons to serve as electron donors and carbon sources decreased after 21 days of souring, the SRCs began to transform more complex aromatic material. The total microbial community analysis revealed changes in the relative abundances of SRCs that aligned with changes in the hydrocarbon transformation patterns in the biosoured oil. Aliphatic hydrocarbon degrading SRCs dominated the microbial communities in the first 21 days of souring in the control column. As souring continued and sulfide production increased (Figure 3.1), the relative abundance of monoaromatic hydrocarbon degrading SRCs increased. This shift in community abundance coincided with a decrease in aliphatic hydrocarbon degradation and an increase in monoaromatic hydrocarbon degradation as souring progressed. The microbial community analysis confirms that the relative abundances of microbial communities is a driving factor in hydrocarbon degradation during biosouring. This microbial community analysis was done outside of the scope of this dissertation in a collaboration with Professor John Coates's research group.

Monoaromatic compound transformation patterns in oil samples from the nitrate and perchlorate treated columns are illustrated in Figures 3.3b and 3.3c, respectively. These transformations follow similar patterns to those of aliphatic transformations in each respective treatment. As the nitrate treatment began, C_{12}-C_{26} monoaromatic compounds in oil samples were depleted to ~40-60% of the original parent oil concentrations after 21 days. These transformations continued as the treatment progressed, resulting in monoaromatic hydrocarbon concentrations ~30-50% of the original parent oil concentrations. Monoaromatic species in oil samples from the perchlorate treated column were only depleted to ~10-20% of the parent oil concentrations after 70 days, further supporting the conclusion that perchlorate injections hinder biotransformation of crude oil.

3.4.5 Biotransformations of Polycyclic Aromatic Hydrocarbons

The C_{10}-C_{26} PAHs in oil samples from the souring control column were depleted to ~85-95% of the parent oil concentrations in the first 28 days, ~65-90% after 43 days, and ~60-85% after 70 days, as shown in Supplemental Figure 3.3a. Transformation of monoaromatic species in oil samples from the souring control column was ~1.5 times greater than transformation of PAHs of the same carbon number in the souring control column over the experimental timeline, implying that SRCs favor monoaromatic compound degradation over PAH degradation. PAHs in oil samples from the nitrate treated column were depleted to ~40-60% of the parent oil concentrations without any preference based on molecular weight, while PAHs in oil samples from the perchlorate treated column were depleted to ~80-90% of the parent oil concentrations.

This chapter describes those crude oil hydrocarbons susceptible to microbial degradation by illustrating the transformation of complete chemical classes of labile crude oil components. Rather than focusing only on specific compounds prone to biodegradation, such as cyclohexane or benzene, GC-VUV-TOF allows a complete class of hydrocarbon isomers to be summed in order

to understand how a complete N_{DBE} class of one molecular mass is degraded by microbial communities. Biotransformation of crude oil by microbial communities in the biosouring column was found to be highly selective. The SRCs first degraded C_{10}-C_{19} aliphatic compounds before degrading C_{10}-C_{26} monoaromatic hydrocarbons. The nitrate treatment enhanced biotransformation of all crude oil hydrocarbons regardless of molecular weight, while the perchlorate treatment inhibited biotransformation of the crude oil. Previous studies have only shown microbial communities targeting a select group of hydrocarbons, such as n-alkanes or C_6-C_{10} monoaromatic compounds,[47-51] for degradation. The GC-VUV-TOF technique revealed that hydrocarbon degrading microbial communities transform isomers of C_{10}-C_{30} compounds of different structural classes and that the transformation patterns vary depending on the abundances of microbial communities and the availability of the terminal electron acceptor.

3.4.6 Biodegradation Products

The heteroatom class distributions, based on relative abundance in the mass spectrum, of the most abundant chemical species observable with +ESI and -ESI combined with FT-ICR MS in the parent crude oil, oil from the souring control column, oil from the nitrate treated column, and oil from the perchlorate treated column are shown in Figure 3.4. The distributions were normalized to the most-abundant peak in each spectrum. Compounds containing a single pyridinic nitrogen atom (N_1) comprised the most-abundant chemical class in all the oil samples (Figure 3.4a). The relative abundance of the N_1 class decreased from ~60% to ~40% in the oil after 70 days of souring. This depletion suggests selective transformation of these species into other compounds, such as oxygenated species, or degradation by SRCs. Compounds with two pyridinic nitrogen atoms (N_2) fell from ~2.5% to ~1.5% relative abundance in the same souring time span as the depletion of the N_1 class. This decline in the relative abundances of pyridinic nitrogen classes during souring was matched by an increase in species that contain both oxygen and nitrogen. Compounds with one oxygen and one nitrogen atom (N_1O_1) in the oil increased in relative abundance from ~2.0% to ~5.0% after 70 days of souring. The relative abundance of N_1O_2 compounds also grew from ~0.3% to ~2.0% during the same time span in the oil from the souring column. Pyridinic nitrogen species detectable in +ESI-FT-ICR MS in the oils from the nitrate or perchlorate treatments did not decrease in relative abundance to the same extent as was observed in the oil from the souring control column. There was a ~5% decrease in the relative abundance of the N_1 class in the oils from both treatments and a minimal (<0.5%) change in the relative abundances of the N_1O_1 and N_1O_2 classes.

An increase in the relative abundances of compounds containing either 2 or 4 oxygen atoms (O_2 and O_4 classes) in both the oils from the biosouring control and nitrate treated columns is illustrated in Figure 3.4b. There was a ~6-fold increase in the relative abundances of compounds belonging to the O_2 and O_4 classes in the oil from the biosouring control column when compared to those relative abundances in the parent crude oil. There was also a similar increase in the relative abundances of compounds belonging to the O_2 and O_4 classes in the oil from the nitrate treated column. There was not an increase in the relative abundances of compounds containing either 1 or 3 oxygen atoms (O_1 and O_3 classes) in either of these oils. There were minimal increases in oxygenated content (O_1-O_4 classes) in the oil from the perchlorate treatment, further corroborating the conclusion that the perchlorate treatment inhibited hydrocarbon degradation and product formation.

The O_2 and O_4 compound classes detected in -ESI-FT-ICR MS are most likely dominated by compounds containing one or two carboxylic acid functional groups, respectively. The increasing abundance of these carboxylic acids provides further support for microbiological transformations, as they are typical products of biodegradation.[52,53] These compounds form via the activation and transformation of monoaromatic hydrocarbons and PAHs by bacteria endogenously incorporating fumaric acid to a benzyl radical,[54] thereby creating benzylsuccinate derivatives by charging and detoxifying the aromatic ring. This microbial process results in carboxylic acid formation. Microbial communities can then utilize these products as an electron donor or carbon source.[54-56]

Smaller molecular weight compounds of the C_{20}-C_{30} molecular size range containing two or four oxygen atoms were successfully identified in the oils from the biosouring control and nitrate treated columns using GC-VUV-TOF. While the position of the carboxyl group on most of the observed compounds is unknown, authentic standards (Sigma-Aldrich, St. Louis, MO, USA) confirmed the identification of a subset of the broader range of C_{20}-C_{30} carboxylic acids in these oil samples. The results of -ESI combined with FT-ICR MS illustrated that the range of carboxylic acids produced extended to C_{30}-C_{60} compounds, which are outside the analytical range of GC-VUV-TOF. The combination of monoaromatic hydrocarbon and PAH degradation and production of $C_xH_yO_2$ and $C_xH_yO_4$ compounds supports the interpretation that a fumarate addition to hydrocarbons occurred during biodegradation.

3.4.7 Molecular Distribution of Biodegradation Products

Compositional changes of crude oil between timepoints for all members of a heteroatom class can be visualized in images of N_{DBE} versus carbon number. Isoabundance-contoured plots of N_{DBE} versus carbon number for the N_1, N_1O_1, N_1O_2, and N_1S_1 classes derived from +ESI combined with FT-ICR MS of the parent crude oil, oil from the souring control column, oil from the nitrate treated column, and oil from the perchlorate treated column are shown in Figure 3.5a. Compounds pertaining to the N_1O_1 class in the oil from the soured column increased in carbon number range from C_{20}-C_{60} to C_{10}-C_{75} and N_{DBE} range from 5-25 to 3-30 when compared to the ranges of the parent crude oil. Similarly, compounds of the N_1O_2 class in the oil from the soured column increased from C_{30}-C_{55} to C_{20}-C_{80} and from 7-17 to 7-27 N_{DBE} when compared to the ranges of the parent crude oil. The increase of species containing both nitrogen and oxygen atoms within the soured oil's chemical composition indicates that microbial catabolism of crude oil can result in the production of larger molecular weight compounds that were not present in the original parent oil. There was an increase in the carbon number and N_{DBE} ranges of compounds belonging to the N_1O_1 and N_1O_2 classes in the oils from the nitrate and perchlorate treated columns, but the ranges are far less than they are in the oil from the souring control column.

Isoabundance-contoured plots of N_{DBE} versus carbon number for the O_1, O_2, O_3, and O_4 classes derived from -ESI combined with FT-ICR MS of the parent crude oil, oil from the souring control column, oil from the nitrate treated column, and oil from the perchlorate treated column are shown in Figure 3.5b. While there are minimal changes in the molecular distributions of O_1 and O_3 compounds in any of the oils, the relative abundances of O_2 compounds of C_{10}-C_{60} and 5-25 N_{DBE} increased in both the oils from the souring and nitrate treated columns compared to the abundances in the parent crude oil. The O_4 compounds of C_{10}-C_{60} and 3-23 N_{DBE} also increased in relative abundance in both the oils from the souring and nitrate treated columns compared to the abundances in the parent crude oil. The increases in abundances and changes in O_2 and O_4

compound distributions were not as apparent in the oil from the perchlorate treated column, further bolstering the conclusion that perchlorate injections inhibited biotransformation of the parent crude oil.

3.4.8 Environmental and Industrial Applications

This chapter provides a comprehensive temporal characterization of microbial transformations of crude oil as a result of biosouring and subsequent treatments. In the oil from the souring control column, C_{10}-C_{15} aliphatic compounds were first degraded followed by transformation of C_{10}-C_{26} monoaromatic species. Both the nitrate and perchlorate treatments mitigated sulfide production, but the nitrate treatment accelerated the rate of biotransformation of crude oil hydrocarbons while the perchlorate treatment inhibited the majority of biotransformation. +ESI and -ESI combined with FT-ICR MS revealed increases in the relative abundances of oxygenated biodegradation products, involving the addition of two or four oxygen atoms to existing hydrocarbons, in both the oils from the biosouring control and nitrate treated columns. These products are indicative of monocarboxylic and dicarboxylic acids. No such increases were observed in the oil from the perchlorate treated column. Based on the lack of hydrocarbon degradation and product formation, perchlorate injections may be the preferred treatment for industrial biosouring.

The differences in transformation patterns observed in the oils from the souring control column, the nitrate treated column, and the perchlorate treated column demonstrate that the degree of microbial biotransformation of crude oil is specific to the presence of a dominant electron acceptor, the relative abundances of microbial communities,[35] and the availability of specific crude oil components as electron donors and carbon sources. While it has been shown that microbial communities can activate a range of hydrocarbons for degradation that is significantly greater than that which can be metabolized,[56] this chapter reveals that hydrocarbon degradation and product formation of crude oil is not limited to a narrow range of compound classes or molecular weights. Isomers of hydrocarbons from C_{10}-C_{30} were degraded and carboxylic acid products were formed up to molecular sizes of C_{60}. The biotransformation patterns and product formations revealed in this chapter can constrain and strengthen existing models of crude oil degradation patterns for industrial and environmental applications.

3.5 Acknowledgements

The authors acknowledge Kevin Wilson for his assistance at the Chemical Dynamics Beamline 9.0.2 at the Advanced Light Source, Dana Loutey for sample extraction from the bioreactor columns, and Ryan Rodgers at the National High Magnetic Field Laboratory for valuable discussion and insight. The authors acknowledge the Energy Biosciences Institute (EBI) for funding this work under Fund 86217. A portion of this work was performed at the National High Magnetic Field Laboratory, which is funded by the National Science Foundation through DMR 11-57490 and the State of Florida.

3.6 References

(1) Youssef, N.; Elshahed, M. S.; McInerney, M. J. Microbial processes in oil fields: culprits, problems, and opportunities. *Advances in Applied Microbiology*. **2009**, *66*, 141-251.

(2) Gieg, L. M.; Jack, T. R.; Foght, J. M. Biological souring and mitigation in oil reservoirs. *Applied Microbiology and Biotechnology*. **2011**, *92* (2), 263-282.

(3) Myhr, S.; Lillebo, B. L. P.; Sunde, E.; Beeder, J.; Torsvik, T. Inhibiton of microbial H_2S production in an oil reservoir model column by nitrate injection. *Applied Microbiology and Biotechnology*. **2002**, *58* (3), 400-408.

(4) Greene, E. A.; Hubert, C.; Nemati, M.; Jenneman, G. E.; Voordouw, G. Nitrite reductase activity of sulphate-reducing bacteria prevents their inhibition by nitrate-reducing, sulphide-oxidizing bacteria. *Environmental microbiology*. **2003**, *5* (7), 607-617.

(5) Tang, K.; Baskaran, V.; Nemati, M. Bacteria of the sulphur cycle: An overview of microbiology, biokinetics and their role in petroleum and mining industries. *Biochemical Engineering Journal*. **2009**, *44*, 73-94.

(6) Williamson, N. Chapter 18: Health and safety issues from the production of hydrogen sulphide. *Applied Microbiology and Molecular Biology of Oilfield Systems*. **2008**, *13*, 151-157.

(7) Hubbard, C. G.; Cheng, Y.; Engelbrektson, A.; Druhan, J. L.; Li, L.; Ajo-Franklin, J. B.; Coates, J. D.; Conrad, M.E. Isotopic insights into microbial sulfur cycling in oil reservoirs. *Frontiers in Microbiology.* **2014**. *5*, 1-12.

(8) Dunsmore, B.; Youldon, J.; Thrasher, D. R.; Vance, I. Effects of nitrate treatment on a mixed species, oil field microbial biofilm. *J. Ind. Microbio. Biotech.* **2006**, *33*, 454-462.

(9) Xue, Y.; Voordouw, G. Control of microbial sulfide production with biocides and nitrate in oil reservoir simulating bioreactors. *Frontiers in Microbiology*. **2015**, *6*, 1387-1398.

(10) Voordouw, G.; Grigoryan, A.A.; Lambo, A.; Lin, S.P.; Park, H.S.; Jack, T.R.; Coombe, D.; Clay, B.; Zhang, F.; Ertmoed, R.; Miner, K.; Arensdorf, J.J. Sulfide remediation by pulsed injection of nitrate into a low temperature Canadian heavy oil reservoir. *Environmental Science & Technology*. **2009**, *43* (24), 9512-9518.

(11) Callbeck, C.M.; Agrawal, A.; Voordouw, G. Acetate production from oil under sulfate-reducing conditions in bioreactors injected with sulfate and nitrate. *Appl Environ Microbiol*. **2013**, *79* (16), 5059-5068.

(12) Grigoryan, A.A.; Cornish, S.L.; Buziak, B.; Lin, S.; Cavallaro, A.; Arensdorf, J.J.; Voordouw, G. Competitive oxidation of volatile fatty acids by sulfate- and nitrate-reducing bacteria from an oil field in Argentina. *Appl. Environ. Microbiol.* **2008**, *74* (14), 4324-4335.

(13) Callbeck, C.; Dong, X.; Chatterjee, I.; Agrawal, A.; Caffrey, S.; Sensen, C. Microbial community succession in a bioreactor modeling a souring low-temperature oil reservoir subjected to nitrate injection. *Appl. Microbiol. Biotechnol*. **2001**, *91* (3), 799–810.

(14) Hubert, C.; Nemati, M.; Jenneman, G.; Voordouw, G. Containment of biogenic sulfide production in continuous up-flow packed-bed bioreactors with nitrate or nitrite. *Biotech. Prog.* **2003**, *19* (2), 338-345.

(15) Engelbrektson, A.; Hubbard, C. G.; Tom, L. M.; Boussina, A.; Jin, Y. T.; Wong, H.; Piceno, Y. M.; Carlson H. K.; Conrad, M. E.; Anderson, G.; Coates, J. D. Inhibition of microbial sulfate reduction in a flow-through column system by (per)chlorarte treatment. *Frontiers in Microbiology*. **2014**, *5*, 1-11.

(16) Baeuerle, P. A.; Huttner, W. B. Chlorate—a potent inhibitor of protein sulfation in intact cells. *Biochem. Biophys. Res. Commun*. **1986**, *141* (2), 870–877.

(17) Coates, J. D.; Achenbach, L. Microbial perchlorate reduction: rocket-fueled metabolism. A. *Nat. Rev. Microbiol*. **2004**, *2* (7), 569–580.

(18) Gregoire, P.; Engelbrektson, A.; Hubbard, C. G.; Metlagel, Z.; Csencsits. R.; Auer, M. Control of sulfideogenesis through bio-oxidation of H_2S coupled to (per)chlorate reduction. *Environ. Microbiol*. **2014**, *6* (16), 558-564.

(19 Gieg, L. M.; Davidova, I. A.; Duncan, K. E.; Suflita, J. M. Methanogenesis, sulfate reduction and crude oil biodegradation in hot Alaskan oilfields. *Environmental Microbiology*. **2010**, *12* (11), 3074-3086.

(20) Drozd, G. T.; Worton, D. R.; Aeppli, C.; Reddy, C. M.; Zhang, H.; Variano, E.; Goldstein, A. G. Modeling comprehensive chemical composition of weathered oil following a marine spill to predict ozone and potential secondary aerosol formation and constraint transport pathways. *J. Geophys. Res. Oceans.* **2015**, *120*, (11), 7300-7315.

(21) Aitken, C. M.; Jones, D. M.; Larter, S. R. Anaerobic hydrocarbon biodegradation in deep subsurface oil reservoirs. *Nature*. **2004**, *431* (7006), 291-294.

(22) Townsend, G. T.; Prince, R. C.; Suflita, J. M. Anaerobic oxidation of crude oil hydrocarbons by the resident microorganisms of a contaminated anoxic aquifer. *Environ. Sci. Technol*. **2003**, *37* (22), 5213–5218.

(23) Townsend, G. T.; Prince, R. C.; Suflita, J. M. Anaerobic biodegradation of alicyclic constituents of gasoline and natural gas condensate by bacteria from an anoxic aquifer. *FEMS Microbiology Ecology*. **2004**, *49* (1), 129–135.

(24) Walters, C. C.; Wang, F .C.; Qian, K.; Wu, C.; Mennito, A. S.; Wei, Z. Petroleum alteration by thermochemical sulfate reduction-A comprehensive molecular study of aromatic hydrocarbons and polar compounds. *Geochimica et Cosmochimica Acta*. **2015**, *153*, 37-71.

(25) Fingas, M. *Handbook of Oil Spill Science and Technology*. **2015**.

(26) Reddy, C. M.; Quinn, J. G. GC-MS analysis of total petroleum hydrocarbons and polycyclic aromatic hydrocarbons in seawater samples after the north cape oil spill. *Marine Pollution Bulletin*. **1999**, *38*, 126-135.

(27) White, H. K.; Xu, L.; Hartmann, P.; Quinn, J. G.; Reddy, C. M. Unresolved complex mixture (UCM) in coastal environments is derived from fossil sources. *Environ. Sci. Technol*. **2013**, *47*, 726-731.

(28) Isaacman, G.; Wilson, K.; Chan, A.; Worton, D.; Kimmel, J.; Nah, T.; Hohaus, T.; Gonin, M.; Kroll, J. H.; Worsnop, D. R.; Goldstein, A. H. Improved resolution of hydrocarbon structures and constitutional isomers in complex mixtures using gas chromatography-vacuum ultraviolet-mass spectrometry. *Anal. Chem*. **2012**, *84* (5), 2335−2342.

(29) Kaiser, N. K.; Quinn, J. P.; Blakney, G. T.; Hendrickson, C. L.; Marshall, A. G. A novel 9.4 tesla FTICR mass spectrometer with improved sensitivity, mass resolution, and mass range. *J. Am. Soc. Mass Spectrom.* **2011,** *22* (8), 1343-1351.

(30) A. G. Marshall.; Rodgers, R. P. Petroleomics: Chemistry of the underworld. *PNAS*. **2008**, *105* (47), 18090-18095.

(31) Hughey, C. A.; Hendrickson, C. L.; Rodgers, R. P.; Marshall, A. G. Elemental composition analysis of processed and unprocessed diesel fuel by electrospray ionization Fourier transform ion cyclotron resonance mass spectrometry. *Energy Fuels*. **2001**, *15* (5), 1186−1193.

(32) Marshall, A. G.; Hendrickson, C. L.; Jackson, G. S. Fourier transform ion cyclotron resonance mass spectrometry: a primer. *Mass Spectrom. Rev.* **1998**, *17* (1), 1-35.

(33) McKenna, A. M.; Williams, J. T.; Putman, J. C.; Aeppli, C. Reddy, C. M.; Valentine, D. L.; Lemkau, K. L.; Kellermann, M. Y.; Savory, J. J.; Kaiser, N. K.; Marhsall, A. G.; Rodgers, R. P. Unprecedented ultrahigh resolution FT-ICR mass spectrometry and parts-per-billion mass accuracy enable direct characterization of nickel and vanadyl porphyrins in petroleum from natural seeps. *Energy Fuels*. **2014**, *28* (4), 2454-2464.

(34) Kaiser, N.; Savory, J.; McKenna, A.; Quinn, J.; Hendrickson, C. L. Electrically compensated fourier transform ion cyclotron resonance cell for complex mixture mass analysis. *Anal. Chem*. **2011**, *83* (17), 6907−6910.

(35) Shrestha, P. M.; Williamson, A. J.; Barnum, T. P.; Liu, Y.; Nowak, J.; Loutey, D.; Louie, W.; Kim, H.; Chin, W. S.; Mayilvahanan, K. S.; Shabbir, T.; Goldstein, A.; Coates, J. D. Microbial biosouring control using perchlorate treatment in crude oil reservoir simulated condition. *In prep.*

(36) Cline, J. Spectrophotometric determination of hydrogen sulfide in natural waters. *Limnology and Oceanography*. **1969**, *14*, 454-458.

(37) Worton, D.; Zhang, H.; Isaacman, G.; Chan, A.; Wilson, K.; Goldstein, A. Comprehensive chemical characterization of hydrocarbons in NIST standard reference material 2779 Gulf of Mexico crude oil. *Environ. Sci. Tech.* **2015**, *49* (22), 13130-13138.

(38) Chan, A.; Isaacman, G.; Wilson, K.; Worton, D.; Ruehl, C.; Nah, T.; Gentner, D. R.; Dallmann, T. R.; Kirchstetter, T.; Harley, R.; Gilman, J.; Kuster, W.; de Gouw, J.; Offenberg, J.; Kleindienst, T.; Lin, Y.; Rubitschun, C.; Surratt, J.; Hayes, P.; Jimenez, J.; Goldstein, A. H. Detailed chemical characterization of unresolved complex mixtures in atmospheric organics: insights into emission sources, atmospheric processing, and secondary organic aerosol formation. *Journal of Geophysical Research: Atmospheres*. **2013**, *118*, 6783−6796.

(39) McKenna, A. M.; Nelson, R. K.; Reddy, C. M.; Savory, J. J.; Kaiser, N. K.; Fitzsimmons, J. E.; Marshall, A. G.; Rodgers, R. P. Expansion of the analytical window for oil spill characterization by ultrahigh resolution mass spectrometry: beyond gas chromatography. *Environ. Sci. Tech*. **2013**, *47* (13), 7530-7539.

(40) Lobodin, V. V.; Juyal, P.; McKenna, A. M.; Rodgers, R. P.; Marshall, A. G. Tetramethylammonium hydroxide as a reagent for complex mixture analysis by negative ion electrospray ionization mass spectrometry. *Anal. Chem.* **2013,** *85* (16), 7803-7808.

(41) Ruddy, B. M.; Huettel, M.; Kostka, J. E.; Lobodin, V. V.; Bythell, B. J.; McKenna, A. M.; Aeppli, C.; Reddy, C. M.; Nelson, R. K.; Marshall, A. G.; Rodgers, R. P. Targeted petroleomics: analytical investigation of macondo well oil oxidation products from pensacola beach. *Energy Fuels*, **2014**, *28* (6), 4043-4050.

(42) Rodgers, R. P.; Schaub, T. M.; Marshall, A. G. Petroleomics: MS return to its roots. *Anal. Chem.* **2005**, *77*, 20A-27A.

(43) McLafferty, F. W.; Turecek, F., *Interpretation of Mass Spectra, 4th ed.* University Science Books: Mill Valley, CA, 1993.

(44) Worton, D. R.; Isaacman, G.; Gentner, D. R.; Dallmann, T. R.; Chan, A. W. H.; Ruehl, C.; Kirchstetter, T. W.; Wilson, K. R.; Harley, R. A.; Goldstein, A. H. Lubricating oil dominates primary organic aerosol emissions from motor vehicles. *Environ. Sci. Technol.* **2014**, *48*, 3698−3706.

(45) Mao, D.; Van De Weghe, H.; Lookman, R.; Vanermen, G.; De Brucker, N.; Diels, L. Resolving the unresolved complex mixture in motor oils using high-performance liquid chromatography followed by comprehensive two-dimensional gas chromatography. *Fuel*. **2009**, *88*, 312−318.

(46) Aeppli, C.; Nelson, R.K.; Radović, J.R.; Carmichael, C.A.; Valentine, D.L.; Reddy, C.M. Recalcitrance and degradation of petroleum biomarkers upon abiotic and biotic natural weathering of *Deepwater Horizon* oil. *Environ. Sci. Tech*. **2014**, *48*, (12), 6726-6734.

(47) Aitken, C. M.; Jones, D. M.; Maguire, M. J.; Gray, N. D.; Sherry, A.; Bowler, B. F. J.; Dicthfield, A. K.; Larter, S. R.; Head, I. M. Evidence that crude oil alkane activation proceeds by different mechanisms under sulfate-reducing and methanogenic conditions. *Geochimica et Cosmochimica Acta*. **2013**, *109*, 162-174.

(48) Rueter, P.; Rabus, R.; Wilkest, H.; Aeckersberg, F.; Rainey, F. A.; Jannasch, H. W.; Widdel, F. Anaerobic oxidation of hydrocarbons in crude oil by new types of sulphate-reducing bacteria. *Nature*. **1994**, *372*, 455-458.

(49) Ommedal, H.; Torsvik, T. Desulfotignum toluenicum sp. nov., a novel toulene-degrading, sulphate-reducing bacterium isolated from an oil-reserovir model column. *International Journal of Systematic and Evolutionary Microbiology*. **2007**. *57* (12), 2865-2869.

(50) Nakagawa, T.; Sato, S.; Yamamoto, Y.; Fukui, M. Successive changes in community structure of an ethylbenzene-degrading sulfate-reducing consortium. *Water Research*. **2002**, *36* (11), 2813-2823.

(51) Zedelius, J.; Rabus, R.; Grundmann, O.; Werner, I.; Brodkorb, D.; Schreiber, F.; Ehrenreich, P.; Behrends, A.; Wilkes, H.; Kube, M.; Reinhardt, R.; Widdel, F. Alkane degradation under anoxic conditions by a nitrate-reducing bacterium with possible involvement of the electron acceptor in substrate activation. *Environ. Microbiol. Rep.* **2011**, *3* (1), 125–135.

(52) Atlas, R. M. Microbial degradation of petroleum hydrocarbons: an environmental perspective. *Microbiol. Rev.* **1981**, *45* (1), 180−209.

(53) Aeppli, C.; Carmichael, C. A.; Nelson, R. K.; Lemkau, K. L.; Graham, W. M.; Redmond, M. C.; Valentine, D. L.; Reddy, C. M. Oil weathering after the *Deepwater Horizon* disaster led to the formation of oxygenated residues. *Environ. Sci. Tech*. **2012**, *46*, 8799-8807.

(54) Bharadway, V.; Vyas, S.; Villlano, S.; Maupin, C.; Dean, A. Unraveling the impact of hydrocarbon structure on the fumarate addition mechanism-a gas-phase ab initio study. *Phys. Chem. Chem. Phys*. **2015**, *17* (6), 4054-4066.

(55) Kühner, S.; Wöhlbrand, L.; Fritz, I.; Wruck, W.; Hultschig, C.; Hufnagel, P.; Kube, M.; Reinhardt, R.; Rabus, R. Substrate-dependent regulation of anaerobic degradation pathways for toluene and ethylbenzene in a denitrifying bacterium, strain EbN1. *J. Bacteriol*. **2005**, *187* (4), 1493–1503.

(56) Jarling, R.; Kuhner, S.; Basilio Janke E.; Gruner, A.; Drozdowska, M.; Golding, B.T.; Rabus, R.; Wilkes, R. Versatile transformations of hydrocarbons in anaerobic bacteria: substrate ranges and regio- and stereo-chemistry of activation reactions. *Frontiers in Microbiology*. **2015**, *6*, 5-14.

3.7 Figures

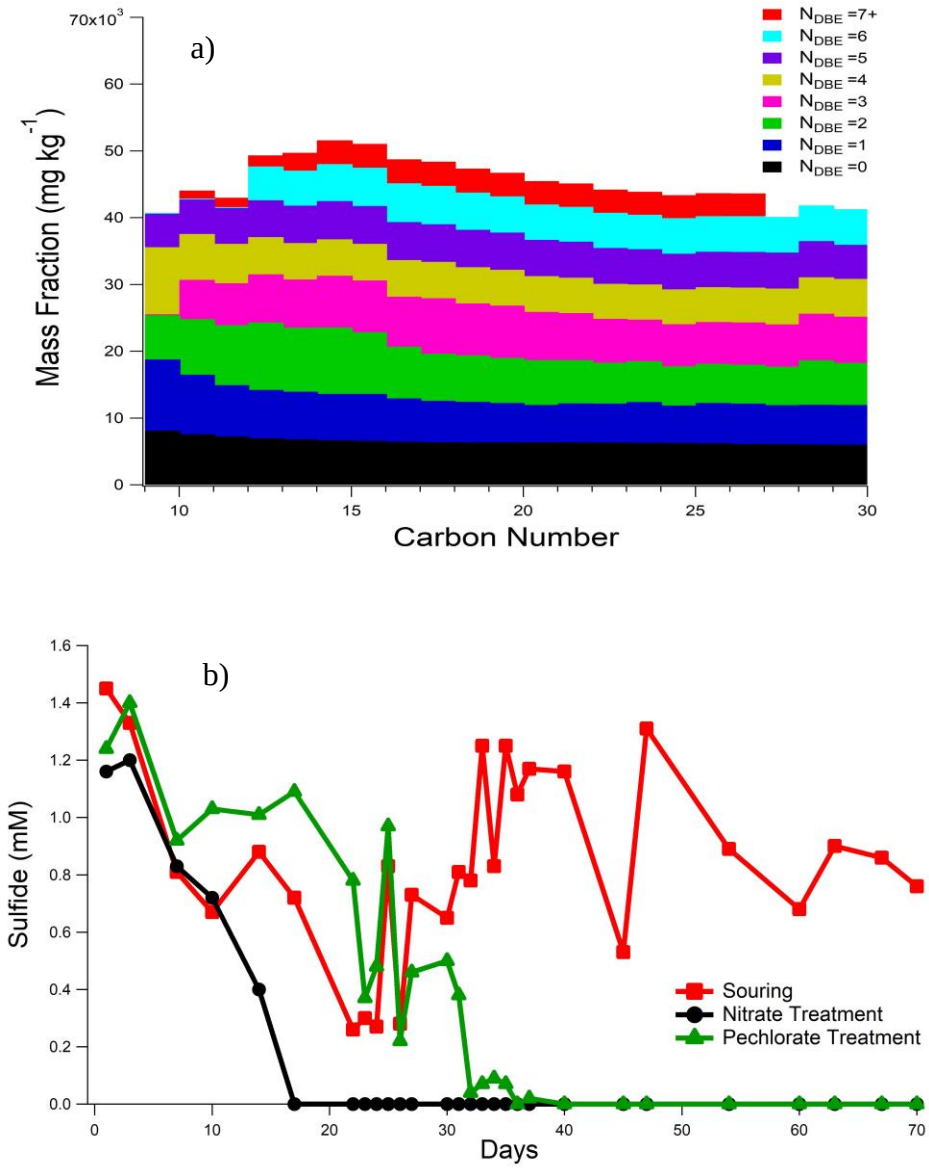

Figure 3.1. (a) Chemical composition of the original parent North Sea crude oil as a function of both carbon number (C_9-C_{30}) and double bond equivalent (N_{DBE}) chemical class. (b) Sulfide concentrations as a function of time in the souring control column, nitrate treated column, and perchlorate treated column.

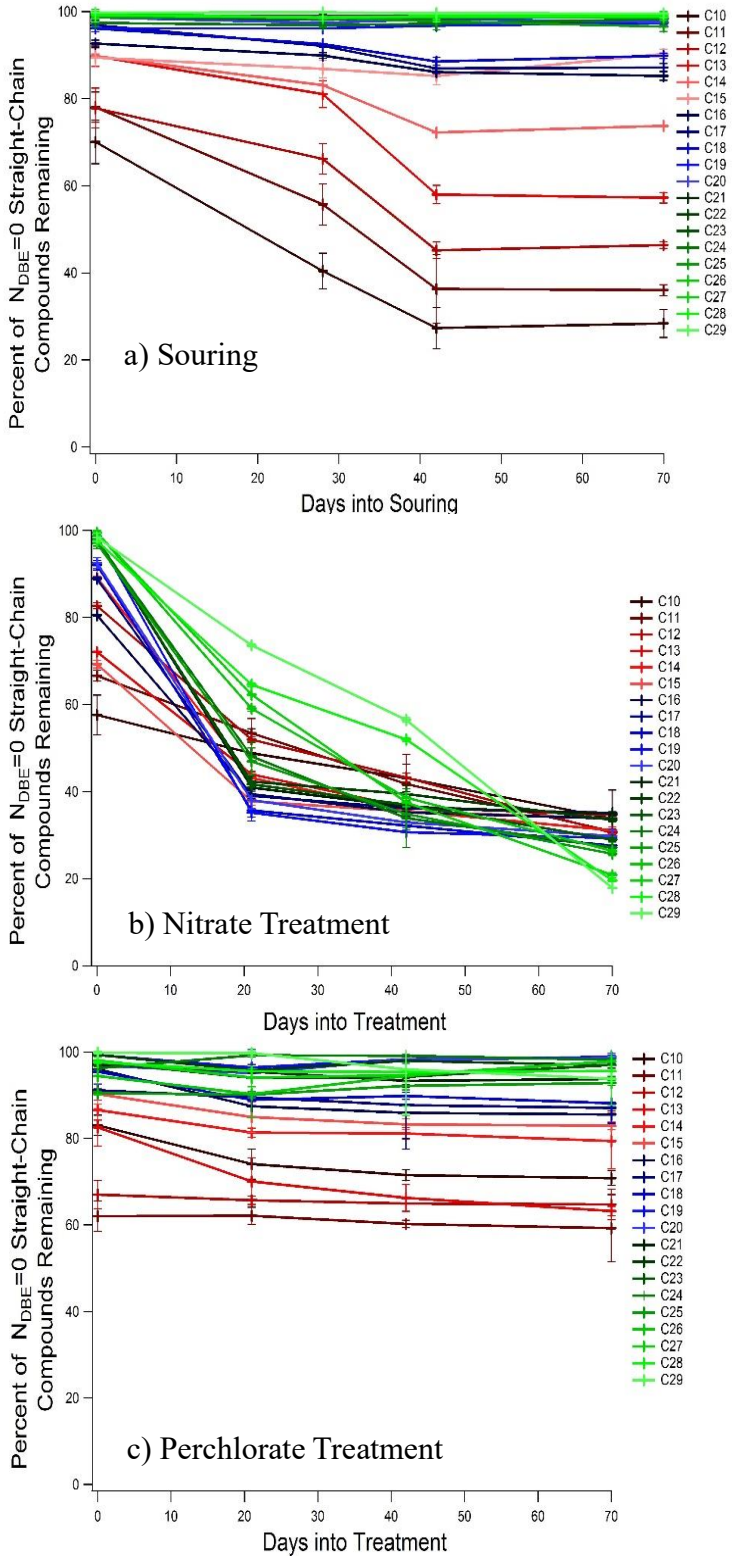

Figure 3.2. Transformations of straight-chain alkanes (N_{DBE}=0) as a function of time in oils from the (a) souring control, (b) nitrate treated, and (c) perchlorate treated columns, measured by GC-VUV-TOF. Bars indicate minimum and maximum percentages (n=2).

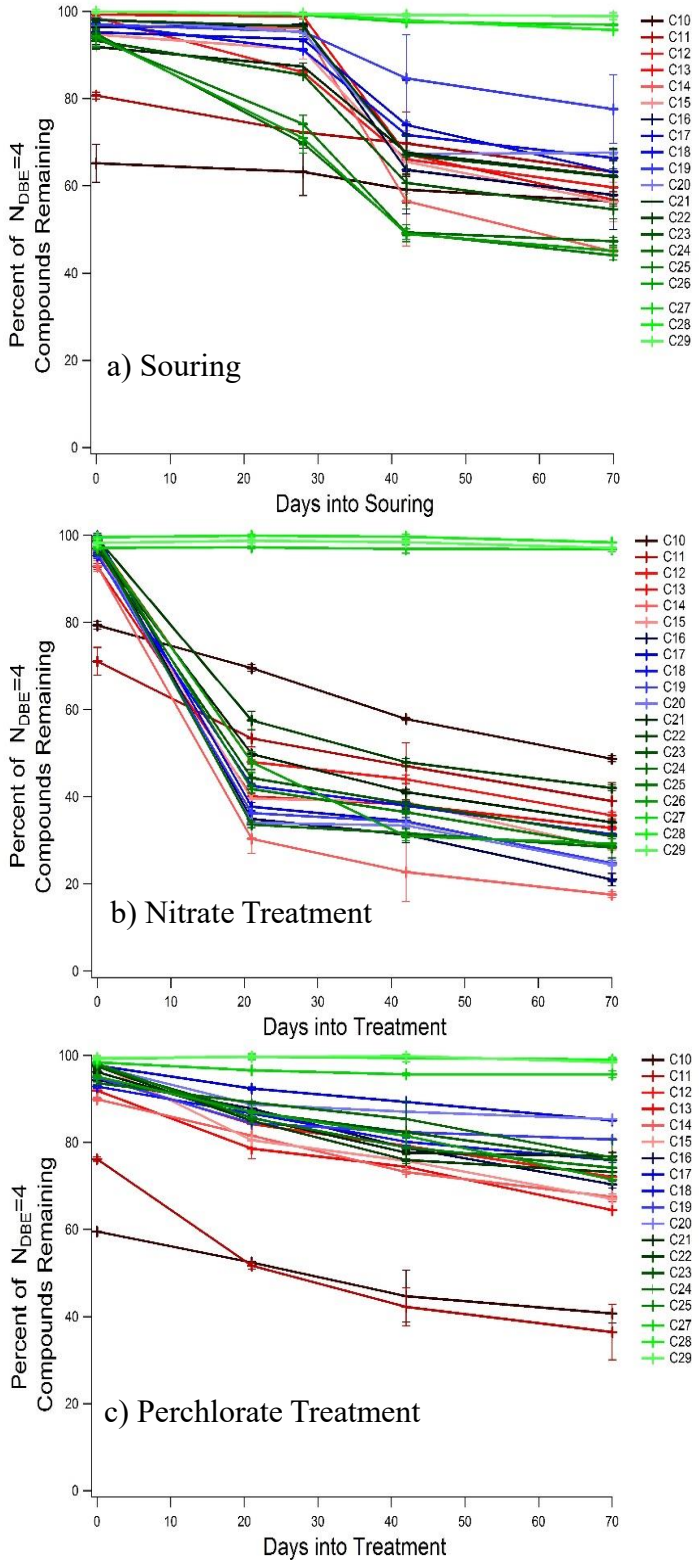

Figure 3.3. Transformations of isomerically summed monoaromatic compounds (N_{DBE}=4) as a function of time in oils from the a) souring control, (b) nitrate treated, and (c) perchlorate treated columns, measured by GC-VUV-TOF. Bars indicate minimum and maximum percentages (n=2).

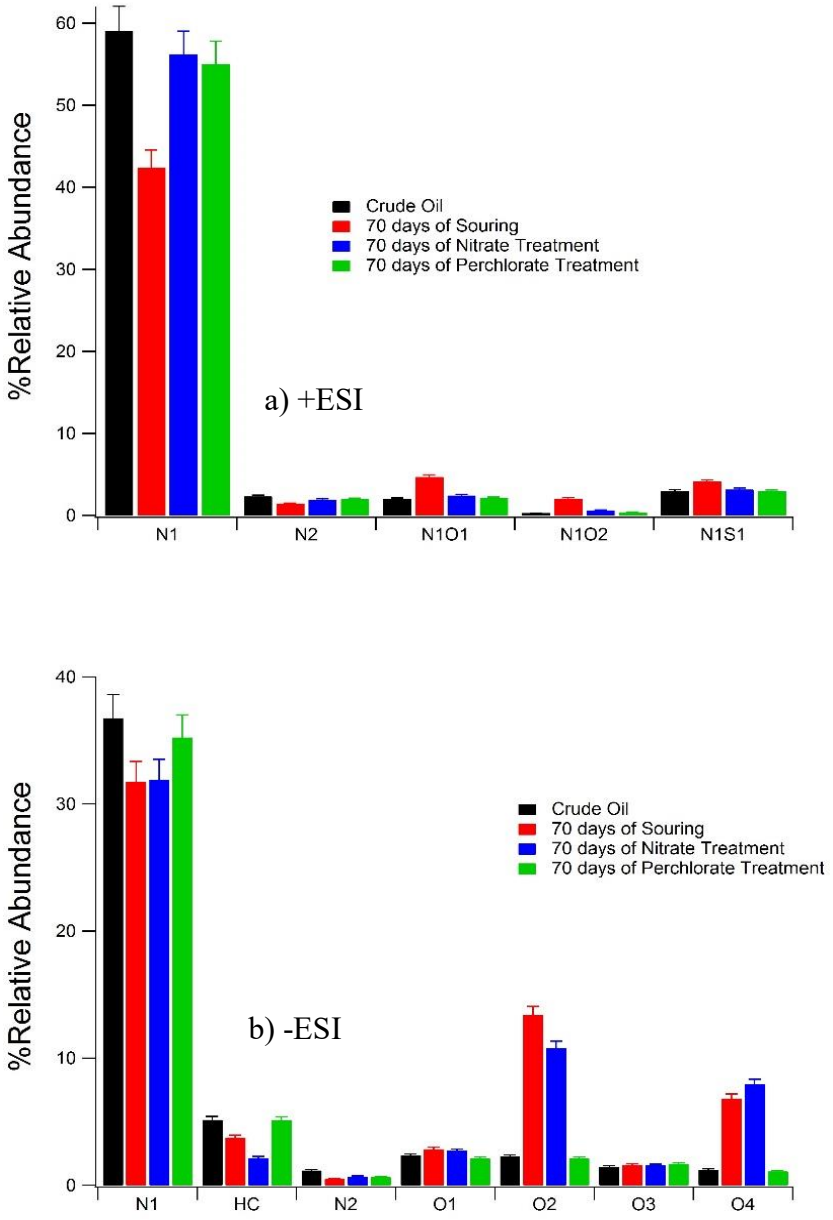

Figure 3.4. Relative abundance (%) of molecular formulas containing different heteroatoms observed using (a) positive electrospray ionization and (b) negative electrospray ionization combined with FT-ICR MS of parent North Sea crude oil, oil from 70 days into souring, oil from 70 days into the nitrate treatment, and oil from 70 days into the perchlorate treatment.

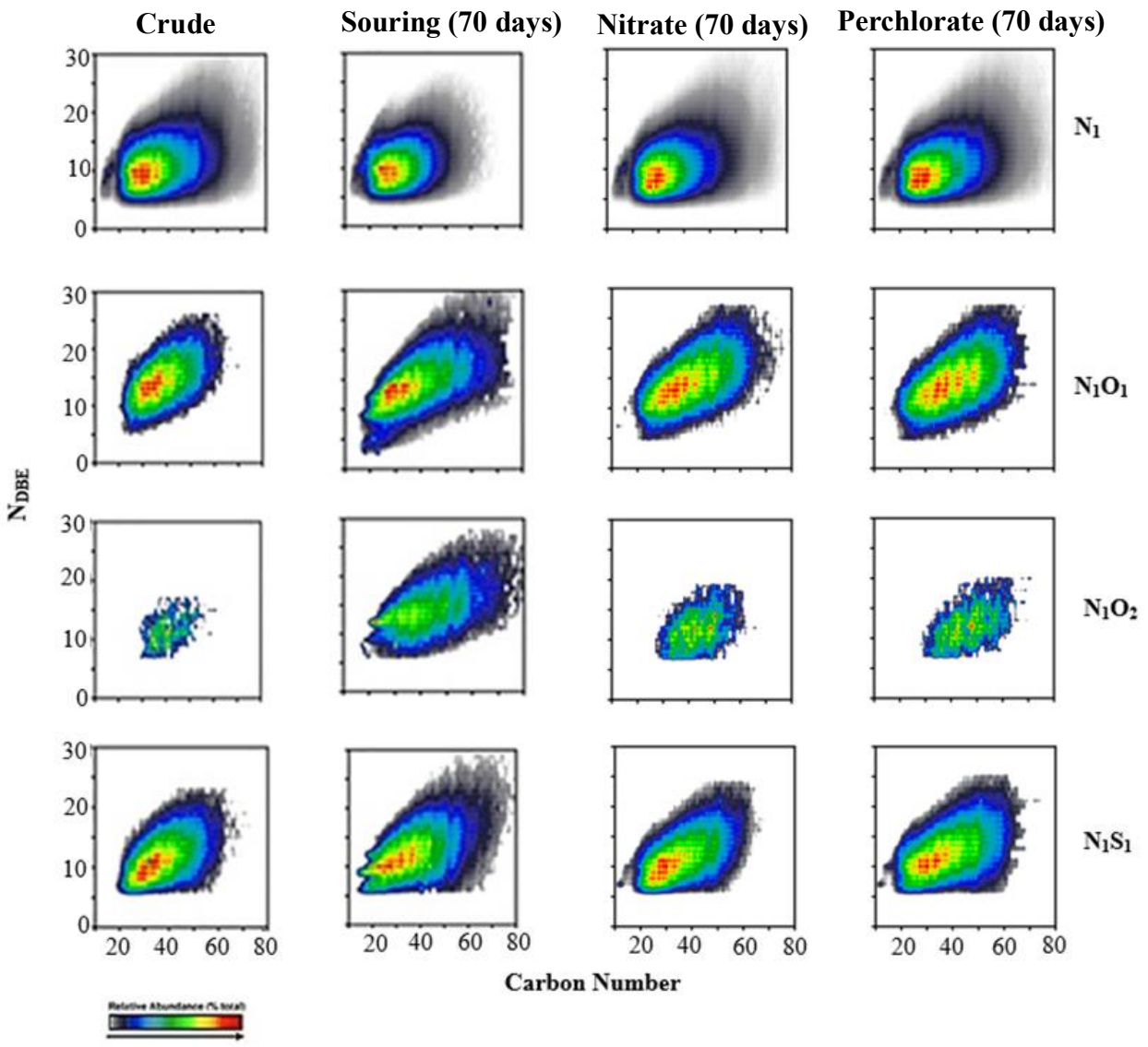

Figure 3.5a. Isoabundance-contoured plots of double bond equivalents (N_{DBE}) vs carbon number for parent North Sea crude oil, oil from 70 days into souring, oil from 70 days into the nitrate treatment, and oil from 70 days into the perchlorate treatment measured by positive electrospray ionization. Each compositional image is normalized to the most abundant species within that heteroatom class for each mass spectrum.

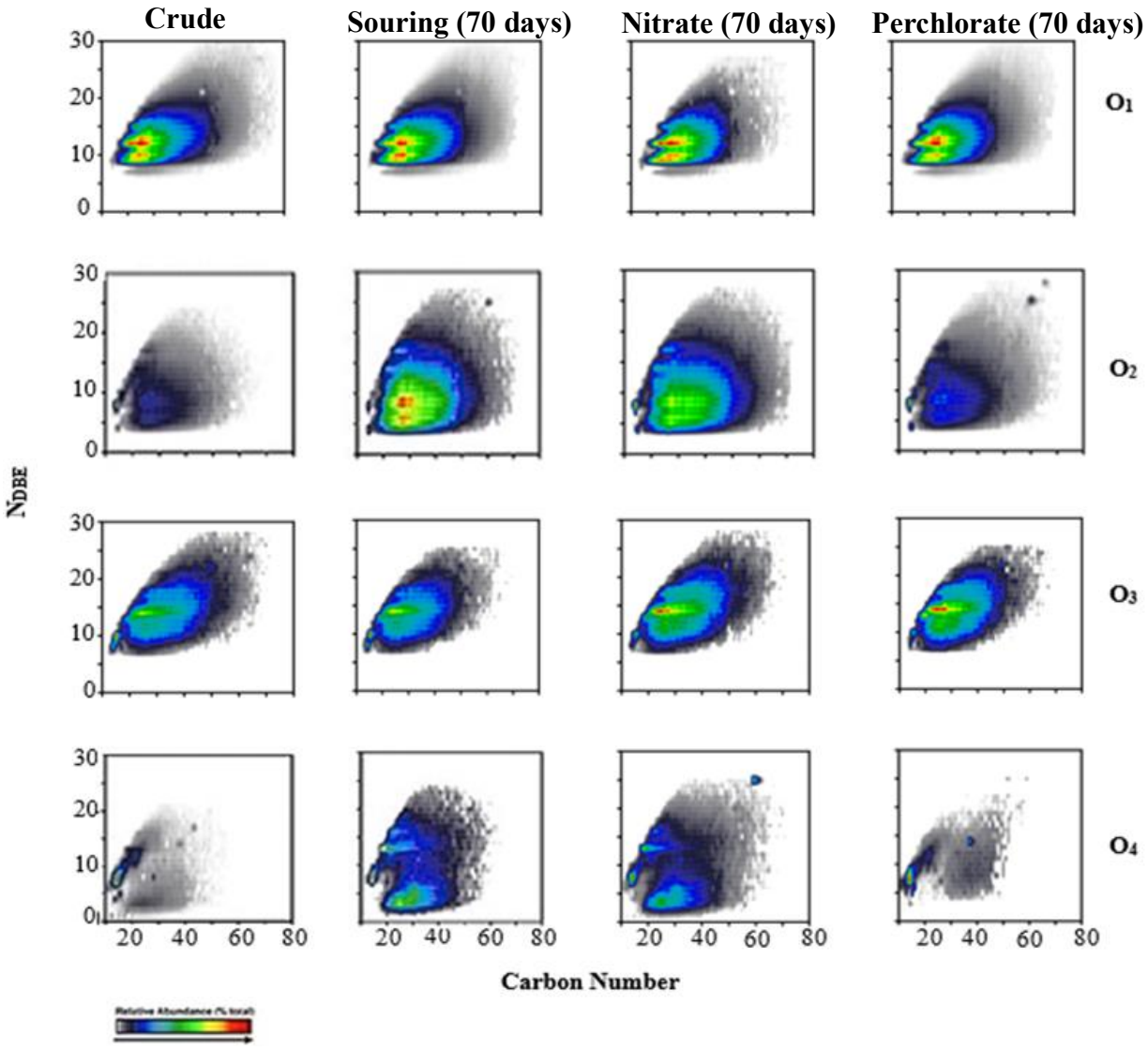

Figure 3.5b. Isoabundance-contoured plots of double bond equivalents (N_{DBE}) vs carbon number for parent North Sea crude oil, oil from 70 days into souring, oil from 70 days into the nitrate treatment, and oil from 70 days into the perchlorate treatment measured negative electrospray ionization combined with FT-ICR MS. Each compositional image is normalized to the most abundant species within that heteroatom class for each mass spectrum.

3.8 Supplemental Information

3.8.1 Analytical Methods and Calibration Methodology for Gas Chromatography

Conventional chemical characterization of crude oil relies on gas chromatography-mass spectrometry with electron ionization (EI).[1,2] This technique incorporates hard ionization (~70 eV) that is unable to separate, identify, and quantify many hydrocarbons in oil which elute as an organic unresolved complex mixture (UCM).[3] Over 80% of the oil's chemical composition is represented by this UCM in typical GC-MS analyses.[4] Even with comprehensive two-dimensional gas chromatography,[5,6] it is difficult to separate isomeric hydrocarbon species as molecular weights increase. Soft single-photon ionization using a rare-gas excimer vacuum ultraviolet lamp enhances a compound's parent ion signal to allow identification based on molecular weight, but lowers compound signal sensitivity compared to that of EI.[7] Gas chromatography combined with vacuum ultraviolet radiation and time-of-flight mass spectrometry (GC-VUV-TOF) overcomes the limitations of traditional chromatographic techniques to comprehensively summarize the chemical composition of complex organic mixtures up to the molecular volatility limit of the GC columns (~320^{o}C).[8] Vacuum ultraviolet light from the Advanced Light Source (ALS) at the Lawrence Berkeley National Laboratory (LBNL) provides a soft ionization source (~10.5 eV) with high photon flux (~10^{15} photons/s)[9] to minimize compound fragmentation and allow mass spectral resolution based on carbon number and chemical class. This technique has been used previously to characterize complex atmospheric aerosol mixtures and crude oil obtained from the *Deepwater Horizon* oil spill (NIST SRM 2779).[8-10]

The molecular ion signal for each compound class is used as the basis for quantification. The molecular ion's signal strength is dependent on the compound's transfer efficiency through the GC column, ionization efficiency, and degree of fragmentation.[9] Authentic standards (Sigma-Aldrich, St. Louis, MO, USA), including alkanes, branched alkanes, cycloalkanes, monoaromatic hydrocarbons, hopanes, steranes, polycyclic aromatic hydrocarbons (PAHs), alkylated PAHs, and acids were used for identification and quantification of hydrocarbons. Compounds were classified based on carbon number and double bond equivalent (N_{DBE}) chemical class.[11] Compounds of the same N_{DBE} class fragment similarly upon VUV photoionization regardless of carbon number,[9,10] yielding the same mass-response calibration curves used to quantify hydrocarbon classes. Perdeuterated alkanes (Sigma-Aldrich, St. Louis, MO, USA) from C_{10}-C_{36} were used as an internal standard in all samples to establish a relationship between transfer efficiency and retention time. All response signals upon calibration were normalized to a recalcitrant $C_{30}H_{52}$ hopane biomarker.[10]

3.8.2 Analytical Methods and Calibration Methodology for Mass Spectrometry

Nitrogen, oxygen, and sulfur-containing compounds in crude oil challenge GC-based analytical approaches due to increased polarity and decreased volatility that require higher temperatures to volatilize to elute from the GC. The GC-VUV-TOF technique is limited to compounds with volatilities below the temperature limits of the column phase (~320^{o}C) to prevent both compound and column degradation. The mass resolution of the time-of-flight instrument ($m/\Delta m_{50\%} \approx 4000$) in GC-VUV-TOF is also insufficient to separate the overlaps in molecular weights that result from heavier oxygenated compounds.[12] Ultrahigh resolution Fourier transform ion cyclotron resonance mass spectrometry (FT-ICR MS) is used to compare the compositional changes that occur between oil samples as a function of time to both expand the analytical window of identifiable compounds and to identify biodegradation products.

The immense chemical and structural diversity of crude oil challenges nearly all ionization techniques. Previous studies on crude oil by FT-ICR MS have applied electrospray ionization (ESI) to target polar compounds[13-15] and atmospheric pressure photoionization (APPI) to target nonpolar compounds.[16,17] Heavy oil studies have also applied field desorption, field ionization, and atmospheric pressure laser-induced acoustic desorption to target specific chemical functionalities.[18,19] The selectivity of ESI highlights polar compounds and has been combined with FT-ICR MS and applied extensively to analyze weathered crude oils, identifying over 80,000 unique elemental compositions in weathered and biotransformed oil residues.[20-22] This ionization method generates quasimolecular ions, $[M+H]^+$ in +ESI and $[M-H]^-$ in -ESI,[23] where ionization efficiency is a function of analyte acidity or basicity and dependent on chemical structure and composition. More conjugated systems and electronegative functional groups (i.e. carboxylic acids) possess a lower ionization potential, and thus a higher ionization efficiency, and are more efficiently ionized in ESI.[13,23]

For ESI in this chapter, the sample solution was infused via a microelectrospray source[24] (50 µm internal diameter fused silica emitter) at 400 nL/min by a syringe pump. For –ESI the emitter voltage was -2.5 kV, the tube lens voltage was -350 V, and the heated metal capillary current was 4 A. Cations in +ESI were formed under the same conditions as anions, but with positive voltages.

Ions were accumulated in an external linear quadrupole ion trap for 500-5000 ms and transferred by rf-only quadrupoles (2.1 MHz and 255 V_{p-p} amplitude) to the ICR cell[25,26] equipped with a 9.4 T horizontal 220 mm bore diameter superconducting solenoid magnet operated at room temperature. The ICR cell had a 7 segment open cylindrical configuration with capacitively coupled excitation electrodes based on the Tolmachev configuration.[27,28] Time-domain transients of 6.1 s were collected (n=100) and averaged, half–Hanning apodized, and zero-filled prior to fast Fourier transformation.[29,30] A modular ICR data station (Predator)[31] facilitated instrument control, data acquisition, and analysis.

Broadband phase correction[32] was applied to all collected spectra to increase resolution of isobaric species. Fourier transformation of time-domain data yields real and imaginary frequency-domain spectra, Re(ω) and Im(ω), that are linear combinations of absorption and dispersion-mode components, A(ω) and D(ω). The FT-ICR spectra are typically displayed in magnitude (absolute-value) mode, $M(\omega)=[[Re(\omega)]^2+[Im(\omega)]^2]^{1/2}$. It is possible to determine the phase angle, $\varphi=\tan^{-1}[Im(\omega)/Re(\omega)]$, for each peak[32] and construct the appropriate linear combination of real and imaginary spectra to recover the absorption mode. This correction results in spectra with resolving power a factor of 2 higher than that of magnitude mode.[32]

The ICR frequencies were converted to masses based on the quadrupolar trapping potential approximation.[33,34] Each spectrum was internally calibrated to an abundant homologous alkylation series whose members differ in mass by integer multiples of 14.01565 Da (mass of CH_2). A "walking" calibration equation was then used to further increase mass accuracy.[35] Masses were converted from the International Union of Pure and Applied Chemistry (IUPAC) mass scale to the Kendrick mass scale[36] to identify homologous series for each heteroatom class (species with the same $C_cH_hN_nO_oS_s$ elemental composition differing only by the degree of alkylation). Peak assignments were accomplished by Kendrick mass defect analysis.[37,38] Data visualization was rendered with PetroOrg software.[39]

3.8.3 Supplemental Figures

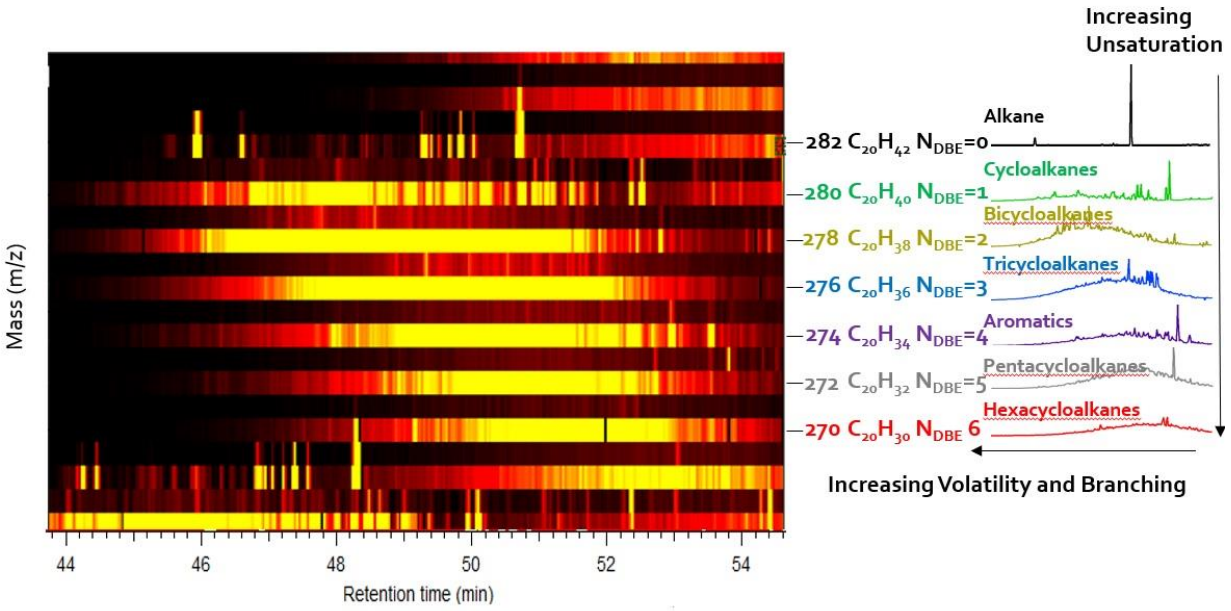

Supplemental Figure 3.1. A portion of a GC-VUV-TOF chromatogram of crude oil. Hydrocarbon classes are separated based on carbon number, degree of saturation, and degree of volatility. Straight-chain alkanes are separated from branched alkanes by volatility and are quantified separately. For N_{DBE}=1 and higher, the integral of all isomers is quantified as a sum, providing a comprehensive approach to analysis of the crude oil's chemical composition.

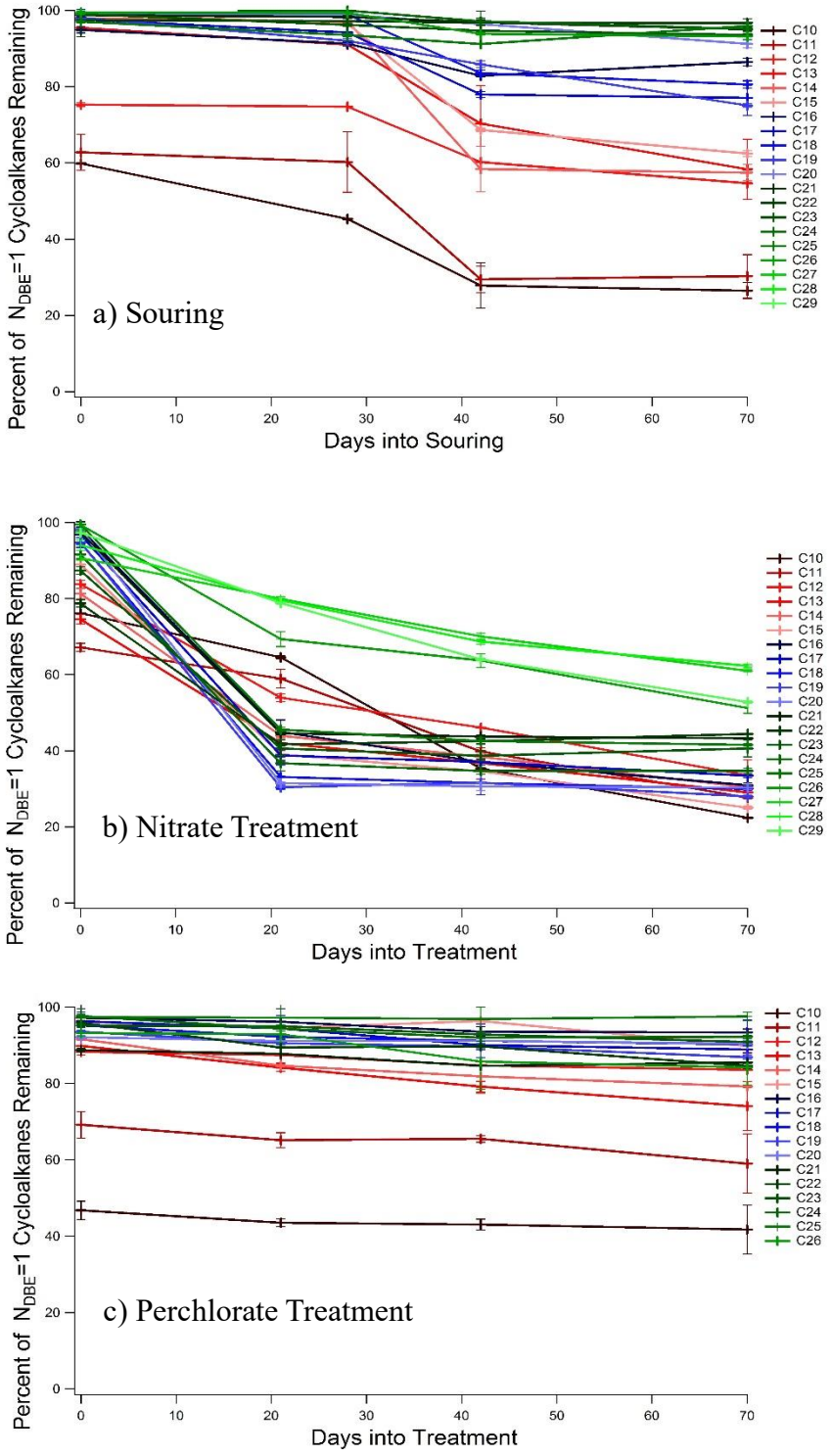

Supplemental Figure 3.2. Transformations of isomerically summed N_{DBE}=1 monocycloalkanes as a function of time in oils from the (a) souring control, (b) nitrate-treated, and (c) perchlorate-treated columns, measured by GC-VUV-TOF. Bars indicate minimum and maximum percentages (n=2).

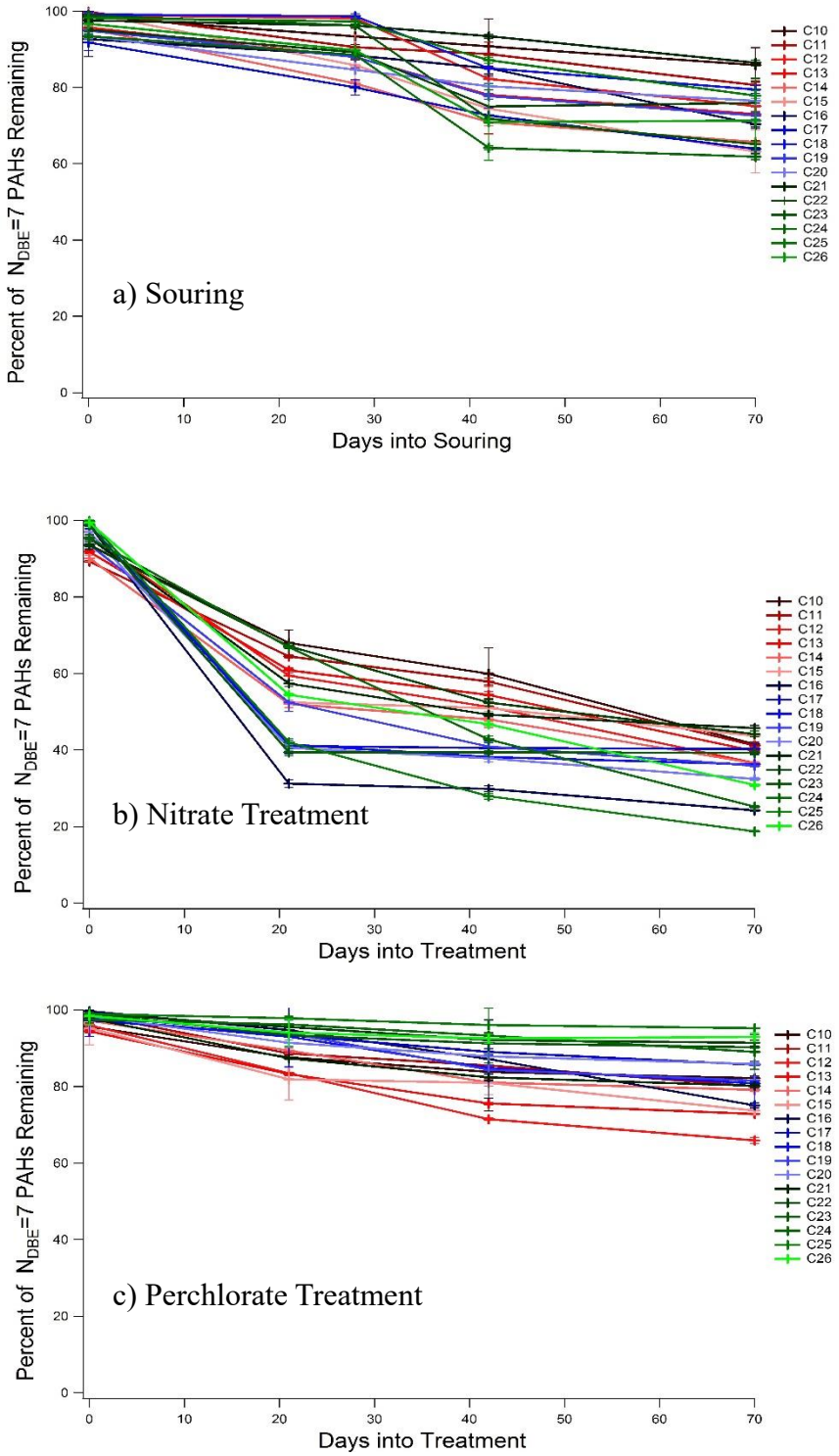

Supplemental Figure 3.3. Transformations of isomerically summed N_{DBE}=7 polycyclic aromatic hydrocarbons (PAHs) as a function of time in oils from the (a) souring control, (b) nitrate-treated, and (c) perchlorate-treated columns, measured by GC-VUV-TOF. Bars indicate minimum and maximum percentages (n=2).

3.8.4 Supplemental References

(1) Fingas, M. *Handbook of Oil Spill Science and Technology.* **2015**.

(2) Reddy, C. M.; Quinn, J. G. GC-MS analysis of total petroleum hydrocarbons and polycyclic aromatic hydrocarbons in seawater samples after the north cape oil spill. *Marine Pollution Bulletin*. **1999**, *38*, 126-135.

(3) Wang, Z.; Fingas, M. Development of oil hydrocarbon fingerprinting and identification techniques. *Marine Pollution Bulletin.* **2003,** *47*, 423-452.

(4) White, H. K.; Xu, L.; Hartmann, P.; Quinn, J. G.; Reddy, C. M. Unresolved complex mixture (UCM) in coastal environments is derived from fossil sources. *Environ. Sci. Technol*. **2013**, *47*, 726-731.

(5) Frysinger, G. S.; Gaines, R. B.; Xu, L.; Reddy, C.M. Resolving the unresolved complex mixture in petroleum-contaminated sediments. *Environ. Sci. Technol*. **2003**, *37*, 1653-1662.

(6) van Mispelaar, V. G.; Smilde, A. K.; de Noord, O. E.; Blomberg, J.; Schoenmakers, P. J. Classification of highly similar crude oils using data sets from comprehensive two-dimensional gas chromatography and multivariate techniques. *J Chrom. A.* **2005**, *1096*, 156-164.

(7) Zimmermann, R.; Mühlberger, F.; Fuhrer, K.; Gonin, M.; Welthagen, W. An ultracompact photo-ionization time-of-flight mass spectrometer with a novel vacuum ultraviolet light source for on-line detection of organic trace compounds as a detector for gas chromatography. *Journal of Material Cycles and Waste Management*. **2008**, *10*, 24-31.

(8) Isaacman, G.; Wilson, K.; Chan, A.; Worton, D.; Kimmel, J.; Nah, T.; Hohaus, T.; Gonin, M.; Kroll, J. H.; Worsnop, D. R.; Goldstein, A. H. Improved resolution of hydrocarbon structures and constitutional isomers in complex mixtures using gas chromatography-vacuum ultraviolet-mass spectrometry. *Anal. Chem*. **2012**, *84* (5), 2335−2342.

(9) Chan, A.; Isaacman, G.; Wilson, K.; Worton, D.; Ruehl, C.; Nah, T.; Gentner, D. R.; Dallmann, T. R.; Kirchstetter, T.; Harley, R.; Gilman, J.; Kuster, W.; de Gouw, J.; Offenberg, J.; Kleindienst, T.; Lin, Y.; Rubitschun, C.; Surratt, J.; Hayes, P.; Jimenez, J.; Goldstein, A. H. Detailed chemical characterization of unresolved complex mixtures in atmospheric organics: insights into emission sources, atmospheric processing, and secondary organic aerosol formation. *Journal of Geophysical Research: Atmospheres*. **2013**, *118*, 6783−6796.

(10) Worton, D.; Zhang, H.; Isaacman, G.; Chan, A.; Wilson, K.; Goldstein, A. Comprehensive chemical characterization of hydrocarbons in NIST standard reference material 2779 Gulf of Mexico crude oil. *Environ. Sci. Tech.* **2015**, *49* (22), 13130-13138.

(11) McLafferty, F. W.; Turecek, F., *Interpretation of Mass Spectra, 4th ed.* University Science Books: Mill Valley, CA, 1993.

(12) Rodgers, R. P.; Schaub, T. M.; Marshall, A. G. Petroleomics: MS return to its roots. *Anal. Chem.* **2005**, *77*, 20A-27A.

(13) Hughey, C. A.; Hendrickson, C. L.; Rodgers, R. P.; Marshall, A. G. Elemental composition analysis of processed and unprocessed diesel fuel by electrospray ionization Fourier transform ion cyclotron resonance mass spectrometry. *Energy Fuels*. **2001**, *15* (5), 1186−1193.

(14) Hughey, C. A.; Minardi, C. S.; Galasso-Roth, S. A.; Paspalof, G. B.; Mapolelo, M. M.; Rodgers, R. P.; Marshall, A. G.; Ruderman, D. L. Naphthenic acids as indicators of crude oil biodegradation in soil, based on semi-quantitative electrospray ionization Fourier transform ion cyclotron resonance mass spectrometry. *Rapid Commun. Mass Spectrom*. **2008**, *22*, 3968−3976.

(15) Chen, H.; Hou, A.; Corilo, Y. E.; Lin, Q.; Lu, J.; Mendelssohn, I. A.; Zhang, R.; Rodgers, R.P.; McKenna, A.M. 4 years after the *Deepwater Horizon* spill: molecular transformation of Macondo well oil in Louisiana salt marsh sediments revealed by FT-ICR mass spectrometry. *Environ. Sci. Tech.* **2016**, *50*, 9061-9069.

(16) Purcell, J. M.; Hendrickson, C. L.; Rodgers, R. P.; Marshall, A. G. Atmospheric pressure photoionization Fourier transform ion cyclotron resonance mass spectromety for complex mixture analysis. *Anal. Chem.* **2006**, *78*, 5906-5912.

(17) Purcell, J. M.; Rodgers, R. P.; Hendrickson, C. L.; Marshall, A. G. Atmospheric pressure photoionization proton transfer for complex organic mixtures investigated by fourier transform ion cyclotron resonance mass spectrometry. *J. Am. Soc. Mass Spectrom.* **2007**, *18*, 1682-1689.

(18) Podgorski, D.C.; Hamdan, R.; McKenna, A. M.; Nyadong, L.; Rodgers, R. P.; Marshall, A. G.; Cooper, W. T. Characterization of pyrogenic black carbon by desorption atmospheric pressure photoionization Fourier transform ion cyclotron resonance mass spectrometry. *Anal. Chem*. **2012**, *84*, 1281-1287.

(19) Nyadong, L.; McKenna, A. M.; Hendrickson, C. L.; Rodgers, R. P.; Marshall, A. G. Atmospheric pressure laser-induced acoustic desorption chemical ionization Fourier transform ion cyclotron resonance mass spectrometry for the analysis of complex mixtures. *Anal. Chem*. **2011**, *83*, 1616-1623.

(20) McKenna, A. M.; Williams, J. T.; Putman, J. C.; Aeppli, C. Reddy, C. M.; Valentine, D. L.; Lemkau, K. L.; Kellermann, M. Y.; Savory, J. J.; Kaiser, N. K.; Marhsall, A. G.; Rodgers, R. P. Unprecedented ultrahigh resolution FT-ICR mass spectrometry and parts-per-billion mass accuracy enable direct characterization of nickel and vanadyl porphyrins in petroleum from natural seeps. *Energy Fuels*. **2014**, *28* (4), 2454-2464.

(21) Ruddy, B. M.; Huettel, M.; Kostka, J. E.; Lobodin, V. V.; Bythell, B. J.; McKenna, A. M.; Aeppli, C.; Reddy, C. M.; Nelson, R. K.; Marshall, A. G.; Rodgers, R. P. Targeted petroleomics: analytical investigation of macondo well oil oxidation products from Pensacola Beach. *Energy Fuels*, **2014**, *28* (6), 4043-4050.

(22) McKenna, A. M.; Nelson, R. K.; Reddy, C. M.; Savory, J. J.; Kaiser, N. K.; Fitzsimmons, J. E.; Marshall, A. G.; Rodgers, R. P. Expansion of the analytical window for oil spill characterization by ultrahigh resolution mass spectrometry: beyond gas chromatography. *Environ. Sci. Tech*. **2013**, *47* (13), 7530-7539.

(23) Zhan, D. L.; Fenn, J. B. Electrospray mass spectrometry of fossil fuels. *Int. J. Mass Spectrom*. **2000**, *194*, 197–208.

(24) Emmett, M. R.; White, F. M.; Hendrickson, C. L.; Shi, S. D.-H.; Marshall, A. G. Application of micro-electrospray liquid chromatography techniques to FT-ICR MS to enable high-sensitivity biological analysis. *J. Am. Soc. Mass Spectrom.* **1998,** *9*, 333-340.

(25) Podgorski, D.; Corilo, Y.; Nyadong, L.; Lobodin, V.; Bythell, B.; Robbins, W.; McKenna, A.; Marshall, A.; Rodgers, R. Heavy petroleum composition 5. Compositional and structural continuum of petroleum revealed. *Energy Fuels*. **2013**, *27*, 1268−1276.

(26) Kaiser, N. K.; Savory, J. J.; Hendrickson, C. L. Controlled ion ejection from an external trap for extended m/z range in FT-ICR mass spectrometry. *J. Am. Soc. Mass Spectrom.* **2014,** *25*, 943-949.

(27) Tolmachev, A. V.; Robinson, E. W.; Wu, S.; Kang, H.; Lourette, N. M.; Pasa-Tolic, L.; Smith, R. D. Trapped-ion cell with improved dc potential harmonicity for FT-ICR MS. *J. Am. Soc. Mass Spectrom.* **2008,** *19*, 586-597.

(28) Tolmachev, A. V.; Robinson, E. W.; Wu, S.; Smith, R. D.; Pasa-Tolic, L. Trapping radial electric field optimization in compensated FTICR cells. *J Am Soc Mass Spectrom.* **2011,** *22*, 1334-1342.

(29) Xian, F.; Corilo, Y. E.; Hendrickson, C. L.; Marshall, A. G. Baseline correction of absorption-mode Fourier transform ion cyclotron resoancne mass spectra. *Int. J. Mass Spectrom.* **2012,** *325*, 67-72.

(30) Xian, F.; Hendrickson, C. L.; Blakney, G. T.; Beu, S. C.; Marshall, A. G. Automated broadband phase correction of fourier transform ion cyclotron resonance mass spectra. *Anal. Chem.* **2010,** *82*, 8807-8812.

(31) Blakney, G. T.; Hendrickson, C. L.; Marshall, A. G. Predator data station: a fast data acquisition system for FT-ICR MS experiments. *Int. J. Mass Spectrom.* **2011,** *306*, 246-252.

(32) Beu, S. C.; Blakney, G. T.; Quinn, J. P.; Hendrickson, C. L.; Marshall, A. G. Broadband phase correction of FT-ICR mass spectra via simultaneous excitation and detection *Anal. Chem.* **2004,** *76*, 5756-5761.

(33) Shi, S. D.-H.; Drader, J. J.; Freitas, M. A.; Hendrickson, C. L.; Marshall, A. G. Comparison and interconversion of the two most common frequency-to-mass calibration functions for Fourier transform ion cyclotron resonance mass spectrometry. *Int. J. Mass Spectrom.* **2000,** *195/196*, 591-598.

(34) Grosshans, P. B.; Chen, R.; Limbach, P. A.; Marshall, A. G. Linear excitation and detection in Fourier transform ion cyclotron resonance mass spectrometry. *Int. J. Mass Spectrom. And Ion Procceses.* **1994,** *139*, 169-189.

(35) Savory, J. J.; Kaiser, N. K.; McKenna, A. M.; Xian, F.; Blakney, G. T.; Rodgers, R. P.; Hendrickson, C. L.; Marshall, A. G. Parts-Per-Billion Fourier Transform Ion Cyclotron Resonance Mass Measurement Accuracy with a "Walking" Calibration Equation. *Anal. Chem.* **2011,** *83*, 1732-1736.

(36) Kendrick, E. A mass scale based on CH_2=14.0000 for high resolution mass spectrometry of organic compounds. *Anal. Chem.* **1963,** *35*, 2146-2154.

(37) Hughey, C. A.; Hendrickson, C. L.; Rodgers, R. P.; Marshall, A. G.; Qian, K. Kendrick mass defect spectrum: a compact visual analysis for ultrahigh-resolution broadband mass spectra. *Anal. Chem.* **2001,** *73*, 4676-4681.

(38) Wu, Z.; Rodgers, R. P.; Marshall, A. G. Two- and three-dimensional van Krevelen diagrams: a graphical analysis complementary to the Kendrick mass plot for sorting elemental compositions of complex organic mixtures based on ultrahigh-resolution broadband Fourier transform ion cyclotron resonance mass measurements. *Anal. Chem.* **2004,** *76*, 2511-2516.

(39) Coril, Y. E., PetroOrg Software. *Florida State University; All Rights reserved.* *http://www.petroorg.com*

Chapter 4

Dependence of Crude Oil Microbial Catabolism on Hydrocarbon Isomer Structure

This chapter is adapted from:

Jeremy A. Nowak, Robert J. Weber, Herbert Volk, Pravin M. Shrestha, John D. Coates, Allen H. Goldstein
"Dependence of Crude Oil Microbial Catabolism on Hydrocarbon Isomer Structure"
Submitted to *Organic Geochemistry,* March 2019.

4.1 Abstract

Microbial catabolism is a natural biological process that can sour crude oil reservoirs, transform spilled oil, and is an engineering tool in hydrocarbon pollution remediation strategies. Crude oil typically contains a wide number of hydrocarbon isomers of a broad range of molecular formulas and structures. It is important to advance the understanding of how differences in structure (such as degree of branching or position of alkyl substituents) affect relative catabolic attack of alkanes, monocycloalkanes, or monoaromatic hydrocarbons in order to determine which compounds will be altered most by these processes and which will be recalcitrant. This study used gas chromatography combined with variable ionization time-of-flight-mass spectrometry (GC-Select-eV-TOF-MS) at 14 eV to characterize catabolic patterns of hydrocarbon isomers in crude oil from four different oil fields exposed to a single complex microbial community. We comprehensively characterized changes in alkanes, monocycloalkanes, and monoaromatic hydrocarbons to identify differences in biodegradation as a function of degree of branching and alkyl position. Hydrocarbon isomers with terminal alkyl branches were more prone to biotransformation than those with methyl groups further from the terminal position. Compounds with alkyl branches adjacent to each other experienced less biodegradation than isomers with nonadjacent methyl groups. These patterns were consistent regardless of hydrocarbon structural class or oil composition, implying that isomeric structure, including the shape of the carbon chain and the alkyl position, dictates patterns of catabolism of hydrocarbons of a particular molecular class. The patterns identified in this work demonstrate that microbial metabolism leaves a distinct signature from other transformation processes occurring in spilled oil, such as atmospheric oxidation or evaporation, providing a unique fingerprint to distinguish biodegradation from those of other processes involved in oil weathering.

4.2 Introduction

Ancient and extant microbial metabolism plays an important role in the physical-chemical characteristics of crude oil produced from oil reservoirs. In oil recovery processes, sulfate-reducing microbial communities inadvertently catabolize crude oil hydrocarbons in situ as sources of energy and electrons, producing copious quantities of toxic, corrosive, and explosive hydrogen sulfide in a process known as biosouring.[1,2] Alternatively, crude oil-derived hydrocarbons can enter natural marine environments through anthropogenic activities such as oil spills[3,4] and pose a significant

threat to wildlife and marine ecosystems. Over the last 50 years, numerous diverse microorganisms have been identified and characterized that are capable of utilizing complex hydrocarbons as carbon sources and electron donors for metabolism and growth.[5-7] In many instances, such as the Deepwater Horizon oil spill in 2010, the abundance of these oil degrading microbial communities has been the basis of intrinsic hydrocarbon remediation strategies.

Several strains of bacteria are known to be capable of degrading straight-chain alkanes, monocycloalkanes, monoaromatic hydrocarbons, and polycyclic aromatic hydrocarbons under either aerobic or anaerobic conditions.[8,9] Past studies have demonstrated microbial communities degrading oil-derived aromatic products in marine sediments, aliphatic compounds in polluted tropical streams, and hydrocarbons in marine ecosystems after major oil spills.[10-12]

Microbial catabolism depends on a variety of environmental and biological factors, including the availability of suitable microbial communities and labile crude oil components.[13-15] The chemical composition of crude oil is ~90% pure hydrocarbons[16] and the hydrocarbon distribution, based on structural class and branching, can vary depending on the oil's origin, initial composition, or degree of weathering[17,18]. While most alkanes, monocycloalkanes, and aromatic species in a crude oil are presumed to be susceptible to microbial attack,[19,20] hopanes and steranes are less susceptible and act as recalcitrant biomarkers in crude oil to which the degradation of other compounds can be compared.[21] Anaerobic biodegradation of crude oil hydrocarbons through β-oxidation and the incorporation of benzylsuccinate derivatives occurs at a slower rate than in aerobic biodegradation.[2,22,23]

Previous studies have illustrated how microbial communities preferentially catabolize linear alkanes of crude oil hydrocarbons over branched.[24-26] The position of the alkyl branch on a straight-chain alkane influences the relative catabolism of branched hydrocarbon isomers.[27-29] These studies have been limited to characterizing alkanes of lower molecular weights ($<C_8$), rather than extending compound transformation patterns as a function of branching to heavier alkanes. To our knowledge, it has not been previously reported how the degree of branching or the position of an alkyl substituent affects microbial metabolism of isomers of cycloalkanes or aromatic species.

Studies of crude oil catabolism have typically utilized traditional gas chromatography (GC) that couples a volatility separation of the oil's hydrocarbons with a flame ionization detector (FID) or with an electron ionization mass spectrometer (EI MS) at 70 eV.[3,30] This classic hard ionization technique imparts a large excess of energy to organic molecules, resulting in fragmentation that complicates quantification and identification of branched hydrocarbon isomers.[31] In order to overcome the limitations of traditional GC-MS to characterize the effects of structural branching and oil composition on hydrocarbon biodegradation, this chapter incorporates GC combined with variable ionization time-of-flight-mass spectrometry (GC-Select-eV-TOF-MS) at 14 eV. This soft ionization technique enhances the molecular ion and reduces compound fragmentation to more easily identify and quantify branched hydrocarbon isomers in crude oil.

In this chapter, an active crude-oil degrading, sulfate-reducing marine microbial community was used to inoculate microcosm bottles containing crude oils from four different oil fields (North Sea, Azerbaijan, Texas, and the Gulf of Mexico). The compositions of these four oils have been previously characterized and reported in extensive detail.[32] Samples were extracted from the bottles at different time points throughout a 20-week incubation timeline and analyzed via GC-Select-eV-TOF-MS in order to understand the extent of microbial catabolism as a function of a crude oil's hydrocarbon distribution. While no attempt was made to trace the products of microbial hydrocarbon metabolism due to the complexity of analysis and the lack of specific tracers (e.g.

^{13}C), loss of hydrocarbon components from the crude oil in comparison to heat-killed and uninoculated controls was considered indicative of microbial catabolism. This chapter identifies how microbial catabolism of crude oil affects the isomeric distribution of alkanes, monocycloalkanes, and monoaromatic hydrocarbons. Furthermore, the chemical signature of biotransformation is shown to differ from that of other environmental removal pathways, such as atmospheric oxidation or evaporation of hydrocarbons.[4,33] Analysis of the isomer distributions in weathered oil potentially provides a novel forensic approach to differentiating the dominant weathering processes for crude oil produced from an oil reservoir or for spilled oil remaining in the environment.

4.3 Experimental Methods

4.3.1 Bottle Experiment Setup

Microbial media for growth was created by combining 35.9 g Instant Ocean (Spectrum Brands, Blacksburg, VA), 0.05 g KH_2PO_4, 0.32 g NH_4Cl, 4.26 g Na_2SO_4, and 1 mL trace element solution[34] with 1 liter of deionized water. 70 mL of this media were dispensed into 125 mL serum bottles. These bottles were flushed with N_2 to establish an anaerobic environment. The bottles were autoclaved and a 10% v/v microbial inoculum enrichment subculture from reactor columns used in a previous study[2] was added into each bottle. Autoclaved controls were created by inoculating bottles with the same enrichment from the reactor columns after it had been autoclaved. Abiotic controls were created by not adding microbial inocula to the anaerobic environments in the bottles. All bottles received 3 mL of oil from one of four sources: North Sea, the Gulf of Mexico, Texas, and Azerbaijan. All microcosm studies were performed in triplicate. Bottles were incubated at 30°C and inverted to avoid contact of the hydrocarbons with the rubber stoppers. Oil samples were extracted from the individual microcosms after 0, 3, 10, 13, and 20 weeks and analyzed for changes in chemical composition.

4.3.2 GC-Select-eV-TOF-MS

Oil dissolved in chloroform was directly injected, without prior fractionation or chromatographic separation, into the 250°C inlet of a gas chromatograph (GC, Agilent 7890B, Santa Clara, CA, USA). Analytes were separated based on volatility using a nonpolar column (60 m x 0.25 mm x 0.25 um Rxi-5Sil-MS; Restek, Bellefonte, PA, USA) with a helium gas flow rate of 2 mL/min. The GC program began at 40°C, ramped at 3.5°C/minute to 320°C, and was held isothermal for a final 10 minutes.

The GC was interfaced with a BenchTOF-Select time-of-flight mass spectrometer (Markes International, Llantrisant, UK) with a $m/\Delta m_{50\%} \approx 1000$. The ion source in the mass spectrometer generates electrons from the surface of a negatively charged filament and uses ion optics to retain a high potential difference and accelerate the electrons from the filament, therefore reducing their energy prior to arriving at the positively charged ion chamber.[35,36] The analyte from the GC column was transferred from the GC to the mass spectrometer's 200°C ion source via a 320°C transfer line. These temperatures reduced the thermal energy imparted to the hydrocarbons, subsequently reducing compound fragmentation. An ionization energy of 14 eV was chosen to maximize both compound molecular ion signal. Mass spectra were collected at 50 Hz and data processing was performed using custom code written in Igor 6.3.7.[2] To correct for

thermal transfer efficiency of high- and low-volatility analytes through the GC column, a series of perdeuterated alkanes (Sigma-Aldrich, St. Louis, MO, USA) of even carbon numbers from C_{10}-C_{30} were used as an internal standard to establish a relationship between transfer efficiency and retention time. Data calibration and visualization procedures followed previously established methods.[2]

4.3.3 Identification of Specific Isomers

The GC-Select-eV-TOF-MS technique enhances the abundance of molecular ions and reduces fragmentation of branched hydrocarbons in crude oil, allowing confident identification and quantification of all major straight-chain and branched lower molecular weight hydrocarbons by their parent mass, with clear separation from hydrocarbons with different chemical formulas. Hydrocarbon volatility increases with branching, therefore branched isomers elute earlier in the chromatogram than the straight-chain hydrocarbon. To identify specific hydrocarbon isomers in all four oils as a function of carbon number and molecular structure, authentic standards (Sigma-Aldrich, St. Louis, MO, USA), including alkanes, branched alkanes, cycloalkanes, branched cycloalkanes, alkylbenzenes, hopanes, and steranes were analyzed at 14 eV. The elution order of these authentic standards was used to identify the molecular structure of isomers of one molecular weight and compound class. For compounds that were not identified using authentic standards, chromatograms were compared to those previously established in the literature under similar chromatographic conditions, including column length and stationary phase. The elution orders of compounds in these chromatograms were used to identify the remaining isomers in a crude oil chromatogram.[29,31,37,38,39]

Figure 4.1 illustrates the overlayed single ion chromatographic traces of all major isomers of the four compound classes analyzed in this chapter from the four oils, with identified isomeric peaks. The four compound classes analyzed in this chapter for differences in biodegradation as a function of isomeric structure were C_9 alkanes, C_9 monocycloalkanes, C_9 monoaromatic compounds, and C_{10} monoaromatic compounds. The elution order of these compounds was the same throughout the 20-week timeline in all four oils used in this study, but the relative contribution and distribution of each isomer to the full compound class varied as a function of oil origin. These chromatographic traces, combined with previous work analyzing the complete composition of these oils in detail,[32] show the extent to which the four oils' initial chemical compositions differed at the start of this study.

4.4 Results and Discussion

Biodegradation of C_{30} hopane compounds in all four oils was <5% of the initial concentrations throughout the 20-week incubation period, corroborating previous studies illustrating the recalcitrance of hopane biomarkers to biodegradation.[21] The lack of biodegradation of hopanes is consistent with current understanding of microbial oil transformations, and demonstrates that recalcitrant compounds remained stable as expected in these experiments.

4.4.1 Alkane and Monocycloalkane Transformations

The dimethylheptane C_9 compounds eluted earliest in all four oils, as illustrated in Figure 4.1a, followed by the ethylheptanes and methylheptanes, and subsequently the *n*-nonane straight-

chain alkane. The relative biotransformation of the identified C_9 alkanes in the four oils across the 20-week incubation are illustrated in Figure 4.2. Hydrocarbon losses expressed as percentages of initial value at each time point are averages of three replicate bottles of the same crude oil, with a standard deviation of 5-10%. There was no change in the C_9 alkane composition of any of the crude oils in the control bottles without microbial inocula or with heat-killed inocula, indicating that all reported transformations were microbiologically mediated. In all oils, the C_9 straight-chain alkanes were degraded to ~50-60% of the original amount after 20 weeks incubation. The methyloctane isomers decreased to ~60-80% of the original amount in all oils, while the dimethylheptane isomers decreased to ~85-95% of the original amount in all oils over the same time period. This result corroborates previous work illustrating preferential biodegradation of crude oil hydrocarbons in the order of straight-chain alkanes > methyl branched alkanes > dimethyl branched alkanes > ethyl branched alkanes.[24-26]

The position of the alkyl branch on the carbon chain of the C_9 hydrocarbon affected the biodegradation of C_9 alkanes in all oils. The methyloctane isomers with methyl groups closer to the terminal position (2-methyloctane and 3-methyloctane) had ~10-20% more degradation than the methyloctane isomer with the methyl group in the middle (4-methyloctane) at each time point. These structural differences imply that branched hydrocarbons with terminal methyl groups are more prone to microbial attack than those with methyl groups further from the terminal position. In all four oils, the isomer of dimethylheptane with the alkyl branches adjacent to each other (2,3-dimethylheptane) was degraded ~5% less than the isomer with nonadjacent methyl groups (3,5-dimethylheptane) at each time point. This transformation difference was likely due to steric hindrance of adjacent alkyl carbon positions on the carbon backbone.[25,29,40] The same isomer specific C_9 biodegradation patterns were present in all four oils, indicating that these microbial transformation preferences were consistent and independent of initial oil composition.

All major isomers of C_9 monocycloalkanes are shown in Figure 4.1b as a function of branching in all four oils. Trimethylcyclohexanes eluted the earliest in the chromatogram, followed by ethylmethylcyclohexanes, and subsequently propylcyclohexanes. Figure 4.3 illustrates the transformation of C_9 monocycloalkanes in the four oils across the 20-week incubation as a function of hydrocarbon structure. Trimethylcyclohexanes were the least degraded species in all oils with ~90-95% of the original composition remaining at the end of the incubation. This recalcitrance is most likely due to the steric hindrance of the closely positioned alkyl species making them less susceptible to microbial attack. 1,4-ethylmethylcyclohexane was degraded ~5-10% more than 1,2-ethylmethylcyclohexane in all the oils due to the alkyl substituents being further separated on the carbon chain. This pattern was similar to the pattern observed in the C_9 alkanes, where isomers with alkyl substituents adjacent to each other were degraded more slowly than those isomers with alkyl substituents further apart on the carbon backbone. Propylcyclohexanes were the most completely degraded monocycloalkanes in all four oils (~65-80% of the original composition by week 20), possibly due to the single alkyl substituent on the cycloalkane carbon chain being more susceptible to microbial attack compared to the multiple alkyl substituents in the trimethylcyclohexanes and ethylcyclohexanes. These C_9 monocycloalkane isomer biodegradation patterns were consistent in all four oils regardless of the initial isomer composition.

4.4.2 Monoaromatic Hydrocarbon Transformations

All major isomers of C_9 monoaromatic compounds in all four oils are shown in Figure 4.1c. These compounds can be grouped into isomers of propylbenzenes, methylethylbenzenes, and

trimethylbenzenes based on their volatilities which determine the elution order. These identifications in all four oils were used to determine the transformation of C_9 monoaromatic compounds as a function of the 20-week incubation timeline, as illustrated in Figure 4.4. Methylethylbenzenes degraded the most rapidly of all the C_9 monoaromatic isomers in all four oils. The extent of degradation increased as a function of the ethyl group's adjacency to the methyl group. 1-methyl-4-ethylbenzene degraded the most over 20 weeks in all four oils, followed by 1-methyl-3-ethylbenzene, and subsequently 1-methyl-2-ethylbenzene. These degradation patterns as a function of alkyl position recapitulated the patterns observed in the C_9 alkane and C_9 monocycloalkane isomers in the four oils, implying that the relative extent of biodegradation of a hydrocarbon isomer was primarily dependent on alkyl position on the carbon chain. The trimethylbenzenes and propylbenzenes showed little susceptibility to microbial attack (<10% compared to the starting concentration) in all four oils, similarly to previously established findings.[27,29,41] These biodegradation patterns of C_9 alkanes, C_9 monocycloalkanes, and C_9 monoaromatic compounds implied that isomeric structure, carbon chain, and alkyl position dictate biodegradation of lower molecular weight crude oil hydrocarbons independent of the oil's initial composition.

As the molecular weight of a hydrocarbon increases, the number of isomers of a molecular formula exponentially increases.[42] This increase is visualized in Figure 4.1d, which illustrates 17 individually identified C_{10} monoaromatic compounds in all four oils. These benzenes are grouped into ethyldimethylbenzenes, tetramethylbenzenes, methylpropylbenzenes, diethylbenzenes, and butylbenzenes. The concentration of C_{10} monoaromatic compounds changed in all four oils throughout the 20-week incubation, as illustrated in Figure 4.5. In each case, the ethyldimethyl monoaromatic compounds were the most extensively degraded and degradation increased with increasing separation between the ethyl and dimethyl groups. These patterns corroborated the finding that the position of alkyl substituents is a primary factor dictating susceptibility to biotransformation of hydrocarbon isomers. As previously illustrated,[29,40] tetramethylbenzenes, methylpropylbenzenes, and butylbenzenes were more recalcitrant to microbial catabolism than ethyldimethyl benzenes in all four oils in this chapter.

The monoaromatic compound transformation pattern observed here extends previous microbial catabolism studies by separating and quantifying all isomers of individual hydrocarbon molecular formulas and illustrates observed changes over 20 weeks of microbial activity. Hydrocarbon branching, including alkyl position on the carbon chain, controlled the extent of biotransformation of one isomeric hydrocarbon molecular formula. Lower molecular weight alkanes, monocycloalkanes, and monoaromatic compounds with alkyl substituents closer together on the carbon chain proved to be more recalcitrant than isomers with alkyl substituents further apart.

4.4.3 Heavier Isomeric Crude Oil Hydrocarbon Transformations

The separation and identification of hydrocarbons isomers in a chromatogram becomes increasingly difficult as molecular mass increases due to the exponential increase in the number of isomers.[42,43] Figures 4.6 and 4.7 illustrate this concept with chromatographic traces of C_{12} monocycloalkanes and C_{12} monoaromatic compounds, respectively, in all four oils at the beginning of the biodegradation timeline and after 20 weeks incubation. While concentrations of essentially all compounds are lower after 20 weeks due to microbial biodegradation, different isomers degraded to different extents depending on their structure, which also affected their retention order

in the chromatogram. Compounds eluting at a later retention time were biodegraded to a greater extent than those eluting at an earlier retention time, implying that compounds eluting later had less branched substituents from the carbon chain or had alkyl substituents spaced further apart from each other along the carbon chain. These implications are consistent with those compounds having lower vapor pressures and thus later retention times. Even though exact structures cannot be identified for all the compounds in these samples, the chromatograms of C_{12} monocycloalkanes and monoaromatic compounds implied that branching and alkyl positions of isomeric hydrocarbons affect the degree of biodegradation independent of oil composition.

This chapter illustrates that the lability of crude oil hydrocarbons to microbial attack increases as the degree of branched substituents decreases and alkyl substituents are further separated on a carbon chain. These patterns can potentially be used to model the expected change in chemical composition of oil across greater carbon numbers, isomers, and more complex compound classes, such as polycyclic aromatic hydrocarbons. This technique provides a clear fingerprint for biotransformation and can be used in environmental applications such as biosouring investigations and hydrocarbon remediation responses.

4.5 Conclusions and Environmental Implications

This chapter extends previous works examining the effects of compound structure on biodegradation of crude oil hydrocarbons in order to understand how compound branching impacts the biodegradation of alkanes, monocycloalkanes, and monoaromatic hydrocarbons. C_9 alkanes, C_9 monocycloalkanes, C_9 monoaromatic compounds, and C_{10} monoaromatic compounds follow biodegradation patterns that vary as a function of structural branching and alkyl position, independent of oil composition. Hydrocarbon isomers with fewer branched substituents were biodegraded more rapidly than isomers with more branched substituents. Alkyl position also impacted biodegradation, as compounds with alkyl substituents spaced further apart on a carbon chain were degraded more quickly than those with alkyl substituents spaced closer together. This biodegradation pattern was most likely due to steric hindrances of closer positioned alkyl groups inhibiting microbial attack. These patterns are consistent and independent of oil composition and hydrocarbon molecular weight, as heavier compounds with more isomers also followed a pattern where certain isomers were biodegraded faster than others. We infer this pattern must also be indicative of alkyl position and structural branching.

The patterns identified in this chapter demonstrate that biodegradation leaves a distinctly different chemical signature from that of other transformation processes occurring in spilled oil. The most branched alkanes are most volatile and therefore evaporate first when oil is spilled and exposed to air, followed by less branched alkanes, and then the straight-chain alkanes.[4] Hydrocarbons can also undergo atmospheric oxidation directly at the oil surface, with oxidation rates increasing as branching increases.[33,44] These isomeric relative transformation patterns for evaporation and atmospheric oxidation are opposite from the isomeric biodegradation pattern observed in this anaerobic sulfate-reducing marine environment, where compounds with fewer or more separated alkyl substituents along a carbon chain were more susceptible to biodegradation. Even in nitrate-reducing marine environments where different crude oil hydrocarbon degradation extents were observed,[2] the degradation patterns with respect to alkyl chain position on the carbon skeleton were consistent with the patterns observed in this chapter. These differences in isomeric transformation patterns may be useful in developing forensic analyses of the fate of spilled oil

remaining in the environment, providing a novel approach for determining the relative amounts of atmospheric oxidation, evaporation, and biodegradation that occurred in weathered oil.

4.6 Acknowledgements

The authors acknowledge the Energy Biosciences Institute (EBI) for funding this work under Fund 86217.

4.7 References

(1) Engelbrektson, A., Hubbard, C.G., Tom, L.M., Boussina, A., Jin, Y.T., Wong, H., Piceno, Y.M., Carlson H.K. Conrad, M. E.; Anderson, G.; Coates, J. D. Inhibition of microbial sulfate reduction in a flow-through column system by (per)chlorate treatment. *Frontiers in Microbiology*. **2014**, *5*, 1-11.

(2) Nowak, J.A., Shrestha, P.M., Weber, R.J., McKenna, A.M., Chen, H., Coates, J.D., Goldstein, A.H. Comprehensive analysis of changes in crude oil chemical composition during biosouring and treatments. *Environmental Science & Technology*. **2018**, *52*, 1290-1300.

(3) Reddy, C.M., Quinn, J.G. GC-MS analysis of total petroleum hydrocarbons and polycyclic aromatic hydrocarbons in seawater samples after the north cape oil spill. *Marine Pollution Bulletin*. **1999**, *38*, 126-135.

(4) Drozd, G.T., Worton, D.R., Aeppli, C., Reddy, C.M., Zhang, H., Variano, E., Goldstein, A.G. Modeling comprehensive chemical composition of weathered oil following a marine spill to predict ozone and potential secondary aerosol formation and constraint transport pathways. *Journal of Geophysical Research Oceans*. **2015**, *120*, 7300-7315.

(5) Atlas, R.M. Microbial degradation of petroleum hydrocarbons: an environmental perspective. *Microbiology Reviews*. **1981**, *45*, 180-209.

(6) Harayama, S., Kishira, H., Kasai, Y., Shutsubo K. Petroleum biodegradation in marine environments. *Journal of Molecular Microbiology and Biotechnology*. **1999**, *1*, 63-70.

(7) Venosa, A.D., Campo, P., Suidan, M.T. Biodegradability of lingering crude oil 19 years after the Exxon Valdez oil spill. *Environmental Science & Technology*. **2010**, *44*, 7613-7621.

(8) Rahman, K.S., Rahman, T.J., Kourkoutas, Y., Petsas, I., Marchant, R., Banat, I.M. Enhanced bioremediation of n-alkane in petroleum sludge using bacterial consortium amended with rhamnolipid and micronutrients. *Bioresource Technology*. **2003**, *90*, 159-168.

(9) Brooijmans, R.J.W., Pastink, M.I., Siezen, R.J. Hydrocarbon-degrading bacteria: the oil-spill clean-up crew. *Microbial biotechnology*. **2009,** *2*, 587-594.

(10) Jones, D.M., Douglas, A.G., Parkes, R.J., Taylor, J., Giger, W., Schaffner, C. The recognition of biodegraded petroleum-derived aromatic hydrocarbons in recent marine sediments. *Marine Pollution Bullentin*. **1983**, *14*, 103-108.

(11) Adebusoye, S.A., Iloir, M.O., Amund, O.O., Teniola, O.D., Olatope, S.O. Microbial degradation of petroleum hydrocarbons in a polluted tropical stream. *World Journal of Microbiology and Biotechnology*. **2007**, *23*, 1149-1159.

(12) Atlas, R.M., Bragg, J. Bioremediation of marine oil spills: when and when not—the Exxon Valdez experience. *Microbial Biotechnology*. **2009**, *2*, 213-221.

(13) Harayama, S., Kasai, Y., Hara, A. Microbial communities in oil-contaminated seawater. *Current Opinion in Biotechnology*. **2004**, *15*, 205-214.

(14) Head, I.M., Jones, D.M., Röling, W.F.M. Marine microorganisms make a meal of oil. *Nature Reviews Microbiology*. **2006**, *4*, 173-182.

(15) Yakimov, M.M., Timmis, K.N., Golyshin, P.N. Obligate oil-degrading marine bacteria. *Current Opinions in Biotechnology*. **2007,** *18*, 257-266.

(16) Colati, K. A. P.; Dalmaschio, G. P.; de Castro, E. V. R.; Gomes, A. O.; Vaz, B. G.; Romão, W. Monitoring the liquid/liquid extraction of naphthenic acids in brazilian crude oil using electrospray ionization FT-ICR mass spectrometry (ESI FT-ICR MS). *Fuel*. **2013**, *108*, 647-655.

(17) Chen, H.; Hou, A.; Corilo, Y. E.; Lin, Q.; Lu, J.; Mendelssohn, I. A.; Zhang, R.; Rodgers, R.P.; McKenna, A.M. 4 years after the Deepwater Horizon Spill: Molecular transformation of Macondo well oil in Louisiana salt marsh sediments revealed by FT-ICR mass spectrometry. *Environ. Sci. Tech.* **2016**, *50*, (17), 9061-9069.

(18) Ruddy, B. M.; Huettel, M.; Kostka, J. E.; Lobodin, V. V.; Bythell, B. J.; McKenna, A. M.; Aeppli, C.; Reddy, C. M.; Nelson, R. K.; Marshall, A. G.; Rodgers, R. P. Targeted petroleomics: analytical investigation of Macondo well oil oxidation products from Pensacola Beach. *Energy Fuels*. **2014**, *28*, (6), 4043-4050.

(19) Fuchs. G., Boll, M., Heider, J. Microbial degradation of aromatic compounds - from one strategy to four. *Nature Reviews Microbiology*. **2011**, 9, 803-816.

(20) Rojo, F. Degradation of alkanes by bacteria. *Environmental Microbiology*. **2009**, *11*, 2477-2490.

(21) Aeppli, C.; Nelson, R.K.; Radović, J.R.; Carmichael, C.A.; Valentine, D.L.; Reddy, C.M. Recalcitrance and degradation of petroleum biomarkers upon abiotic and biotic natural weathering of *Deepwater Horizon* oil. *Environ. Sci. Tech*. **2014**, *48*, (12), 6726-6734.

(22) Vogt, C., Kleinsteuber, S., Richnow, H.H. Anaerobic benzene degradation by bacteria. *Microbial Biotechnology*. **2011**, *4*, 710-724.

(23) Zedelius, J., Rabus, R., Grundmann, O., Werner, I., Brodkorb, D., Schreiber, F., Ehrenreich, P., Behrends, A., Wilkes, H., Kube, M., Reinhardt, R., Widdel, F. Alkane degradation under anoxic conditions by a nitrate-reducing bacterium with possible involvement of the electron acceptor in substrate activation. *Environmental Microbiology Reports*. **2011**, *3*, 125-135.

(24) Schaeffer, T.L., Cantwell, S.G., Brown, J.L., Watt, D.S., Fall, R.R. Microbial growth on hydrocarbons: terminal branching inhibits biodegradation. *Applied and Environmental Microbiology*. **1979**, *38*, 742-746.

(25) Robson, J.N., Rowland, S.J. Biodegradation of highly branched isoprenoid hydrocarbons: a possible explanation of sedimentary abundance. *Organic Geochemistry*. **1987**, *13*, 691-695.

(26) Ulrici, W. Contaminant soil areas, different countries and contaminant monitoring of contaminants in Environmental Process II. *Soil Decontamination Biotechnology*., **2000**. Rehm, H. J.; and Reed, G. Eds., 11, 5-42.

(27) Eganhouse, R.P., Cozzarelli, I.M., Scholl, M.A., Matthews, L.L. Natural attenuation of volatile organic compounds (VOCs) in the leachate plume of a municipal landfill: using alkylbenzenes as process probes. *Ground Water*. **2001**, *39*, 192-202.

(28) Masterson, W.D., Dzou, L.I.P., Holba, A.G., Fincannon, A.L., Ellis, L. Evidence for biodegradation and evaporative fractionation in West Sak, Kuparuk and Prudhoe Bay field areas, North Slope, Alaska. *Organic Geochemistry*. **2001**, *32*, 411-441.

(29) George, S.C., Boreham, C.J., Minifie, S.A., Teerman, S.C. The effect of minor to moderate biodegradation on C_5 to C_9 hydrocarbons in crude oils. *Organic Geochemistry*. **2002**, *33*, 1293-1317.

(30) Fingas, M. *Handbook of Oil Spill Science and Technology*. **2015**

(31) Wang, Z.; Fingas, M. Differentiation of the source of spilled oil and monitoring of the oil weathering process using gas chromatography-mass spectrometry. *Journal of Chromatography A*. **1995**, 712 (2), 321− 343.

(32) Nowak, J.A., Weber, R.J., Goldstein, A.H. Quantification of isomerically summed hydrocarbon contributions to crude oil by carbon number, double bond equivalent, and aromaticity using gas chromatography with tunable vacuum ultraviolet ionization. *The Analyst*. **2018**, *143*, 1396-1405.

(33) Chan, A.; Isaacman, G.; Wilson, K.; Worton, D.; Ruehl, C.; Nah, T.; Gentner, D. R.; Dallmann, T. R.; Kirchstetter, T.; Harley, R.; Gilman, J.; Kuster, W.; de Gouw, J.; Offenberg, J.; Kleindienst, T.; Lin, Y.; Rubitschun, C.; Surratt, J.; Hayes, P.; Jimenez, J.; Goldstein, A. H. Detailed chemical characterization of unresolved complex mixtures in atmospheric organics: insights into emission sources, atmospheric processing, and secondary organic aerosol formation. *Journal of Geophysical Research: Atmospheres*. **2013**, *118*, 6783−6796.

(34) Widdel, F., Pfennig, N. Studies on dissimilatory sulfate-reducing bacteria that decompose fatty acids. *Archives of Microbiology*. **1981**, *129*, 395-400.

(35) Alam, M.S., Stark, C., Harrison, R.M. Using variable ionization energy time-of-flight mass spectrometry with comprehensive GCxGC to identify isomeric species. *Analytical Chemistry*. **2016**, *88*, 4211-4220.

(36) Markes International, Ltd. Application Note 528. **2014**.

(37) Wilkes, H., Boreham, C., Harms, G., Zengler, K., Rabus, R. Anaerobic degradation and carbon isotopic fractionation of alkylbenzenes in crude oil by sulphate-reducing bacteria. *Organic Geochemistry*. **2000**, *31*, 101-115.

(38) McIntyre, C.P., Harvey, P.M., Ferguson, S.H., Wressnig, A.M., Volk, H., George, S.C., Snape, I. Determining the Extent of Biodegradation of Fuels Using the Diastereomers of Acyclic Isoprenoids. *Environmental Science & Technology*. **2007**, *41*, 2452-2458.

(39) Tran, T.C., Logan, G.A., Grosjean, E., Ryan, D., Marriott, P.J. Use of comprehensive two-dimensional gas chromatography/time-of-flight mass spectrometry for the characterization of biodegradation and unresolved complex mixtures in petroleum. *Geochimica et Cosmochimica Acta*. **2010**, *74*, 6468-6484.

(40) Volkman, J.K., Alexander, R., Kagi, R.I., Rowland, S.J., Sheppard, P.N. Biodegradation of aromatic hydrocarbons in crude oils from the Barrow sub-basin of Western Australia. *Organic Geochemistry*. **1984**, *6*, 619-632.

(41) Cozzarelli, I.M., Eganhouse, R.P., Baedecker, M.J. Transformation of mono-aromatic hydrocarbons to organic acids in anoxic groundwater environment. *Environmental Geology and Water Science*. **1990,** *16*, 135-141.

(42) Goldstein, A. H.; Galbally, I. E. Known and unexplored organic constituents in the earth's atmosphere. *Environ. Sci. Technol*. **2007**, 41, (5), 1514−1521.

(43) Worton, D.; Zhang, H.; Isaacman, G.; Chan, A.; Wilson, K.; Goldstein, A. Comprehensive Chemical Characterization of Hydrocarbons in NIST Standard Reference Material 2779 Gulf of Mexico Crude Oil. *Environ. Sci. Tech.* **2015**, *49*, (22), 13130-13138.

(44) Ruehl, C.R., Nah, T., Isaacman, G., Worton, D.R., Chan, A.W., Kolesar, K.R., Cappa, C.D., Goldstein, A.H., Wilson, K.R. The influence of molecular structure and aerosol phase on the heterogeneous oxidation of normal and branched alkanes by OH. *The Journal of Physical Chemistry A*. **2013**, *117*, 3990-4000.

4.8 Figures

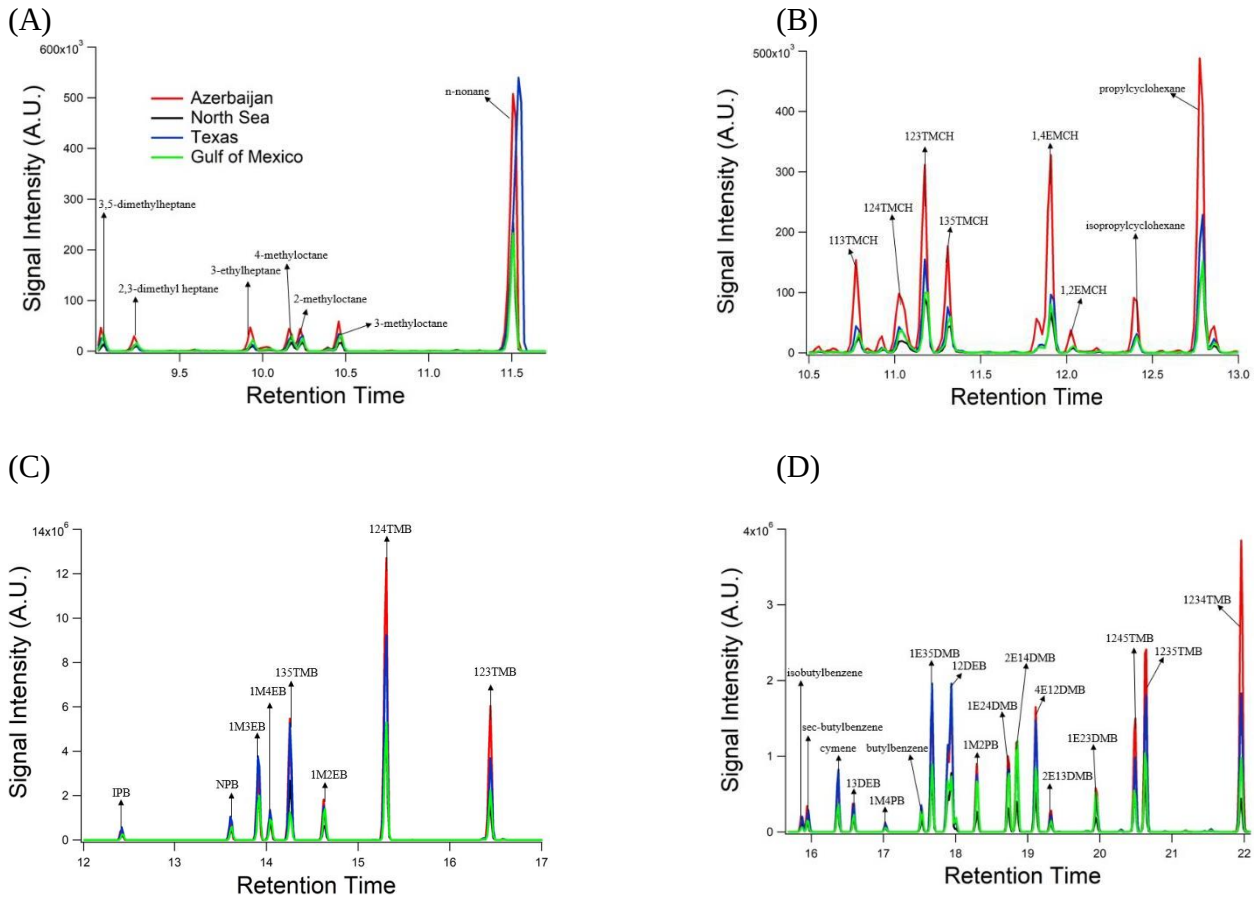

Figure 4.1. Single ion chromatograms of (A) C_9 alkanes (*m/z*=128), (B) C_9 monocycloalkanes (*m/z*=126), (C) C_9 monoaromatic compounds (*m/z*=120), and (D) C_{10} monoaromatic compounds (*m/z*=134) of Azerbaijan, North Sea, Texas, and Gulf of Mexico oils.

(A) North Sea

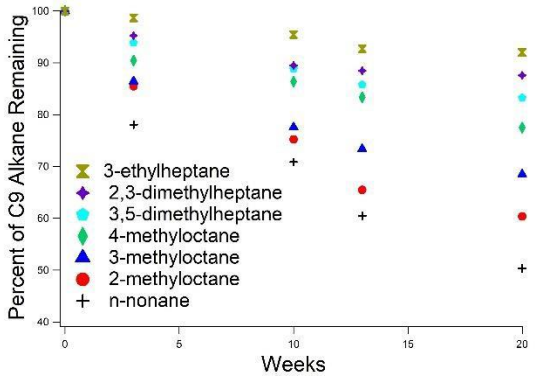

(B) Gulf of Mexico

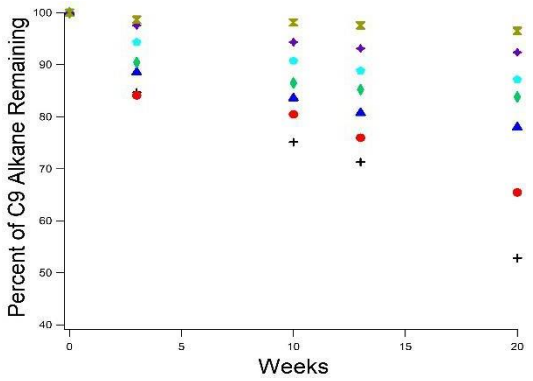

(C) Texas

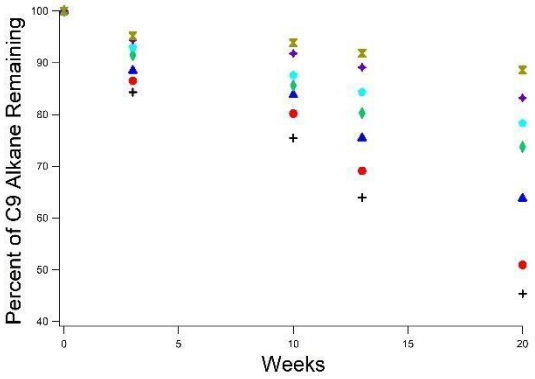

(D) Azerbaijan

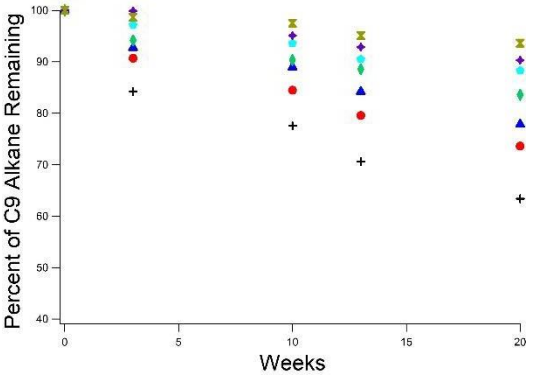

Figure 4.2. Transformations of isomers of C_9 alkanes in (A) North Sea, (B) Gulf of Mexico, (C) Texas, and (D) Azerbaijan oils through a 20-week incubation.

(A) North Sea

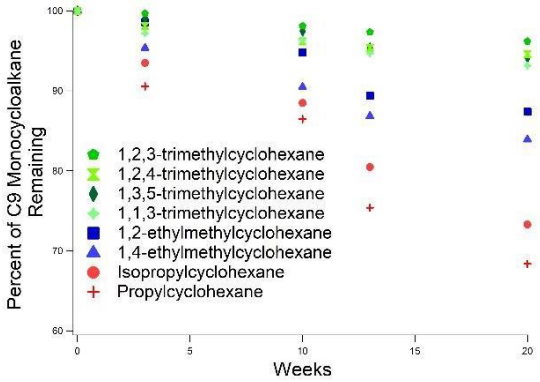

(B) Gulf of Mexico

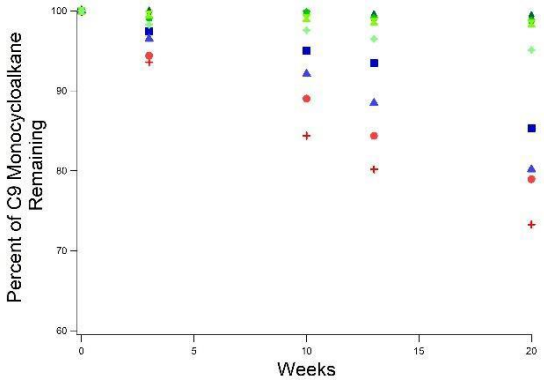

C) Texas

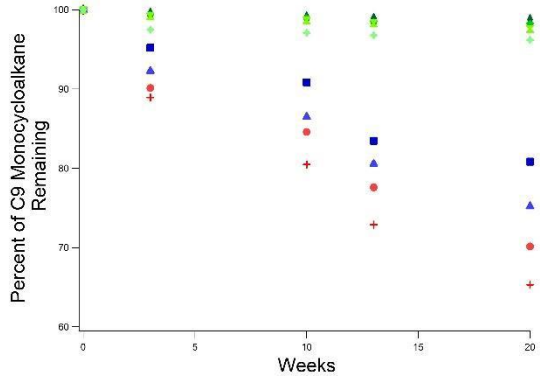

(D) Azerbaijan

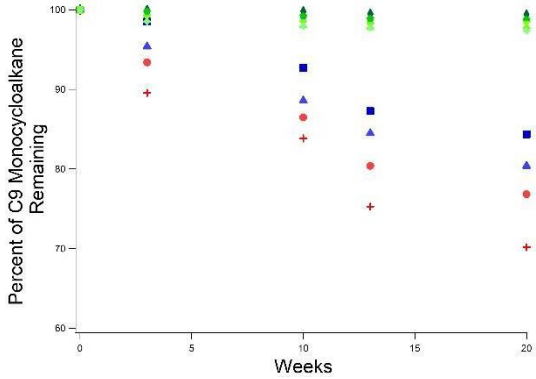

Figure 4.3. Transformations of isomers of C_9 monocycloalkanes in (A) North Sea, (B) Gulf of Mexico, (C) Texas, and (D) Azerbaijan oils through a 20-week incubation.

(A) North Sea

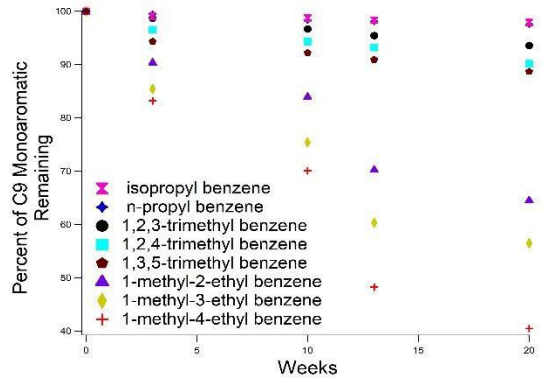

(B) Gulf of Mexico

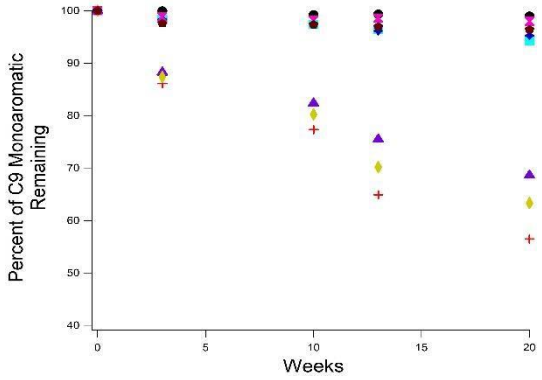

(C) Texas

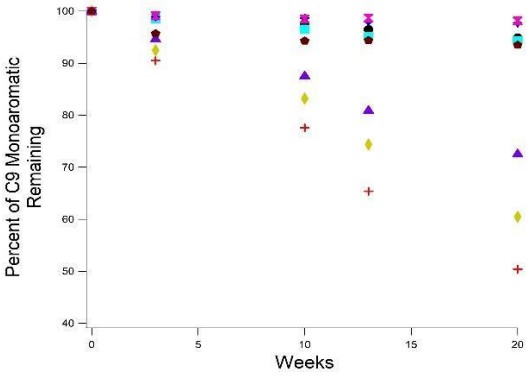

(D) Azerbaijan

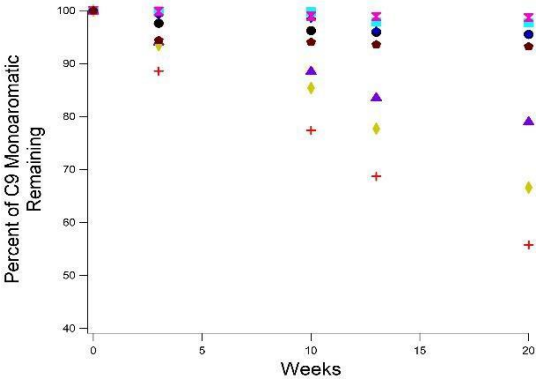

Figure 4.4. Transformations of isomers of C_9 monoaromatic compounds in (A) North Sea, (B) Gulf of Mexico, (C) Texas, and (D) Azerbaijan oils through a 20-week incubation.

(A) North Sea

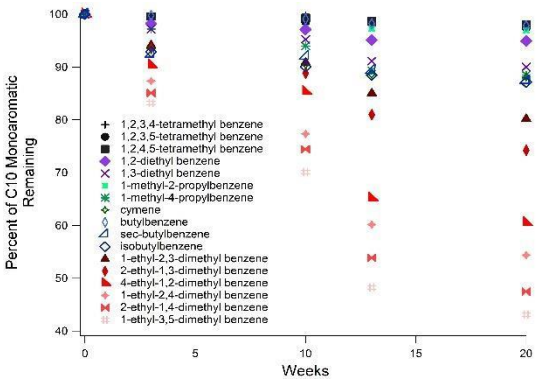

(B) Gulf of Mexico

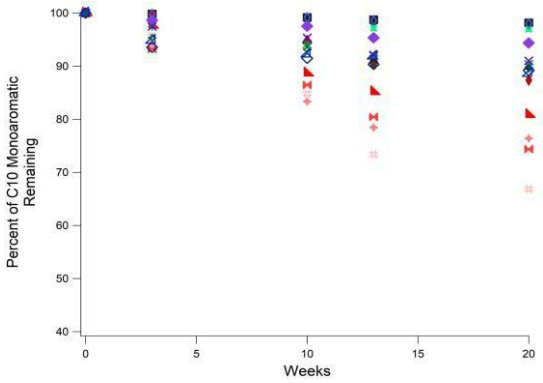

(C) Texas

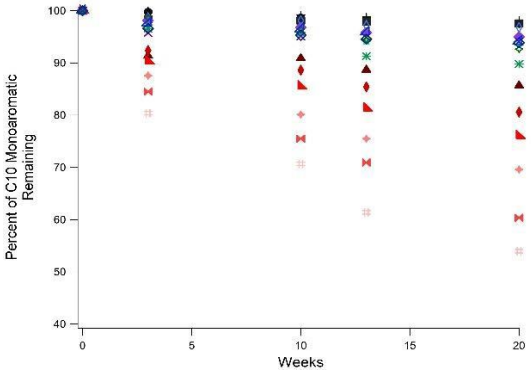

(D) Azerbaijan

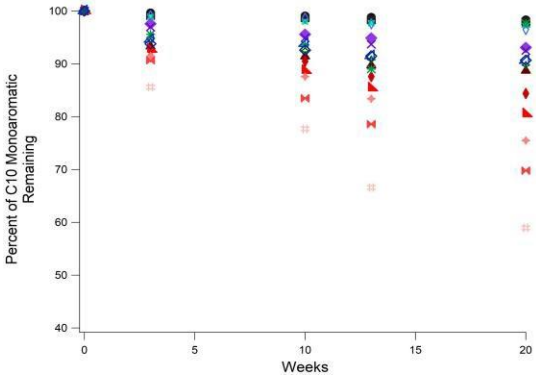

Figure 4.5. Transformations of isomers of C_{10} monoaromatic compounds in (A) North Sea, (B) Gulf of Mexico, (C) Texas, and (D) Azerbaijan oils through a 20-week incubation.

(A) North Sea

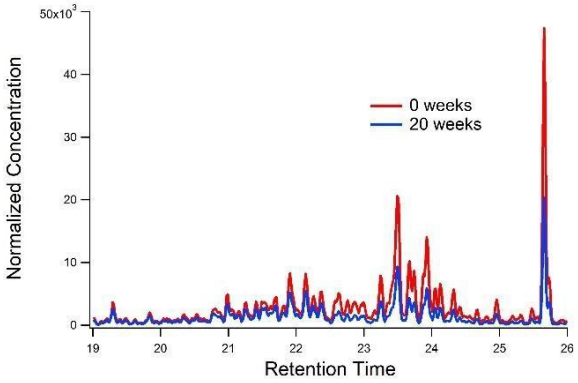

(B) Gulf of Mexico

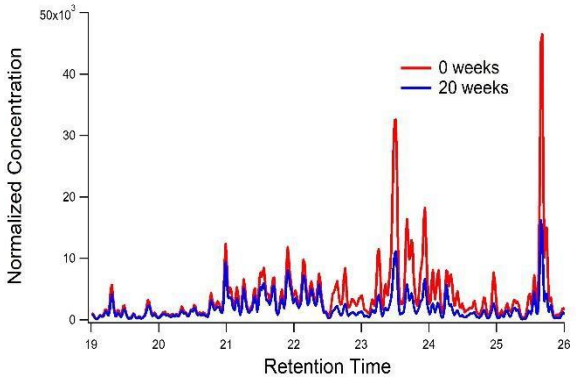

(C) Texas

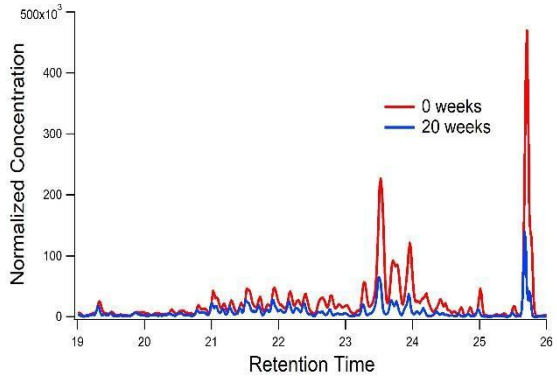

(D) Azerbaijan

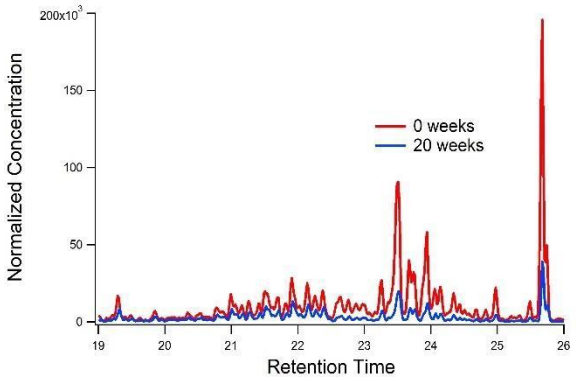

Figure 4.6. Single ion chromatograms of C_{12} monocycloalkanes (*m/z*=168) at week 0 and week 20 of the incubation in the (A) North Sea, (B) Gulf of Mexico, (C) Texas, and (D) Azerbaijan oils.

(A) North Sea

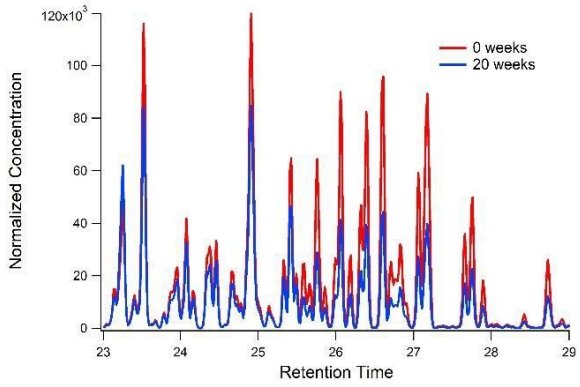

(B) Gulf of Mexico

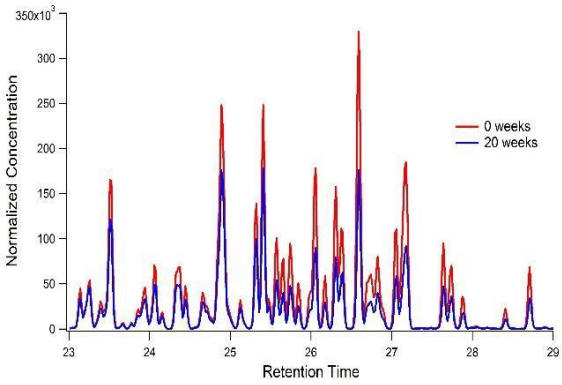

(C) Texas

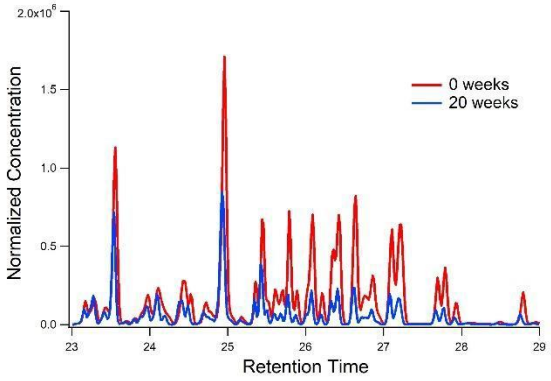

(D) Azerbaijan

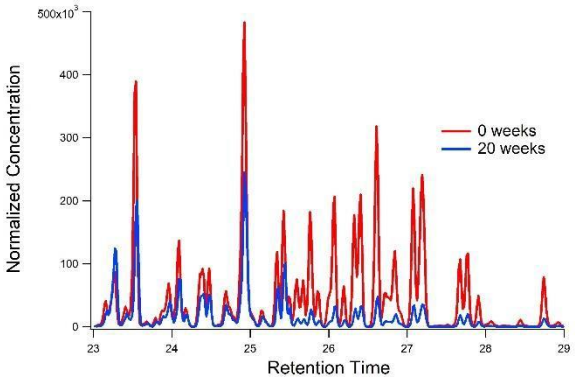

Figure 4.7. Single ion chromatograms of C_{12} monoaromatic compounds (*m/z*=162) at week 0 and week 20 of the incubation in the (A) North Sea, (B) Gulf of Mexico, (C) Texas, and D) Azerbaijan oils.

Chapter 5

Summary and Further Directions

This dissertation presents advances in unravelling the complexity of crude oil's chemical composition to identify biodegradation patterns by hydrocarbon catabolizing microbial communities in different reducing environments. Tunable GC-VUV-TOF at the Advanced Light Source at the Lawrence Berkeley National Laboratory was incorporated to more completely characterize isomeric distributions of hydrocarbons in oil compositions based on molecular weight, carbon number, and compound class. By analyzing four crude oils from different reservoirs, this technique illustrated differences in molecular distributions and aromatic fractions of isomerically summed compound classes that have previously been unidentified.

A deeper understanding of differences in biotransformation under different reducing environments was reached by using GC-VUV-TOF and ultrahigh resolution FT-ICR MS to characterize changes in the chemical composition of crude oil from a North Sea reservoir. These techniques expanded the analytical window of identifiable crude oil hydrocarbons beyond those compounds characterized in previous biodegradation studies. This dissertation illustrated how hydrocarbon degradation patterns and product formations change depending on the presence of a dominant electron acceptor. This work offers significant implications for the fossil fuel industry with respect to biosouring treatments in crude oil fields.

A novel experimental technique, GC-Select-eV-TOF-MS, characterized catabolic patterns of hydrocarbon isomers in crude oil from four different oil fields exposed to the same complex microbial community. Despite different initial compositions, hydrocarbon isomers with terminal alkyl branches were more prone to biodegradation than those with methyl groups further from the terminal position in all four oils. Compounds with alkyl branches adjacent to each other experienced less biodegradation than isomers with nonadjacent methyl groups. This study established a universality of isomeric preferences in catabolism of crude oil by microbial communities despite differences in starting oil compositions. Furthermore, this work illustrated that microbial metabolism leaves a distinct signature from other transformation processes occurring in spilled oil, allowing the effects of biodegradation to be distinguished from those of other processes acting upon weathered oil.

There are several potential areas of further research that provide interesting opportunities for future graduate students or other researchers to investigate microbial biotransformation more deeply. Such areas include addressing compound identifications using additional authentic standards, incorporating isotope labeled tracers to track a compound's specific biodegradation pathway, understanding the effects of different microbial communities degrading the same crude oil, and characterizing volatile organic compounds (VOCs) from biodegrading microbial communities.

The exponential increase in constitutional isomers with molecular hydrocarbon weight makes it challenging to identify structures of all individual contributions to an isomerically summed molecular formula. To comprehensively identify more isomers contributing to summed molecular formulas, additional authentic hydrocarbon standards could be used or synthesized in order to determine structural positions of aromatic functional groups and alkyl substituents. Previous crude oil studies have also combined GC with FT-ICR MS to take advantage of isomeric hydrocarbon characterization and ultrahigh resolution mass spectrometry. It would be interesting

to combine the soft ionization GC technique used in this dissertation with FT-ICR MS in order to identify more isomers across all carbon compounds ranging from C_{10}-C_{80} with an N_{DBE} class of 0-30. This methodology could provide new insights on which isomers are preferentially transformed in crude oil biodegradation studies.

Another avenue for further work analyzing biotransformations of crude oil would be to incorporate isotope labeled hydrocarbons to track specific microbial biodegradation pathways. Isotope labeled compounds are available for smaller molecular weight hydrocarbons such as pentane, cyclohexane, and benzene. Heavier molecular weight isotope labeled compounds could also be synthesized. By combining these compounds with a crude oil degrading microbial enrichment and extracting samples for analysis across a biodegradation timeline, a comprehensive biotransformation pathway of select compounds could be created to identify transformation products and metabolites. This experiment could identify specific hydrocarbon transformations and oxygenated metabolites that arise from the biodegradation of isotope labeled compounds, providing a definitive identification of metabolites and end products of crude oil biodegradation.

While this dissertation illustrates how the same microbial community degrades crude oils from different origins, an extension of this work could examine how different microbial communities degrade the same crude oil. SRCs dominated the microbial inocula incorporated in this work, but further studies could incorporate a single strain of hydrocarbon or non-hydrocarbon degrading bacteria to identify specific bacterial species that contribute to biodegradation of crude oil. The SRCs in this dissertation originated from the North Sea produced waters, but further studies could incorporate microbial enrichments from produced waters from other marine environments. This procedural change could determine if the biodegradation patterns observed here are specific to only North Sea inocula or are consistent with other microbial communities.

No VOCs were characterized in this dissertation, but analysis of a range of highly volatile products could provide an exciting opportunity for further research. Proton transfer reaction time-of-flight mass spectrometry is a powerful analytical technique that can characterize a range of VOCs from microbial biodegradation products, such as sulfur and nitrogen containing compounds. The characterization of VOCs as a result of biodegradation of crude oil could expand on the work described herein to further understand the impact of microbial biodegradation of crude oil on air quality in oil-contaminated marine environments, or the specific mechanisms of biotransformation. This methodology could also further elucidate differences in the chemical signatures of evaporation, oxidation, and biodegradation pathways of crude oil.

These potential areas of further research provide several different ideas for further progress into the understanding of biotransformation pathways of crude oil by utilizing similar methods to those described in this dissertation. The work described here provides insight into biotransformation patterns of crude oil from different origins by incorporating novel chromatographic and mass spectrometric techniques to identify hydrocarbon isomers and biodegradation metabolites. This work expands the molecular range of identifiable hydrocarbons to understand how initial crude oil composition and hydrocarbon structure impact biodegradation patterns. The contributions this dissertation presents to the characterization of biodegradation patterns of crude oil can impact how microbiologists, geochemists, and oil spill scientists study biodegradation of crude oil for industrial and environmental crude oil modeling.